Long-scale evolution of thin liquid films

Alexander Oron*

Department of Mechanical Engineering, Technion-Israel Institute of Technology, Haifa 32000, Israel

Stephen H. Davis

Department of Engineering Sciences and Applied Mathematics, Robert R. McCormick School of Engineering and Applied Science, Northwestern University, Evanston, Illinois 60208

S. George Bankoff

Department of Chemical Engineering, Robert R. McCormick School of Engineering and Applied Science, Northwestern University, Evanston, Illinois 60208

Macroscopic thin liquid films are entities that are important in biophysics, physics, and engineering, as well as in natural settings. They can be composed of common liquids such as water or oil, rheologically complex materials such as polymers solutions or melts, or complex mixtures of phases or components. When the films are subjected to the action of various mechanical, thermal, or structural factors, they display interesting dynamic phenomena such as wave propagation, wave steepening, and development of chaotic responses. Such films can display rupture phenomena creating holes, spreading of fronts, and the development of fingers. In this review a unified mathematical theory is presented that takes advantage of the disparity of the length scales and is based on the asymptotic procedure of reduction of the full set of governing equations and boundary conditions to a simplified, highly nonlinear, evolution equation or to a set of equations. As a result of this long-wave theory, a mathematical system is obtained that does not have the mathematical complexity of the original free-boundary problem but does preserve many of the important features of its physics. The basics of the long-wave theory are explained. If, in addition, the Reynolds number of the flow is not too large, the analogy with Reynolds's theory of lubrication can be drawn. A general nonlinear evolution equation or equations are then derived and various particular cases are considered. Each case contains a discussion of the linear stability properties of the base-state solutions and of the nonlinear spatiotemporal evolution of the interface (and other scalar variables, such as temperature or solute concentration). The cases reducing to a single highly nonlinear evolution equation are first examined. These include: (a) films with constant interfacial shear stress and constant surface tension, (b) films with constant surface tension and gravity only, (c) films with van der Waals (long-range molecular) forces and constant surface tension only, (d) films with thermocapillarity, surface tension, and body force only, (e) films with temperature-dependent physical properties, (f) evaporating/condensing films, (g) films on a thick substrate, (h) films on a horizontal cylinder, and (i) films on a rotating disc. The dynamics of the films with a spatial dependence of the base-state solution are then studied. These include the examples of nonuniform temperature or heat flux at liquid-solid boundaries. Problems which reduce to a set of nonlinear evolution equations are considered next. Those include (a) the dynamics of free liquid films, (b) bounded films with interfacial viscosity, and (c) dynamics of soluble and insoluble surfactants in bounded and free films. The spreading of drops on a solid surface and moving contact lines, including effects of heat and mass transport and van der Waals attractions, are then addressed. Several related topics such as falling films and sheets and Hele-Shaw flows are also briefly discussed. The results discussed give motivation for the development of careful experiments which can be used to test the theories and exhibit new phenomena.
[S0034-6861(97)00803-9]

CONTENTS

*On sabbatical leave at Robert R. McCormick School of Engineering and Applied Science, Department of Engineering Sciences and Applied Mathematics, Northwestern University, Evanston, IL 60208.

I. INTRODUCTION

Thin liquid films are ubiquitous entities in a variety of settings. In geology, they appear as gravity currents under water or as lava flows (Huppert and Simpson, 1980; Huppert, 1982a). In biophysics, they appear as membranes, as linings of mammalian lungs (Grotberg, 1994), or as tear films in the eye (Sharma and Ruckenstein, 1986a; Wong *et al.*, 1996). They occur in Langmuir films (Gaines, 1966) and in foam dynamics (Bikerman, 1973; Edwards *et al.*, 1991; Schramm and Wassmuth, 1994; Wasan *et al.*, 1994; Wong *et al.*, 1995). In engineering, thin films serve in heat and mass transfer processes to limit fluxes and to protect surfaces, and applications arise in paints, adhesives, and membranes.

Thin liquid films display a variety of interesting dynamics. Since the interface between the liquid and the surrounding gas is a deformable boundary, these films display wave motion; the waves can travel and steepen under certain conditions for high flow rates, and the waves can make transitions into quasiperiodic or chaotic structures. The film can rupture, leading to holes in the liquid that expose the substrate to the ambient gas. The connectedness of the film changes in this case, as it does if droplets of liquid are dislodged from the film (fragmentation). Changes in structure occur in flows having contact lines leading to fingered patterns.

Liu *et al.* (1995) performed an experimental study of three-dimensional (3D) instabilities of falling films on an inclined plane driven at the upstream end ($x=0$) in order to understand the transition from two-dimensional (2D) waves to complex disordered patterns. Because 2D disturbances are found to grow more rapidly initially than 3D ones, 2D waves with straight wave fronts are excited first. Nonlinear evolution of the waves depends on the value of the frequency of small perturbations driving the flow. Three-dimensional patterns develop at sufficiently high Reynolds numbers of the flow, and two examples of such patterns are displayed in Fig. 1. Figure 1(a) shows an example of a "synchronous" instability when the deformations of the neighboring wave fronts are in phase. When a 2D wave first becomes large in amplitudes, transverse modulations appear and grow downstream. At $x\approx 40$ cm, nearly periodic spanwise modulations are visible. As the waves travel further downstream ($x>50$ cm), the two-dimensional wave fronts begin to break. Subsequently, the flow becomes disordered. Another type of instability is displayed in Fig.1(b). This is a subharmonic mode when the deformations of the neighboring wave fronts are out of phase,

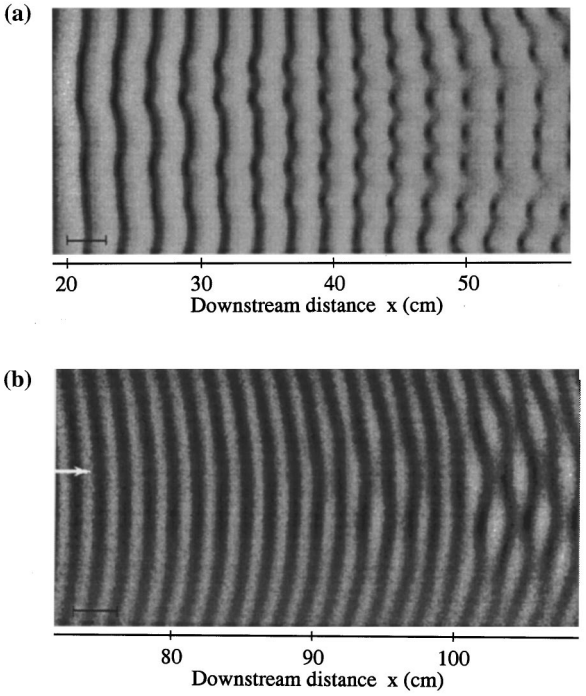

FIG. 1. Photographs of 3D patterns arising in falling films. The film flows on an inclined plane and is perturbed at the upstream end ($x=0$). Visualization is by fluorescence imaging; the film thickness is proportional to the brightness, i.e., the thick region is bright and the thin region is dark. The direction of the flow is from the left to the right. Lines seen on the photograph are of equal heights: (a) synchronous 3D instability of 2D periodic waves. A snapshot taken at the inclination angle of 6.4°, Reynolds number of 72, and imposed perturbation frequency of 10.0 Hz; (b) a herringbone (or checkerboard) pattern due to 3D subharmonic instability. A snapshot taken at the inclination angle of 4.0°, Reynolds number of 50.5, and imposed perturbation frequency of 14 Hz. Reprinted with the permission of the American Institute of Physics from Liu, Schneider, and Gollub (1995).

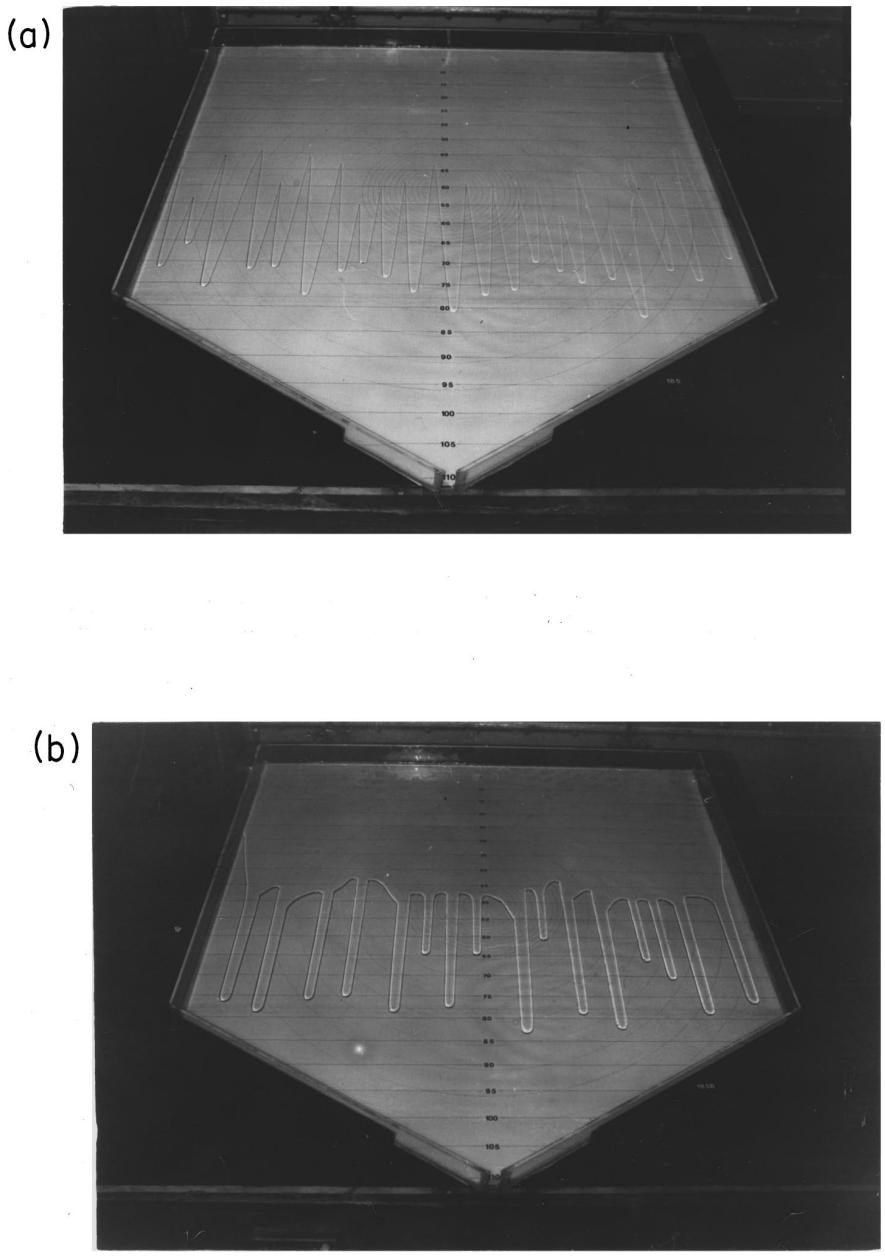

FIG. 2. The various forms of sheet flow down an inclined plane. The marked horizontal lines in each photograph are 5 cm apart: (a) the flow of silicone-oil MS 200/100 of initial cross-sectional area 1.8 cm^2, down a slope of 12°, 185 s after release, showing a well-developed wave form; (b) the flow of glycerine of initial cross-sectional area 7.3 cm^2, down a slope of 12°, 62 s after release, showing a well-developed wave form with characteristic straight edges aligned directly downslope. Reprinted with permission from Huppert (1982b). Copyright © 1982 Macmillan Magazines Ltd.

i.e., the transverse phase of the modulations differs by π for successive wave fronts, and the streamwise period is doubled. These herringbone patterns usually appear in patches, and their locations fluctuate in time. Phenomena such as these will be discussed in Sec. VI.

Figure 2, reproduced from Huppert (1982b), presents various patterns that emerge when a fluid sheet is released on an inclined plane. Some time after the release, the flow front, a contact line, spontaneously develops a series of fingers of fairly constant wavelength across the slope. In the case shown in Fig. 2(a) the front of a silicone-oil layer consists of periodic triangular-shaped waves. The flow of a glycerine layer is shown in Fig. 2(b), where the front displays a periodic structure of fingers with extremely straight contact lines, which are directed down the slope. Phenomena such as these will be discussed in Sec. VI.

Figure 3, reproduced from Fermigier *et al.* (1992), displays a layer of a silicone oil on the underside of a horizontal plane and overlying a fluid of lower density (gas). Gravity causes the planar interface to become unstable, a Rayleigh-Taylor instability, leading to the creation of fingers. Shown is an isolated axisymmetric pattern that has evolved from an initial disturbance. When the thickness of the layer becomes too large, the fluid is opaque and the screen is invisible, as in the center of the drop. Such phenomena are discussed in Sec. II.

Figure 4, reproduced from Burelbach *et al.* (1990), shows two pictures of a layer of silicone oil on a rigid, horizontal surface. The surface is nonuniformly heated and the interface dimples at points where the temperature of the substrate is elevated. Thermocapillarity produces the dimple when the heat flux is sufficiently small, Fig. 4(a), and a dry spot when the heat flux exceeds a

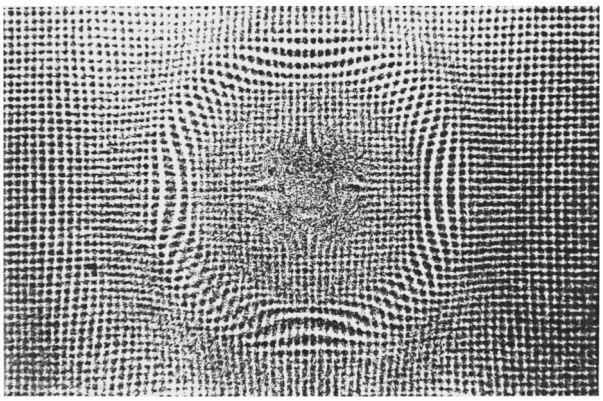

FIG. 3. A snapshot of the Rayleigh-Taylor instability of a silicone-oil layer on the underside of a horizontal plane. The locally axisymmetric perturbation is revealed by the distortion of a ruled screen observed through the interface. The wavelength of the screen is 0.8 mm. Copyright © 1992 Cambridge University Press. Reprinted with the permission of Cambridge University Press from Fermigier, Limat, Wesfreid, Boudinet, and Quilliet (1992).

critical value, Fig. 4(b). Such effects will be discussed in Sec. III.

If one wishes to give mathematical descriptions of such phenomena, one must face the fact that the interfaces of the film are, in part, free boundaries whose configurations must be determined as parts of the solutions of the governing equations. This renders the problem too difficult to treat exactly, which may lead researchers to rely on computing only. Even this becomes formidable when there are many parameters in the problem. If a rupture is to be described in which a film of unit depth is driven to zero depth, it will not suffice to study the corresponding linearized equations, for which well-known and widely employed mathematical tools are available. One must also deal with strongly nonlinear disturbances to the film. Finally, if one is required to deal with coupled phenomena, one must be able to describe, in compact form, simultaneous instabilities that interact in complex ways. This compact form must be tractable and, at the same time, still complex enough to retain the main features of the problem at hand.

One means of treating the above complexities is to analyze *long-scale* phenomena only, in which variations along the film are much more gradual than those normal to it, and in which variations are slow in time. Such theories arise in a variety of areas in classical physics: shallow-water theory for water waves, lubrication theory in viscous films, and slender-body theory in aerodynamics and in fiber dynamics. In all these, a geometrical disparity is utilized in order to separate the variables and to simplify the analysis. In thin viscous films, it turns out that most rupture and instability phenomena do occur on long scales, and a lubrication-theory approach is, in fact, very useful. This is explained below.

The lubrication-theory or long-wave-theory approach is based on the asymptotic reduction of the governing equations and boundary conditions to a simplified system which often consists of a single nonlinear partial

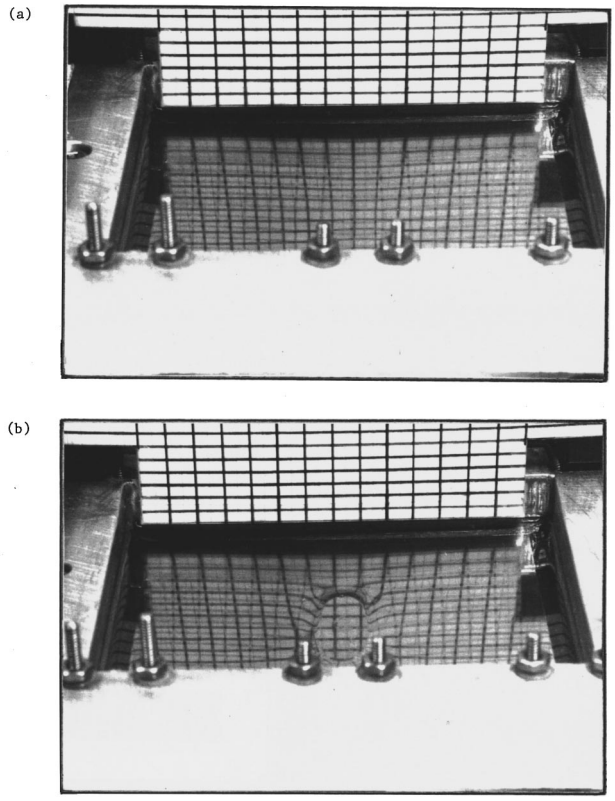

FIG. 4. Photographs of a silicone-oil film on a nonuniformly heated plate: (a) a dimpled film when the heat flux is sufficiently low; (b) the nearly bare region that results at larger heat fluxes. Reprinted with the permission of the American Institute of Physics from Burelbach, Bankoff, and Davis (1990).

differential equation formulated in terms of the local thickness of the film. The rest of the unknowns, i.e., the fluid velocity, fluid temperature, etc., are then determined via functionals of the solution of that differential equation. The notorious complexity of the free-boundary problem is thus removed. However, a resulting penalty is the presence of the strong nonlinearity in the governing equation(s) and the higher-order spatial derivatives appearing there. A simplified linear stability analysis of the problem can be carried out based on the resulting evolution equation. A weakly nonlinear analysis of the problem is also possible through that equation. However, the fully nonlinear analysis that allows one to study finite-amplitude deformations of the film interface must be performed numerically. Still, numerical solution of the evolution equation is considerably less difficult than numerical solution of the original, free-boundary problem.

There has been a great deal of progress in the analysis of thin (macroscopic) liquid films. In the present review such analyses will be unified into a simple framework from which the special cases will naturally emerge. By means of long-scale evolution equations, many interesting cases will be discussed, giving the reader both an overview and representative behaviors typical of thin films. In particular, coupled dynamics and instabilities

will be addressed. Despite the experimental observations mentioned above, there is a critical lack of carefully controlled experiments devoted to uncovering and quantifying phenomena. This review stands as a call for such experiments.

The first topic to be addressed in Sec. II will be bounded films, which have one free surface and one interface with a solid phase. The physical effects discussed will be viscous, surface-tension, and body forces, thermocapillarity, evaporation/condensation, and the presence of van der Waals attractions. The effect of curvature of the solid wall and that of film rotation will be also examined. In Sec. III, bounded films with spatial (geometric and dynamic) nonuniformities will be considered. In Sec. IV, free films in which both interfaces of the films are free boundaries will be considered. Films with interfacial viscosities and internal mass transfer (e.g., surface-active agents) are also discussed. These cases are ones in which systems of evolution equations are needed to describe the dynamics. In Sec. V, the related problem of the spreading of liquid drops on substrates is considered. Here, moving contact lines are present and it is shown how the same long-scale formalism can be applied to describe spreading. Since this topic has been frequently treated in the literature, our discussion will be brief. Section VI will consider the case in which the substrate is inclined to the horizontal and gravity drives a mean flow. Flows in a narrow gap between planes (Hele-Shaw flows) will also be addressed. Finally, in Sec. VII an overview will be given.

II. BOUNDED FILMS

A. Slipper bearing

The long-scale methods that will be used to describe interfacial instabilities have their origins in the lubrication theory of viscous fluids. This theory can be most simply illustrated by considering a fluid-lubricated slipper bearing.

Fluid-lubricated bearings are machine parts in which viscous fluid is forced into a converging channel. The flow creates vertical pressure forces that can be used to support large loads and hence reduce wear. In his pioneering work Reynolds (1886) laid the foundations for the theory of lubrication. He applied hydrodynamics of slow viscous flow and derived the fundamental differential equation of the field, found approximate solutions for this equation, and compared his theoretical results with experiments performed earlier. This idea is illustrated below where the structure called a slipper bearing is displayed. Many more details related to Reynolds's and others' work can be found in Dowson (1979).

In Fig. 5, a (solid) bearing is shown in which a plate at $z=0$ moves in the positive x direction at constant speed U_0 driving fluid into the converging channel. In steady flow, the lower boundary of the bearing (the upper boundary of the channel) is at $z=h(x)$. The fluid is

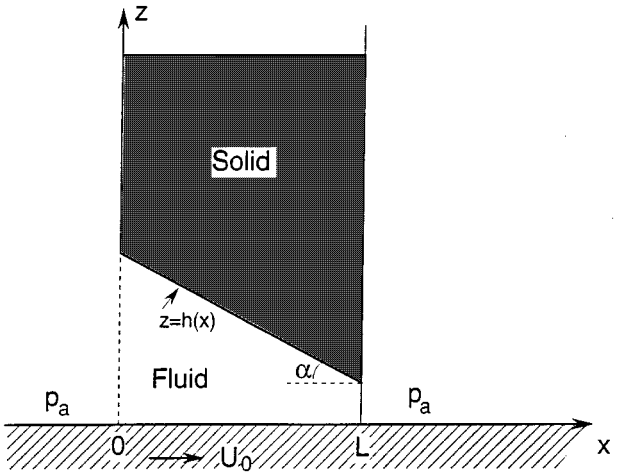

FIG. 5. Slipper bearing. The plate moves with the constant velocity U_0. The lower boundary of the bearing, located at $z=h(x)$, is static and tilted at small angle α. The external pressure is p_a.

taken to be an incompressible, Newtonian viscous fluid of viscosity μ, density ρ, and kinematic viscosity $\nu=\mu/\rho$.

When the length of the plate L is large, the liquid is able to support a load due to the large pressures generated under the bearing. For a fixed channel narrowing $\Delta h=h(0)-h(L)$, the tilt angle

$$\alpha \equiv \frac{dh}{dx} \tag{2.1}$$

is small in this limit. Under this condition and in two dimensions, the Navier-Stokes and continuity equations can be reduced (Schlichting, 1968) to the simplified forms

$$\mu \partial_z^2 u - \partial_x p = 0, \tag{2.2a}$$

$$-\partial_z p = 0, \tag{2.2b}$$

$$\partial_x u + \partial_z w = 0, \tag{2.2c}$$

where the velocity vector is $\vec{\mathbf{v}}=(u,w)$, and p is the pressure in the fluid. Equation (2.2a) tells us that since α is small, the flow is locally parallel. Equation (2.2b) states that the pressure is vertically uniform (or, if gravity were to be included, hydrostatic). Equation (2.2c) is the continuity equation.

The boundary conditions below the bearing, $0<x<L$, are

$$u(0)=U_0, \quad w(0)=0, \tag{2.3a}$$

$$u(h)=0. \tag{2.3b}$$

Beyond the bearing, $x\leqslant 0$ and $x\geqslant L$, the pressure is atmospheric, and in particular

$$p(0)=p(L)=p_a. \tag{2.3c}$$

Given that p depends on x only, one can solve the system (2.2), (2.3) directly to find that

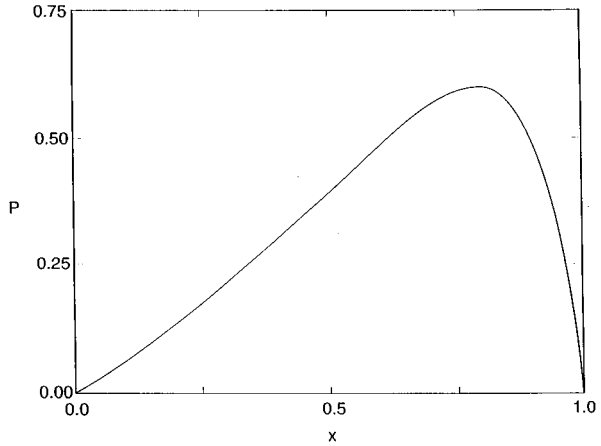

FIG. 6. Distribution of the dimensionless pressure P at the lower boundary of the bearing as a function of the coordinate x/L along the channel. $P \equiv (p-p_a)/6\mu U_0$.

$$\mu u(z) = \frac{1}{2}\partial_x p(z^2 - hz) + \mu U_0\left(1 - \frac{z}{h}\right); \tag{2.4}$$

the flow is a linear combination of plane Poiseuille and plane Couette flows. Of course, $p(x)$ is not yet known.

Given that the flow is steady, the flow rate Q (in the x direction),

$$Q = \int_0^{h(x)} u(z)\,dz, \tag{2.5}$$

must be constant, which gives

$$\mu Q = -\frac{1}{12}h^3\partial_x p + \frac{1}{2}\mu U_0 h. \tag{2.6}$$

Alternatively, one can write the derivative of this equation,

$$\partial_x\left(-\frac{1}{12}h^3\partial_x p + \frac{1}{2}\mu U_0 h\right) = 0. \tag{2.7}$$

Equation (2.7) is the Reynolds lubrication equation. Given $h(x)$, it is an ordinary differential equation for p. In Eq. (2.6) the flow rate Q and the integration constant are determined by conditions (2.3c). In Eq. (2.7) both constants of integration are then determined.

In either case one finds (Schlichting, 1968) that the pressure distribution is given by

$$p(x) = p_a + 6\mu U_0\left[\int_0^x \frac{dx}{h^2} - \frac{\int_0^L dx/h^2}{\int_0^L dx/h^3}\int_0^x \frac{dx}{h^3}\right], \tag{2.8}$$

as shown in Fig. 6. Note that the maximum pressure $p_m \sim 1/\alpha$, so that the upward force F_v exerted by the fluid flow scales as $F_v \sim 1/\alpha^2$. The important fact is that the lubrication pressure behaves like $O(1/\alpha)$ as $\alpha \to 0$.

It is possible to extend the theory to situations in which h depends (slowly) on time t. In this case Eq. (2.7) would have the form

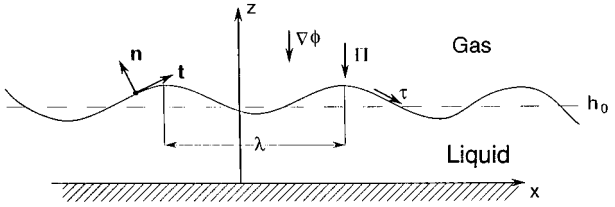

FIG. 7. Sketch of a bounded liquid film. The body force is $\vec{\nabla}\phi$, and the imposed normal and tangential stresses are Π and τ, respectively.

$$\mu\partial_t h + \partial_x\left(-\frac{1}{12}h^3\partial_x p + \frac{1}{2}\mu U_0 h\right) = 0, \tag{2.9a}$$

or in the case of three-dimensional flow, $h = h(x,y,t)$,

$$\mu\partial_t h + \vec{\nabla}_1\cdot\left(-\frac{1}{12}h^3\vec{\nabla}_1 p + \frac{1}{2}\mu\vec{U}_0 h\right) = 0. \tag{2.9b}$$

Here

$$\vec{\nabla}_1 = \left(\frac{\partial}{\partial x}, \frac{\partial}{\partial y}\right), \quad \vec{U}_0 = (U_0, V_0).$$

We now turn to the main subject of the review, starting with the basics of the long-scale methods. The reader will notice the similarity between the time-dependent Reynolds lubrication equation (2.9) and the general evolution equations for thin, bounded liquid films, Eqs. (2.27) and (2.28) derived below. Thus the slipper-bearing theory carries one to the more general cases of films with free surfaces, and so to the phenomena of wave propagation, free-surface instability, and film rupture.

B. The evolution equation for a bounded film

The lubrication approximation will now be applied to a viscous-liquid flow, bounded below by a horizontal plate and above by an interface between the liquid and a passive gas, as shown in Fig. 7. Here one allows the possibility on the interface of external normal $\vec{\Pi}$ and tangential $\vec{\tau}$ stresses, slowly varying in space and time. Further, a conservative body force with potential ϕ is allowed.

The Navier-Stokes and continuity equations in two dimensions have the form

$$\rho(\partial_t u + u\partial_x u + w\partial_z u) = -\partial_x p + \mu\nabla^2 u - \partial_x\phi, \tag{2.10a}$$

$$\rho(\partial_t w + u\partial_x w + w\partial_z w) = -\partial_z p + \mu\nabla^2 w - \partial_z\phi, \tag{2.10b}$$

$$\partial_x u + \partial_z w = 0, \tag{2.10c}$$

where $\nabla^2 = \partial^2/\partial x^2 + \partial^2/\partial z^2$.

The classical boundary conditions between the liquid and the plate are those of no penetration, $w = 0$, and no slip, $u = 0$. These conditions are appropriate for the continuous films to be considered here. However, we wish to derive equations now that will apply not only in this case but also to the case in which a contact line (or

trijunction) exists and liquid on a solid substrate spreads and displaces the surrounding fluid (say, gas). The classical conditions then lead to a nonintegrable singularity at the contact line (Huh and Scriven, 1971; Dussan V. and Davis, 1974), which can be relieved by allowing a relative motion, slip, between the liquid and the solid near the contact line. In order to include such cases, discussed in Sec. V, we generalize the conditions. The condition of no penetration is retained and tangential relative motion is allowed. A Navier model that assumes slip proportional to the shear stress gives

$$\text{at } z=0: \quad w=0, u-\beta\partial_z u=0. \tag{2.11}$$

Here β is the slip coefficient, which will be taken to be zero for the case of continuous films.

On $z=h(x,t)$:

$$w=\partial_t h+u\partial_x h, \tag{2.12a}$$

$$\mathbf{T}\cdot\vec{\mathbf{n}}=-\kappa\sigma\vec{\mathbf{n}}+\frac{\partial\sigma}{\partial s}\vec{\mathbf{t}}+\vec{\mathbf{f}}, \tag{2.12b}$$

where $\mathbf{T}$ is the stress tensor of the liquid, $\vec{\mathbf{n}}$ is the unit outward vector normal to the interface, $\vec{\mathbf{t}}$ is the unit vector tangential to the interface, $\vec{\mathbf{f}}$ is the prescribed forcing at the interface, whose normal and tangential components are $\vec{\Pi}$ and $\vec{\tau}$, respectively, κ is the mean curvature of the interface, and s is the arc length along the interface, such that

$$\vec{\mathbf{n}}=\frac{(-\partial_x h,1)}{[1+(\partial_x h)^2]^{1/2}}, \quad \vec{\mathbf{t}}=\frac{(1,\partial_x h)}{[1+(\partial_x h)^2]^{1/2}}, \tag{2.12c}$$

$$\kappa=-\vec{\nabla}_1\cdot\vec{\mathbf{n}}=\frac{\partial_x^2 h}{[1+(\partial_x h)^2]^{3/2}}. \tag{2.12d}$$

Equation (2.12a) is the kinematic boundary condition (in the absence of interfacial mass transfer) that balances the normal component of the liquid velocity at the interface with the speed of the interface. Equation (2.12b) has two components. Its tangential component states that the shear stress on the interface is balanced by the sum of $\vec{\tau}$ and the surface gradient of the surface tension σ. Its normal component states that the normal stress minus $\vec{\Pi}$ exhibits a jump equal to the surface tension times the mean curvature. When the external force $\vec{\Pi}$ is zero, and the fluid has zero viscosity, then $\mathbf{T}\cdot\vec{\mathbf{n}}\cdot\vec{\mathbf{n}}=-p$, and this component equation reduces to the well-known Laplace equation, which describes the excess pressure in an air bubble, compared to the external pressure, as twice the surface tension divided by the bubble radius (see, for example, Landau and Lifshits, 1987).

Let us now introduce scales for thin films that are motivated by the arguments and scalings used in the analysis of the slipper bearing of Sec. II. Consider length scales in the x direction defined by wavelength λ on a film of mean thickness h_0. Consider the distortions to be of *long scale* if

$$\epsilon=\frac{2\pi h_0}{\lambda}\ll 1. \tag{2.13}$$

It is natural to scale z to h_0; then the dimensionless z coordinate is

$$Z=z/h_0 \tag{2.14a}$$

and x to λ, or equivalently, h_0/ϵ. Then the dimensionless x coordinate is given by

$$X=\frac{\epsilon x}{h_0}. \tag{2.14b}$$

Likewise if there are no rapid variations expected as $\epsilon\to 0$, then

$$\frac{\partial}{\partial X}, \quad \frac{\partial}{\partial Z}=O(1). \tag{2.14c}$$

If $u=O(1)$, the dimensionless fluid velocity in the x direction is

$$U=\frac{u}{U_0}, \tag{2.14d}$$

where U_0 is the characteristic velocity of the problem. Then continuity requires that the dimensionless fluid velocity in the z direction be

$$W=\frac{w}{\epsilon U_0}. \tag{2.14e}$$

Time is scaled to λ/U_0 so that the dimensionless time is

$$T=\frac{\epsilon U_0 t}{h_0}. \tag{2.14f}$$

Finally, one expects, as in the slipper-bearing example, locally parallel flow in the liquid so that $\partial_x p\sim\mu\partial_z^2 u$ and hence the dimensionless stresses, body-force potential, and pressure are

$$(\vec{\tau},\vec{\Pi})=\frac{h_0}{\mu U_0}(\vec{\tau}_0,\epsilon\vec{\Pi}_0), \tag{2.14g}$$

$$(\Phi,P)=\frac{\epsilon h_0}{\mu U_0}(\phi,p). \tag{2.14h}$$

Notice that "pressures" are large due to the lubrication effect. If these forms are substituted into the governing system (2.10)–(2.12), the following scaled system is obtained:

$$\epsilon Re(\partial_T U+U\partial_X U+W\partial_Z U) = -\partial_X P+\partial_Z^2 U+\epsilon^2\partial_X^2 U-\partial_X\Phi, \tag{2.15a}$$

$$\epsilon^3 Re(\partial_T W+U\partial_X W+W\partial_Z W) = -\partial_Z P+\epsilon^2(\partial_Z^2 W+\epsilon^2\partial_X^2 W)-\partial_Z\Phi, \tag{2.15b}$$

$$\partial_X U+\partial_Z W=0. \tag{2.15c}$$

At $Z=0$,

$$W=0, \quad U-\beta_0\partial_Z U=0. \tag{2.16}$$

Here $\beta_0=\beta/h_0$ is the dimensionless slip coefficient.

At $Z=H$,

$$W=\partial_T H+U\partial_X H, \tag{2.17a}$$

$$(\partial_Z U+\epsilon^2\partial_X W)[1-\epsilon^2(\partial_X H)^2]-4\epsilon^2(\partial_X H)(\partial_X U) = \tau_0[1+\epsilon^2(\partial_X H)^2]+\partial_X\Sigma[1+\epsilon^2(\partial_X H)^2]^{1/2}, \tag{2.17b}$$

$$-P-\Pi_0+\frac{2\epsilon^2}{[1+\epsilon^2(\partial_X H)^2]}\{\partial_X U[\epsilon^2(\partial_X H)^2-1] -\partial_X H(\partial_Z U+\epsilon^2\partial_X W)\}=\frac{C^{-1}\epsilon^3\partial_X^2 H}{[1+\epsilon^2(\partial_X H)^2]^{3/2}}, \tag{2.17c}$$

where $H=h/h_0$ is the dimensionless thickness of the film and $\Sigma=\epsilon\sigma/\mu U_0$ is the dimensionless surface tension. The Reynolds number Re and capillary number C are given, respectively, by

$$Re=\frac{U_0 h_0}{\nu}, \tag{2.18}$$

$$C=\frac{U_0\mu}{\sigma}. \tag{2.19}$$

Before taking limits, we integrate the continuity Eq. (2.15c) in Z from 0 to $H(X,T)$, use integration by parts, Eq. (2.17a), and the boundary conditions (2.16) to obtain

$$\partial_T H+\partial_X\left(\int_0^H U dZ\right)=0. \tag{2.20}$$

This equation constitutes a more convenient form of the kinematic condition and ensures conservation of mass on a domain with a deflecting upper boundary.

Finally, we seek the solution of the governing Eqs. (2.10)–(2.12) as a perturbation series in powers of the small parameter ϵ:

$$\begin{aligned} U&=U_0+\epsilon U_1+\epsilon^2 U_2+\cdots,\\ W&=W_0+\epsilon W_1+\epsilon^2 W_2+\cdots,\\ P&=P_0+\epsilon P_1+\epsilon^2 P_2+\cdots. \end{aligned} \tag{2.21a}$$

One lubrication approximation of the governing system is obtained by letting $Re, C=O(1)$ as $\epsilon\to 0$. In the former case the inertial terms, measured by ϵRe, are one order of magnitude smaller than the dominant viscous terms, consistent with the local-parallel-flow assumption. In the latter case, the surface-tension terms, measured by $C^{-1}\epsilon^3$, are two orders of magnitude smaller and would be lost. It will turn out to be essential to retain surface-tension effects at leading order, so that one writes

$$\overline{C}=C\epsilon^{-3} \tag{2.21b}$$

and takes another lubrication limit Re, $\overline{C}=O(1)$ as $\epsilon\to 0$. The latter is applied when surface-tension effects are strong relative to the others. At leading order in ϵ the governing system becomes, after omitting the subscript 0 in U_0, W_0, and P_0,

$$\partial_Z^2 U=\partial_X P+\partial_X\Phi, \tag{2.22a}$$

$$0=\partial_Z P+\partial_Z\Phi, \tag{2.22b}$$

$$\partial_T H+\partial_X\left(\int_0^H U dZ\right)=0. \tag{2.22c}$$

At $Z=0$,

$$U-\beta_0\partial_Z U=0, \tag{2.23}$$

and, at $Z=H$,

$$\partial_Z U=\tau_0+\partial_X\Sigma, \tag{2.24a}$$

$$-\Pi_0-P=\overline{C}^{-1}\partial_X^2 H. \tag{2.24b}$$

For our purposes, there is no need to find W, although it can be obtained by solving Eq. (2.15c) with the first condition of (2.16). Note the similarity to Eqs. (2.2) and (2.3) for the slipper bearing when $\beta_0\equiv h_0\beta=0$ in Eq. (2.23). Again, there is locally parallel flow, but now the upper boundary has prescribed shear stress, normal stress, and surface tension, and there is a conservative body force.

In order to solve these equations it is convenient to introduce a reduced pressure $\overline{P}$,

$$\overline{P}=P+\Phi. \tag{2.25a}$$

It follows from Eqs. (2.22b) and (2.24b) that

$$\overline{P}=\Phi|_{Z=H}-\overline{C}^{-1}\partial_X^2 H-\Pi_0. \tag{2.25b}$$

In this case

$$U=(\tau_0+\partial_X\Sigma)(Z+\beta_0)+\partial_X\overline{P}\left(\frac{1}{2}Z^2-HZ-\beta_0 H\right), \tag{2.26}$$

as follows from Eqs. (2.22a) and (2.25). If form (2.26) is substituted into the mass conservation condition of Eq. (2.22c), one obtains the appropriate evolution equation for the interface,

$$\partial_T H+\partial_X\left[(\tau_0+\partial_X\Sigma)\left(\frac{1}{2}H^2+\beta_0 H\right)\right] -\partial_X\left\{\left(\frac{1}{3}H^3+\beta_0 H^2\right)\partial_X\overline{P}\right\}=0. \tag{2.27}$$

In three dimensions one can show that the evolution equation has the form

$$\partial_T H+\vec{\nabla}_1\cdot\left[(\vec{\tau}_0+\vec{\nabla}_1\Sigma)\left(\frac{1}{2}H^2+\beta_0 H\right)\right] -\vec{\nabla}_1\cdot\left[\left(\frac{1}{3}H^3+\beta_0 H^2\right)\vec{\nabla}_1\overline{P}\right]=0, \tag{2.28}$$

where now $\vec{\tau}_0$ is the vector shear stress imposed on the interface. Equations (2.27) and (2.28) are the appropriate Reynolds lubrication equations for the present system. Whereas in the slipper-bearing problem H is

known and P is determined by this equation, here H is unknown and P is a functional of H determined by Eq. (2.25b) (due to surface tension and the body forces). This distinction is associated with the presence of either a fixed solid boundary or a free gas-liquid interface. Equation (2.27) is a generalization of the evolution equation presented by Sharma and Ruckenstein (1986a) in the case of no slip on the solid and no external forces ($\beta_0=\tau_0=\Pi_0=0$).

The physical significances of the terms is revealed when Eqs. (2.27) and (2.28) are written in the original dimensional variables:

$$\mu\partial_t h+\partial_x\left[(\tau+\partial_x\sigma)\left(\frac{1}{2}h^2+\beta h\right)\right]-\partial_x\left[\left(\frac{1}{3}h^3+\beta h^2\right)\times\partial_x(\phi|_{z=h}-\sigma\partial_x^2 h-\Pi)\right]=0, \tag{2.29}$$

$$\mu\partial_t h+\vec{\nabla}_1\cdot\left[(\vec{\tau}+\vec{\nabla}_1\sigma)\left(\frac{1}{2}h^2+\beta h\right)\right]-\vec{\nabla}_1\cdot\left[\left(\frac{1}{3}h^3+\beta h^2\right)\vec{\nabla}_1(\phi|_{z=h}-\sigma\nabla_1^2 h-\Pi)\right]=0. \tag{2.30}$$

In many of the examples discussed below, all forces are isotropic in the horizontal dimensions x and y, and so only two-dimensional cases will be examined. Further, unless specified, only disturbances periodic in x will be discussed. Thus λ is the wavelength of these disturbances and $2\pi h_0/\lambda$ is the dimensionless wave number.

C. Constant shear stress and constant surface tension only

Suppose that the gas exerts a "wind" stress on an interface that exhibits constant surface tension. In this case $\beta_0=\Pi=\phi=0$, and τ and σ are constant. Equation (2.29) becomes

$$\mu\partial_t h+\tau h\partial_x h+\frac{1}{3}\sigma\partial_x(h^3\partial_x^3 h)=0. \tag{2.31}$$

In the absence of surface tension ($\sigma=0$), Eq. (2.31) is a first-order nonlinear wave equation whose solutions are waves that travel in the direction of the shear and they steepen as they go. No instability is present. When surface tension is present, the steepening is retarded. Our numerical study of the nonlinear equation (2.31) shows that the amplitude of its periodic solutions decays to zero with time.

One can investigate the behavior of small disturbances to the uniform film $h=h_0$ by perturbing it with a small disturbance h', periodic in x: $h=h_0+h'$. If one substitutes this into Eq. (2.31) and linearizes in primed quantities, then one has the linear stability equation for h'. Since this equation has coefficients independent of t and x, one can seek separable solutions of the form

$$h'=h_0'\exp(ikx+st), \tag{2.32}$$

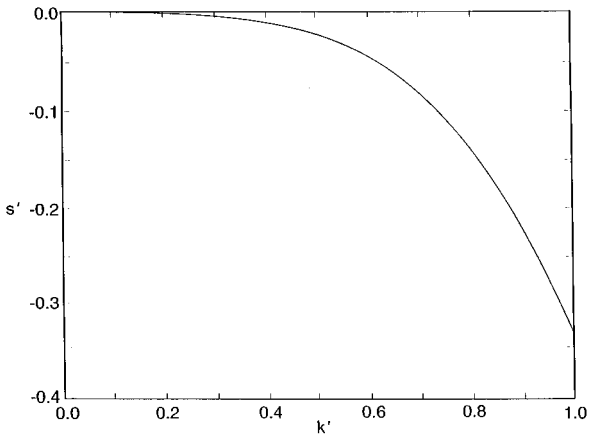

FIG. 8. Characteristic equation given by Eq. (2.35). $s'=\mathrm{Re}(s)h_0\mu/\sigma$ is the dimensionless growth rate of the perturbation with the dimensionless wave number k'. Negative growth rate corresponds to the decay of a perturbation; therefore there is no instability ($s'>0$) in the system.

which is a complete set of "normal modes" that can be used to represent any disturbance. If these are substituted into the linearized disturbance equation, one obtains the following characteristic equation for s:

$$\mu s=-ik'\tau-\frac{\sigma}{3h_0}k'^4, \tag{2.33}$$

where $k'=kh_0$ is the nondimensional wave number and s is the growth rate of the perturbation. The amplitude of the perturbation, therefore, will decay if the real part of the growth rate $\mathrm{Re}(s)$ is negative and will grow if $\mathrm{Re}(s)$ is positive. Purely imaginary values of s correspond to translation along the x axis and give rise to traveling-wave solutions. Finally, zero values of s correspond to neutral, stationary perturbations. The phase speed is thus

$$\mathrm{Im}\left(\frac{s}{k}\right)=-\frac{h_0\tau}{\mu} \tag{2.34}$$

and the growth rate is

$$\mathrm{Re}(s)=-\frac{1}{3h_0\mu}\sigma k'^4, \tag{2.35}$$

and as shown in Fig. 8, no instability exists in the long-wave regime. However, there are unit-order wave-number disturbances that do grow, as shown by Miles (1960) and Smith and Davis (1982).

D. Constant surface tension and gravity only

Consider perhaps the simplest film in which gravity is present and surface tension is constant. Here

$$\beta_0=\partial_x\sigma=\Pi=\tau=0 \quad \text{and} \quad \overline{P}=\rho g h-\sigma\partial_x^2 h, \tag{2.36}$$

so that Eq. (2.29) becomes

$$\mu\partial_t h-\frac{1}{3}\rho g\partial_x(h^3\partial_x h)+\frac{1}{3}\sigma\partial_x(h^3\partial_x^3 h)=0, \tag{2.37a}$$

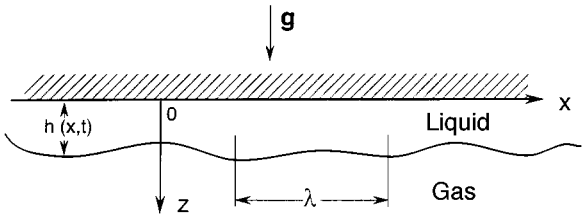

FIG. 9. Sketch of a liquid film lying on the underside of a horizontal plane and subject to Rayleigh-Taylor instability.

and its dimensionless variant is obtained from Eq. (2.27),

$$\partial_T H - \frac{1}{3} G \partial_x (H^3 \partial_X H) + \frac{1}{3} \overline{C}^{-1} \partial_X (H^3 \partial_X^3 H) = 0, \tag{2.37b}$$

where G is the unit-order gravity number,

$$G = \frac{\rho g h_0^2}{\mu U_0}. \tag{2.37c}$$

In the absence of surface tension, Eq. (2.37) is a nonlinear (forward) diffusion equation so that no disturbance to $h = h_0$ grows in time. Surface tension acts through a fourth-order (forward) dissipation term so that no instabilities would occur in the full Eq. (2.37b) for $G > 0$. If Eq. (2.37a) is linearized about $h = h_0$, the characteristic equation is

$$\mu s = -\frac{1}{3h_0}[\rho g h_0^2 + \sigma k'^2] k'^2. \tag{2.38}$$

This equation describes film leveling since $s < 0$; if at time $t = 0$ a small bump is imposed on the interface, Eq. (2.38) governs how it will relax to $h = h_0$.

Equations (2.37a) and (2.37b) also apply to the case of a film on the underside of a plate, the Rayleigh-Taylor instability of a thin viscous layer, as shown in Fig. 9. Here one replaces g by $-g$ in Eq. (2.38) and finds that

$$\mu s = -\frac{1}{3h_0}[-\rho |g| h_0^2 + \sigma k'^2] k'^2.$$

As shown in Fig. 10, the layer is linearly unstable if

$$k'^2 < k_c'^2 \equiv \frac{\rho |g| h_0^2}{\sigma} \equiv Bo, \tag{2.39}$$

i.e., if the perturbations are so long that the (nondimensional) wave number is smaller than the square root of the Bond number Bo, which measures the relative importance of gravity and capillary effects. The value of k_c' is often called the (dimensionless) *cutoff wave number* for neutral stability. It is emphasized that Eq. (2.37) constitutes the valid limit to the governing set of equations and boundary conditions when the Bond number Bo is small. This follows from the relationships $G = Bo/C$, $G = O(1)$, and the smallness of C, as assumed in Eq. (2.21).

The case of Rayleigh-Taylor instability was studied by Yiantsios and Higgins (1989, 1991) for the case of a thin film of a light fluid atop the plate and overlain by a large body of a heavy fluid and by Oron and Rosenau (1992) for the case of a thin liquid film on the underside of a rigid plane. It was found that evolution of an interfacial disturbance of small amplitude leads to rupture of the film, i.e., at a certain location the local thickness of the film becomes zero. Figure 11 shows a typical example of such an evolution. Yiantsios and Higgins showed that Eqs. (2.37a) and (2.37b) with $g < 0$ admit several steady solutions. These consist of various numbers of sinusoidal drops separated by "dry" spots of zero film thickness, as shown in Fig. 8 in Yiantsios and Higgins (1989). The examination of an appropriate Lyapunov functional (Yiantsios and Higgins, 1989) suggests that multiple-

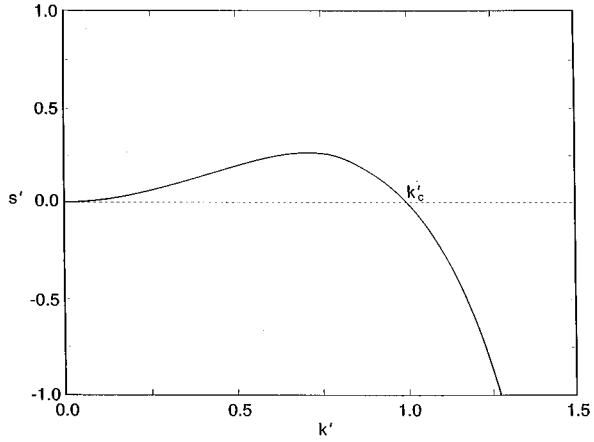

FIG. 10. Characteristic equation given by Eq. (2.38) for the Bond number $Bo = 1$, as defined by Eq. (2.39). $s' = 3s\mu/\rho|g|h_0$ is the dimensionless growth rate of the perturbation with the dimensionless wave number k'. Positive growth rate corresponds to the growth of a perturbation, whereas negative growth rate indicates decay. Therefore the unstable domain is $0 < k' < k_c'$.

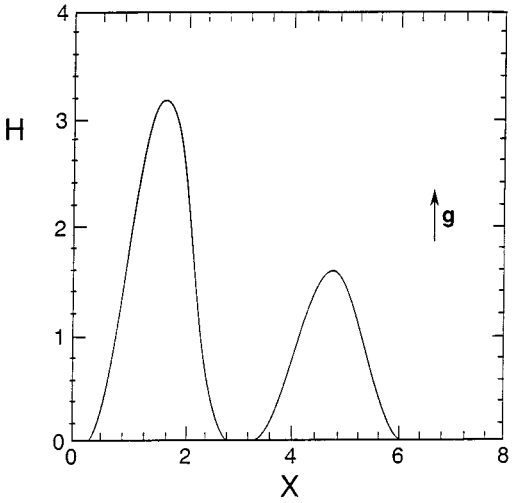

FIG. 11. Film profile close to rupture for Rayleigh-Taylor instability for $G = 20$, $\overline{C}^{-1} = 4$, $\Delta = 2\pi$, and the initial condition $H(X, T = 0) = 1 + 0.005 \sin X$. The arrow indicates the direction of gravity.

drop states are energetically less preferred than a one-drop state. These analytical results were partially confirmed by numerical simulations. As found in the long-time limit, the solutions can asymptotically approach multihumped states with different amplitudes and spacings as well. This suggests that terminal states depend upon the choice of initial data (Yiantsios and Higgins, 1989). It was also found that if the overlying semi-infinite fluid phase is more viscous than the thin liquid film, the process of the film rupture slows down in comparison with the single-fluid case.

It is interesting to note that Eqs. (2.37a) and (2.37b) were also derived and studied by Hammond (1983) in the context of capillary instability of a thin liquid film on the inner side of a cylindrical surface (see Sec. II.J.1). The three-dimensional version of the problem of Rayleigh-Taylor instability was considered by Fermigier *et al.* (1992). Formation of patterns of different symmetries and transition between patterns were observed. Axially symmetric cells and hexagons were found to be preferred. Droplet detachment was observed at the final stage of the experiment. Figure 3 shows the growth of an axisymmetric drop.

Saturation of Rayleigh-Taylor instability of a thin liquid layer by an imposed advection in the longitudinal direction was discussed by Babchin *et al.* (1983). Similarly, capillary instability of an annular film saturates due to a through flow (Frenkel *et al.*, 1987).

The problem of leveling of a film under the action of capillary force on a corrugated substrate at $z=l(x)$ was considered by Stillwagon and Larson (1988). Using the approach described above, they derived the evolution equation, which for the case of zero gravity reads

$$\mu\partial_t h+\frac{1}{3}\sigma\partial_x[h^3\partial_x^3(h+l)]=0. \tag{2.40}$$

Numerical solutions of Eq. (2.40) showed a good agreement with experimental data (Stillwagon and Larson, 1988). At short times there is film deplanarization due to the emergence of capillary humps, but these relax at longer times.

E. Van der Waals (long-range molecular) forces and constant surface tension only

Van der Waals forces can be important when the film thickness is in the range of several hundreds of Angströms, 100–1000 Å. Such forces in general compete with others of electrical or entropic origin (e.g., excess interfacial surface charge or electrical double layers), which exist on both longer and shorter scales than do the van der Waals attractions. At a given thickness of the layer, one or another of these can dominate. Only the h^{-3} forces will be considered here.

Dzyaloshinskii *et al.* (1959) derived a theory for van der Waals attractions in which an integral representation is given for the excess Helmholtz free energy of the layer as a function of the frequency-dependent dielectric properties of the materials in the layered system.

In the special case of a film with parallel boundaries and nonretarded forces in the absence of ionic species, $\phi=\phi_r+A'h^{-3}/6\pi$, where ϕ_r is a reference value for the body-force potential and A' is the dimensional Hamaker constant. When $A'>0$, there is negative disjoining pressure and a corresponding attraction of the two interfaces (solid-liquid and liquid-gas) for each other. When the disjoining pressure is positive, $A'<0$, the interfaces repel each other.

Consider negative disjoining pressure in a film with constant surface tension only, so that $\beta_0=\partial_x\sigma=\Pi=\tau=0$. When $A'>0$, instabilities occur, as shown below. When $A'<0$, the planar film persists. Equation (2.29) then becomes (Williams and Davis, 1982)

$$\mu\partial_t h+\frac{A'}{6\pi}\partial_x\left(\frac{\partial_x h}{h}\right)+\frac{1}{3}\sigma\partial_x(h^3\partial_x^3 h)=0. \tag{2.41a}$$

Its dimensionless version reads

$$\partial_T H+A\,\partial_X\left(\frac{\partial_X H}{H}\right)+\frac{1}{3}\overline{C}^{-1}\partial_X(H^3\partial_X^3 H)=0, \tag{2.41b}$$

where

$$A=\frac{A'\epsilon}{6\pi\rho\nu^2 h_0} \tag{2.41c}$$

is the scaled dimensionless Hamaker constant. Here the characteristic velocity was chosen as $U_0=\nu/h_0$. Alternatively, one can regard the disjoining pressure as an imposed normal stress Π in which $\Pi=A'/(6\pi h^3)$, leading to the same equations.

Linearization of Eq. (2.41a) around $h=h_0$ yields the characteristic equation

$$\mu s=\frac{k'^2}{h_0^2}\left(\frac{A'}{6\pi h_0}-\frac{1}{3}\sigma h_0 k'^2\right). \tag{2.42a}$$

It follows from Eq. (2.42a) that there is instability for $A'>0$, driven by the long-range molecular forces and stabilization is due to surface tension. The cutoff wave number k_c' is then given by

$$k_c'=\frac{1}{h_0}\left(\frac{A'}{2\pi\sigma}\right)^{1/2}, \tag{2.42b}$$

which reflects the fact that an initially corrugated interface has its thin regions thinned further by van der Waals forces while surface tension cuts off the small scales. Instability is possible only if $0<k'<k_c'$, as seen by combining Eqs. (2.42a) and (2.42b):

$$\mu s=\frac{\sigma k'^2}{3h_0}(k_c'^2-k'^2). \tag{2.43}$$

On the periodic domain of wavelength $\lambda=2\pi/k$, the linearized theory predicts that the film is always unstable since all wave numbers are available to the system. In an experimental situation the film resides in a container of finite width, say L. Solution of the linear stability theory for $0\leq X\leq L$ would show that only corrugations of small enough wavelength could "fit" in the box, i.e., $\lambda<L$. *No*

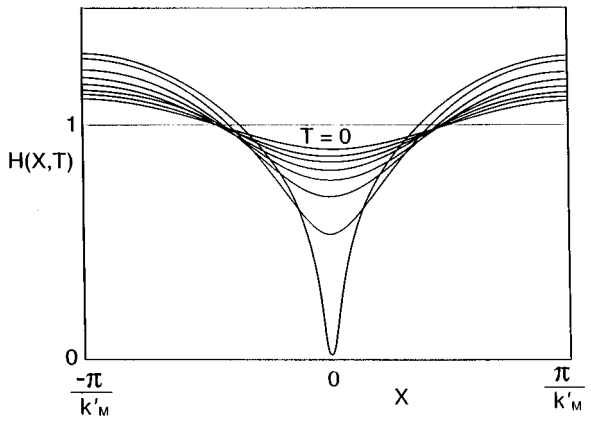

FIG. 12. Film profiles at different times as given by Eq. (2.41b) for $A=\overline{C}^{-1}=1$ solved in the domain $-\pi/k_M \leq X \leq \pi/k_M$ with the initial condition $H(X,T=0)=1+0.1\sin(k_M X)$. The fastest-growing linear mode has a wave number k_M, $2k_M^2=1$. Copyright © 1988 Cambridge University Press. Reprinted with the permission of Cambridge University Press from Burelbach, Bankoff, and Davis (1988).

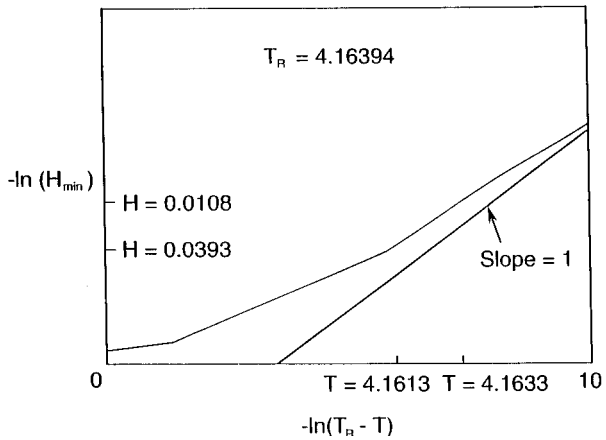

FIG. 13. Local behavior near rupture point for the solution shown in Fig. 12. Copyright © 1988 Cambridge University Press. Reprinted with the permission of Cambridge University Press from Burelbach, Bankoff, and Davis (1988).

instability would then occur by this estimate, if $2\pi h_0/L > k_c'$. One sees from this theory that it is inappropriate to seek a critical thickness from the theory but only a critical thickness for a given experiment, since the condition depends on the system size L.

The evolution of the film interface as described by Eq. (2.41) with periodic boundary conditions and an initial corrugation leads to the rupture of the film in a finite time T_R. This breakup manifests itself by the fact that at a certain time the local thickness of the film becomes zero. Figure 12, reproduced from Fig. 4 in Burelbach *et al.* (1988), displays a typical example of film evolution. Moreover, the rate of film thinning, measured as the rate of decrease of the minimal thickness of the film, increases with time and becomes much larger than the disturbance growth rate given by the linear theory extrapolated ti break up. This fact can be seen in Eq. (2.41). Notice that the "effective" diffusion coefficient, proportional to h^{-1}, in the backward diffusion term increases indefinitely as the film becomes thinner, $h \to 0$, while the local stabilization effect provided by surface tension weakens, proportionally to h^3.

Sheludko (1967) observed experimentally spontaneous breakup of thin, static films and proposed that negative disjoining pressure is responsible for that. He also used a stability analysis in order to calculate a critical thickness of the film below which breakup occurs, while neglecting the presence of electric double layers.

Burelbach *et al.* (1988) used numerical analysis to show that, near the rupture point, surface tension has a minor effect. Therefore the *local* behavior of the interface is governed by the backward diffusion equation

$$\partial_T H + A\,\partial_X\left(\frac{\partial_X H}{H}\right)=0. \tag{2.44}$$

Looking for separable solutions of the form $H(X,T)=\mathcal{T}(T)\mathcal{X}(X)$, Burelbach *et al.* (1988) found that $\mathcal{T}(T)\sim(T_R-T)$. The spatial component $\mathcal{X}(X)$ can be found by solving the ordinary differential equation

$$\frac{d^2y}{dX^2}=\exp(y), \quad \text{with } \mathcal{X}(X)=\exp(y). \tag{2.45}$$

Solving Eq. (2.45) in terms of $\mathcal{X}(X)$ yields

$$\mathcal{X}(X)\sim\frac{b^2}{2}\sec^2\left(\frac{bX}{2}\right),$$

where b is an arbitrary constant whose value can be determined from the numerical solution of Eq. (2.41b). The separable solution for Eq. (2.44) can be thus written in the form

$$H(X,T)=A\,\frac{b^2}{2}(T_R-T)\sec^2\left(\frac{bX}{2}\right). \tag{2.46}$$

The minimal thickness of the film close to the rupture point is therefore expected to decrease linearly with time. This allows the lubrication analysis to be extrapolated very close to the point where adsorbed layers and/or moving contact lines appear. The behavior of solution (2.46), as $T \to T_R$, is shown in Fig. 13, reproduced from Fig. 5 in Burelbach *et al.* (1988).

Several authors (Kheshgi and Scriven, 1991; Mitlin, 1993; Sharma and Jameel, 1993; Jameel and Sharma, 1994; Mitlin and Petviashvili, 1994; Oron and Bankoff, 1997) have considered the dynamics of thin liquid films in the process of dewetting of a solid surface. The effects important for a meaningful description of the process are gravity, capillarity, and, if necessary, the use of a generalized disjoining pressure, which contains a sum of intermolecular attractive and repulsive potentials. The generalized disjoining pressure is destabilizing (attractive) for the film for larger thicknesses and stabilizing (repulsive) for larger (smaller) thicknesses still within the range of several hundreds of Angströms (see, for example, Israelachvili, 1992). Equations (2.28) and (2.29) may be rewritten, respectively, in the form

$$\partial_T H - \frac{1}{3}\partial_X[H^3\partial_X(GH - \overline{C}^{-1}\partial_X^2 H + \Phi)] = 0, \quad (2.47a)$$

$$\mu\partial_t h - \frac{1}{3}\partial_x[h^3\partial_x(\rho g h - \sigma\partial_x^2 h + \phi)] = 0. \quad (2.47b)$$

Different forms for the potential ϕ are encountered in the literature. Teletzke *et al.* (1988) expressed the generalized disjoining pressure as

$$\phi = \sum_{i=1}^{4} a_i h^{-i}, \quad (2.48a)$$

where a_i are coefficients determined by specific intermolecular forces brought into consideration. In particular, the disjoining pressure corresponding to the van der Waals forces used by Williams and Davis (1982),

$$\phi = a_3 h^{-3}, \quad (2.48b)$$

is obtained from Eq. (2.48a) for $a_3 \neq 0, a_i = 0, i \neq 3$. Mitlin (1993) and Mitlin and Petviashvili (1994) used the 6−12 Lennard-Jones potential for solid-liquid interactions

$$\phi = a_3 h^{-3} - a_9 h^{-9}. \quad (2.48c)$$

Polar and apolar (van der Waals) intermolecular interactions give rise to the generalized disjoining pressure expressed by

$$\phi = a_3 h^{-3} - l_1 \exp\left(-\frac{h}{l_2}\right), \quad (2.48d)$$

where l_1 and l_2 are dimensional constants (Williams, 1981; Sharma and Jameel, 1993; Jameel and Sharma, 1994; Paulsen *et al.*, 1996) representing the strength of the repulsive and attractive forces, respectively, and decay lengths. Oron and Bankoff (1997) used

$$\phi = a_3 h^{-3} - a_4 h^{-4} \quad (2.48e)$$

to model the simultaneous action of the attractive ($a_3 > 0$) long-range and repulsive ($a_4 > 0$) short-range intermolecular forces and their influence on the dynamics of the film.

Linearizing Eq. (2.47b) around $h = h_0$, one obtains

$$\mu s = -\frac{1}{3}k'^2 h_0\left[\rho g + \left.\frac{d\phi}{dh}\right|_{h=h_0} + \frac{\sigma k'^2}{h_0^2}\right]. \quad (2.49)$$

It follows from Eq. (2.49) that the necessary condition for linear instability is

$$\left.\frac{d\phi}{dh}\right|_{h=h_0} < -\rho g, \quad (2.50)$$

i.e., the destabilizing effect of the van der Waals force has to be stronger than the leveling effect of gravity.

Kheshgi and Scriven (1991) studied the evolution of the film using Eq. (2.47a) with the potential (2.48b) and found that smaller disturbances decay due to the presence of gravity leveling while larger ones grow and lead to film rupture. Mitlin (1993) and Mitlin and Petviashvili (1994) discussed possible stationary states for the late stage of solid-surface dewetting with the potential (2.48c) and drew a formal analogy between the latter and the Cahn theory of spinodal decomposition (Cahn, 1960). Sharma and Jameel (1993) and Jameel and Sharma (1994) followed the film evolution as described by Eqs. (2.47) and (2.48d) and concluded that thicker films break up, while thinner ones undergo "morphological phase separation" that manifests itself in creation of steady structures of drops separated by ultrathin flat liquid films. Similar patterns were also observed by Oron and Bankoff (1997) in their study of the dynamics of thin spots near film breakup. Figure 14 (Oron and Bankoff, 1997) shows typical steady-state solutions of Eq. (2.47a) with the potential (2.48e) for different sets of parameters.

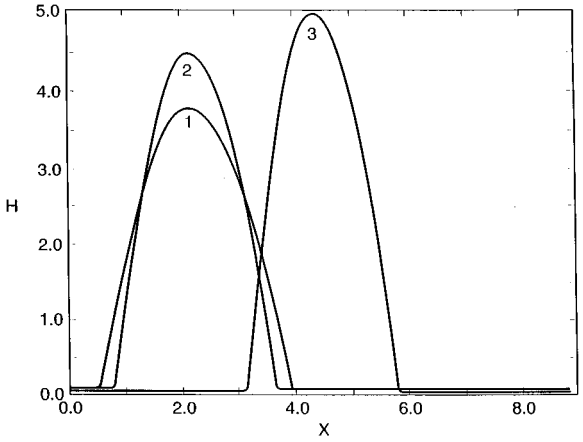

FIG. 14. Steady-state solutions for a film under the simultaneous action of attractive and repulsive intermolecular forces, as described by Eq. (2.47a) with $G = 0$ and $\Phi_0 = H^{-3} - \overline{a}_4 H^{-4}$ [the dimensionless version of Eq. (2.48e)]. Curve 1, $\overline{a}_4 = 0.1, \overline{C}^{-1} = 1$; Curve 2, $\overline{a}_4 = 0.1, \overline{C}^{-1} = 0.05$; Curve 3, $\overline{a}_4 = 0.05, \overline{C}^{-1} = 1$.

F. Thermocapillarity, surface tension, and body force only

The thermocapillary effect (see, for example, Davis, 1987) accounts for the emergence of interfacial shear stresses, owing to the variation of surface tension with temperature ϑ. This shear stress is expressed by $\vec{\nabla}_s\sigma$. In this case $\beta = \Pi = \tau = 0$, $\sigma = \sigma(\vartheta)$. In order to incorporate the thermocapillary effect into the equations, one needs to add to the governing system (2.10)–(2.12) an energy equation and the appropriate boundary conditions related to heat transfer. The energy equation and the boundary conditions have the form

$$\rho c(\partial_t\vartheta + u\partial_x\vartheta + w\partial_z\vartheta) = k_{\text{th}}\nabla^2\vartheta, \quad (2.51)$$

where for $z = 0$

$$\vartheta = \vartheta_0, \quad (2.52a)$$

and for $z = h(x,t)$

$$k_{\text{th}}\vec{\nabla}\vartheta\cdot\vec{\mathbf{n}} + \alpha_{\text{th}}(\vartheta - \vartheta_\infty) = 0. \quad (2.52b)$$

Here c is the specific heat of the fluid, $k_{\rm th}$ is its thermal conductivity, and ϑ_0 is the temperature of the rigid plane, assumed to be uniform. The boundary condition (2.52b) is Newton's cooling law and $\alpha_{\rm th}$ is the heat transfer coefficient describing the rate of heat transfer from the liquid to the ambient gas phase at the constant temperature ϑ_∞.

Scaling the temperature by

$$\Theta=\frac{\vartheta-\vartheta_\infty}{\vartheta_0-\vartheta_\infty} \tag{2.53}$$

and substituting scales (2.14) into Eqs. (2.51) and (2.52) yields

$$\epsilon ReP_r(\partial_T\Theta+U\partial_X\Theta+W\partial_Z\Theta)=\epsilon^2\partial_X^2\Theta+\partial_Z^2\Theta, \tag{2.54}$$

where for $Z=0$:

$$\Theta=1, \tag{2.55a}$$

and $Z=H$:

$$\partial_Z\Theta-\epsilon^2(\partial_X\Theta)(\partial_X H)+B\Theta(1+\epsilon^2(\partial_X H)^2)^{1/2}=0. \tag{2.55b}$$

Here P_r and B are, respectively, the Prandtl and Biot numbers

$$P_r=\frac{\rho c\nu}{k_{\rm th}},\quad B=\frac{\alpha_{\rm th}h_0}{k_{\rm th}}. \tag{2.56}$$

Let us expand the temperature Θ in a perturbation series in ϵ, along with the expansions (2.21a), and substitute these into system (2.54) and (2.55). Again assume that $Re=O(1)$ and further let $P_r,B=O(1)$, so that the convective terms in Eq. (2.54) are delayed to next order, i.e., conduction in the liquid is dominant and the heat flux there balances the heat lost to the environment.

At leading order in ϵ the governing system for Θ_0 consists of condition (2.55a),

$$\partial_Z^2\Theta=0, \tag{2.57}$$

and

$$\partial_Z\Theta+B\Theta=0\quad\text{for } Z=H, \tag{2.58}$$

where the subscript "zero" has been dropped. The solution to this system is

$$\Theta=1-\frac{BZ}{1+BH}\quad\text{and}\quad\Theta_i=\frac{1}{1+BH}, \tag{2.59}$$

where $\Theta_i=\Theta(X,H,T)$ is the surface temperature.

From Eq. (2.27) or (2.29), it is now required that the thermocapillary stress $\partial_X\Sigma$ or $\partial_x\sigma$ be determined. By the chain rule

$$\partial_X\Sigma=M\frac{d\Sigma}{d\Theta}[\partial_X\Theta+(\partial_X H)(\partial_Z\Theta)]$$

$$\equiv -M\frac{\gamma(H)\partial_X H}{(1+BH)^2}, \tag{2.60a}$$

where

$$\gamma(H)=-\left.\frac{d\Sigma}{d\Theta}\right|_{\Theta=\Theta_i}. \tag{2.60b}$$

The sign change is inserted because $d\sigma/d\vartheta$ is negative for common materials. The shear-stress condition, Eq. (2.24a), to leading order in ϵ has the form

$$\partial_Z U+M\frac{\gamma(H)\partial_X H}{(1+BH)^2}=0\quad\text{for } Z=H, \tag{2.61}$$

where

$$M=\left(\frac{\Delta\sigma}{\mu U_0}\right)\epsilon$$

is the Marangoni number. Here $\Delta\sigma$ is the change of surface tension over the temperature domain between the characteristic temperatures, usually ϑ_0 and ϑ_∞. To be more precise, if $\vartheta_\infty<\vartheta_0$ (heating at the bottom of the layer), then $\Delta\sigma>0$ for standard fluid pairs with surface tension decreasing with temperature. For heating at the interface side $\vartheta_\infty>\vartheta_0$ and $\Delta\sigma<0$.

Thus, in the case $\tau_0=\Phi=\Pi_0=\beta_0=0$, Eq. (2.27) becomes

$$\partial_T H+\frac{1}{2}MB\partial_X\left[\frac{H^2\gamma(H)\partial_X H}{(1+BH)^2}\right]+\frac{1}{3}\overline{C^{-1}}\partial_X[H^3\partial_X^3 H]=0. \tag{2.62}$$

If gravity forces are to be included, $\Phi=gZ$ and Eq. (2.62) reads

$$\partial_T H+\partial_x\left\{\left[-\frac{1}{3}GH^3+\frac{1}{2}MB\frac{H^2\gamma(H)}{(1+BH)^2}\right]\partial_X H\right\}+\frac{1}{3}\overline{C^{-1}}\partial_X[H^3\partial_X^3 H]=0. \tag{2.63}$$

For the standard, linearly decreasing function $\sigma=\sigma(\vartheta)$, the value $\partial_\Theta\Sigma$ is constant and $\gamma(H)=1$. Equations (2.62)–(2.63) with $\gamma(H)=1$ appeared in papers of Davis (1983) for $B\ll 1$, Kopbosynov and Pukhnachev (1986), Bankoff and Davis (1987), Burelbach *et al.* (1988), Deissler and Oron (1992), and Oron and Rosenau (1992).

For $B\ll 1$, Eq. (2.63) in dimensional form becomes

$$\mu\partial_t h+\frac{\alpha_{\rm th}\Delta\sigma}{2k_{\rm th}}\partial_x(h^2\partial_x h)-\frac{1}{3}\rho g\partial_x(h^3\partial_x h)+\frac{\sigma}{3}\partial_x(h^3\partial_x^3 h)=0. \tag{2.64}$$

Linearization of Eq. (2.64) around the state $h=h_0$ yields the characteristic equation

$$\mu s=\left(-\frac{1}{3}\rho g h_0+\frac{\alpha_{\rm th}\Delta\sigma}{k_{\rm th}}-\frac{\sigma}{3h_0}k'^2\right)k'^2. \tag{2.65}$$

Equation (2.65) shows that if $g>0$ (gravity acting towards the base of the film) gravity has a stabilizing effect (similar to that described in Sec. II.D), while thermocapillarity has a destabilizing effect on the interface. It is clear from Eq. (2.65) that the thicker the film, the stronger the gravitational stabilization. The dimensionless cutoff wave number k_c' is given in this case by

$$k_c' = \left(3B \frac{\Delta\sigma}{\sigma} - Bo \right)^{1/2}. \tag{2.66a}$$

Thermocapillary destabilization is explained by examining the fate of an initially corrugated interface in the linear temperature field produced by thermal condition. Where the interface is depressed, it lies in a region of higher temperature than its neighbors. Hence, if surface tension is a decreasing function of temperature, interfacial stresses [proportional to the surface gradient of the surface tension (see, for example, Levich, 1962; Landau and Lifshits, 1987)] drive interfacial liquid away from the depression. Since the liquid is viscous, it is dragged away from the depression, causing the depression to deepen further. Hydrostatic and capillary forces cannot prevent this deepening, and as shall be seen, the film will proceed to zero thickness locally.

Studies of Eq. (2.62) with $\gamma(H)=1$ reveal that evolution of initial data of small amplitude usually results in rupture of the film qualitatively similar to that displayed in Fig. 11 (Oron and Rosenau, 1992). In the case of negative gravity, $g<0$, the Rayleigh-Taylor instability (heavy fluid overlying light fluid) enhances the thermocapillary instability and broadens the band of linearly unstable modes:

$$k_c' = \left(3B \frac{\Delta\sigma}{\sigma} + Bo \right)^{1/2}. \tag{2.66b}$$

Stabilization of the Rayleigh-Taylor instability by thermocapillarity was discussed by Oron and Rosenau (1992) and Deissler and Oron (1992) for two- and three-dimensional cases, respectively. It was found that negative thermocapillarity, i.e., $\Delta\sigma<0$, corresponding to heating at the interface side or cooling at the rigid wall, in conjunction with surface tension may lead to saturation of Rayleigh-Taylor instability and to formation of steady drops.

It has been recently discovered that dilute aqueous solutions of long-chain alcohols exhibit nonmonotonic dependence of surface tension on temperature (Legros *et al.*, 1984; Legros, 1986). This dependence can be approximated quite well by the quadratic polynomial

$$\sigma(\vartheta) = \delta(\vartheta - \vartheta_m)^2, \tag{2.67a}$$

where δ is constant and ϑ_m is the temperature corresponding to the minimal surface tension. In this case,

$$\gamma(H) \sim \frac{\vartheta_m - \vartheta_\infty}{\vartheta_0 - \vartheta_\infty} - \frac{1}{1+BH}. \tag{2.67b}$$

The instability arising from the variation of surface tension, given by Eq. (2.67a), has been called "quadratic Marangoni (QM) instability" and studied by Oron and Rosenau (1994). In contrast with the case of the standard thermocapillary instability, described by Eq. (2.62) with $\gamma(H)=1$, the evolution of QM instability may result in a nonruptured steady state. Figure 15, taken from Fig. 4 in Oron and Rosenau (1994), displays such a state along with the streamlines of the flow field. It results from solving Eq. (2.62) with $\gamma(H)$ given by Eq. (2.67b). The intersections of the Θ_0 line with the film interface in Fig. 15 correspond to the locations of the minimal surface tension. This creates surface shear stress acting in opposite directions, as shown by the arrows on the graph, and leads to film stabilization.

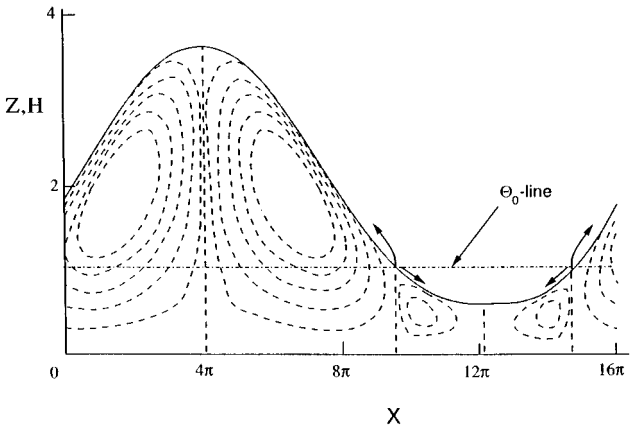

FIG. 15. The steady state obtained from the evolution of a film subject to quadratic Marangoni instability. Dashed lines represent streamlines of the flow field. The periodic domain consists of four convective cells contained between the extremal points of the interface and the points of minimal surface tension. The arrows indicate the direction of the flow at the stagnation points. Copyright © 1994 Cambridge University Press. Reprinted with the permission of Cambridge University Press from Oron and Rosenau (1994).

G. Temperature-dependent physical properties

The temperature variation across a thin film is usually small enough that without appreciable error an average temperature can be used in evaluating the physical properties. However, for liquids of high viscosity, the error may be significant, since viscosities can vary with an Arrhenius-type exponential temperature dependence. Reisfeld and Bankoff (1990) considered this problem with a linear dependence of viscosity on the temperature. Here we generalize the problem for the viscosity as an arbitrary function of the dimensionless temperature.

Let $\mu=\mu_0 f(\Theta)$, where $f(\Theta)$ is a smooth dimensionless function, $0\leqslant\Theta\leqslant1$, $\partial_\Theta f<0, f>0$, and

$$\Theta = \frac{\theta - \theta_i}{\theta_0 - \theta_i} = \Theta(Z), \quad 0\leqslant\Theta\leqslant1. \tag{2.68}$$

Here, the subscript i denotes the interfacial value of the corresponding variable. Let us consider the limiting case of large Biot numbers B. Since $\Theta(0)=1$ and $\Theta(H)=0$, it follows from Eq. (2.57) that

$$\Theta = 1 - \frac{Z}{H}. \tag{2.69}$$

Define $g(Z)=f(\Theta)$. Equation (2.22a) is now modified, using forms (2.25), to read

$$\mu_0 \partial_Z [g(Z)\partial_Z U] = \partial_X \overline{P} \equiv \partial_X (\Phi|_{Z=H} - \overline{C}^{-1} \partial_X^2 H - \Pi_0), \tag{2.70}$$

where $\mu_0=1$ in dimensionless form.

Integrating once from Z to H yields

$$-g(Z)\partial_Z U=\partial_X\overline{P}\,(H-Z)-g(H)[\tau_0+\partial_X\Sigma]. \quad (2.71)$$

Integrating again yields,

$$U=\partial_X\overline{P}\int_0^Z\frac{s-H}{g(s)}ds+g(H)(\tau_0+\partial_X\Sigma)\int_0^Z\frac{ds}{g(s)}. \quad (2.72)$$

From the continuity Eq. (2.20)

$$\partial_T H=-\partial_X[\partial_X\overline{P}\,I_1+(\tau_0+\partial_X\Sigma)g(H)I_2], \quad (2.73)$$

where

$$I_1=\int_0^H\int_0^Z\frac{H-s}{g(s)}dsdZ, \quad (2.74a)$$

$$I_2=\int_0^H\int_0^Z\frac{ds}{g(s)}dZ. \quad (2.74b)$$

These can be simplified by reversing the order of integration

$$I_1=\int_0^H\int_s^H\frac{H-s}{g(s)}dZds=\int_0^H\frac{(H-s)^2}{g(s)}ds, \quad (2.75a)$$

and similarly

$$I_2=\int_0^H\frac{H-s}{g(s)}ds. \quad (2.75b)$$

Equations (2.73), (2.75a), and (2.75b) constitute the generalized evolution equations for arbitrary viscosity-temperature dependence.

For a linear approximation (Reisfeld and Bankoff, 1990)

$$g(Z)=1-\alpha\Theta=1-\alpha\left(1-\frac{Z}{H}\right). \quad (2.76)$$

If only long-range molecular forces and constant surface tension terms are retained, Eq. (2.27) becomes

$$\partial_T H+VA\,\partial_X\left(\frac{\partial_X H}{H}\right)+\frac{1}{3}V\overline{C}^{-1}\partial_X(H^3\partial_X^3 H)=0, \quad (2.77)$$

where

$$V=-\frac{3}{2}\alpha^{-3}[\alpha^2+2\alpha+2\ln(1-\alpha)] \quad \text{for } B\gg 1 \quad (2.78a)$$

and

$$V=1 \quad \text{for } B\ll 1. \quad (2.78b)$$

Equation (2.77) is identical in form to the isothermal equation (2.41) and actually reduces to it by rescaling time, $T\to VT$. Hence linear and nonlinear stability results obtained by Williams and Davis (1982) can be applied directly to this case. Figure 16 shows the graph of function $V(\alpha)$ as given by Eq. (2.78a). The acceleration factor V increases with an increase in the temperature dependence of the viscosity. Thus the effect of variable viscosity is to reduce the time scale for the process, leading to a more rapid rupture of the film. However, for vanishing Biot numbers B the film is effectively isothermal and the resulting Eq. (2.77) reduces to Eq. (2.41), with $V=1$. For larger ranges of temperature variation, an exponential function of the form

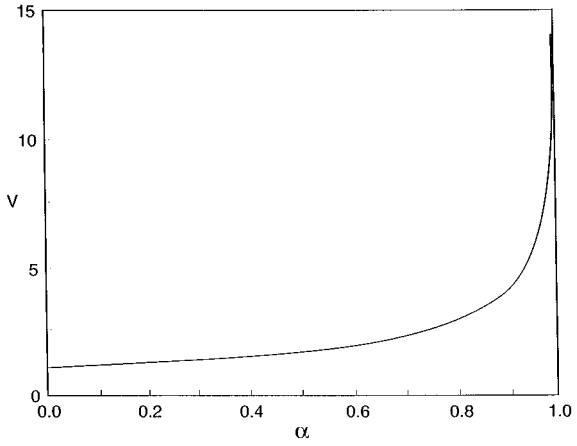

FIG. 16. The function $V(\alpha)$ as given by Eq. (2.78a).

$$g(Z)=f(\Theta)=\exp(-\alpha\Theta), \quad (2.78c)$$

along with Eqs. (2.69) and (2.75), allows the evolution Eq. (2.73) to be explicitly evaluated. Reisfeld and Bankoff (1990) showed that for mineral oil with a temperature difference of 10 K, a 20% decrease in the rupture time is obtained with respect to the constant-viscosity model with a temperature-averaged viscosity.

H. Evaporating/condensing films

1. Formulation

We now consider the two opposing cases of (a) an evaporating thin film of a pure, single-component liquid on a heated plane surface at constant temperature ϑ_0 that is higher than the saturation temperature at the given vapor pressure and (b) a condensing thin film of a pure, single-component liquid on a cooled plane surface at constant temperature θ_0 that is lower than the saturation temperature at a given vapor pressure. The speed of vapor particles is assumed to be sufficiently low that the vapor can be considered to be an incompressible fluid.

Let us first formulate boundary conditions appropriate for phase transformation at the film interface $z=h$. The mass balance at the interface is given by

$$j=\rho_g(\vec{\mathbf{v}}_g-\vec{\mathbf{v}}_i)\cdot\vec{\mathbf{n}}=\rho_f(\vec{\mathbf{v}}_f-\vec{\mathbf{v}}_i)\cdot\vec{\mathbf{n}}, \quad (2.79)$$

where j is the mass flux normal to the interface, which is positive for evaporation and negative for condensation. ρ_g and ρ_f are, respectively, the densities of the vapor and the liquid, $\vec{\mathbf{v}}_g$ and $\vec{\mathbf{v}}_f$ are, respectively, the vapor and liquid velocities at $z=h$, and $\vec{\mathbf{v}}_i$ is the velocity of the interface.

Since $\rho_g/\rho_f\ll 1$, typically $\sim 10^{-3}$, Eq. (2.79) shows that, relative to the interface, the magnitude of the normal velocity of the vapor at the interface is much greater than that of the corresponding liquid. Hence the phase transformation creates large accelerations of the vapor at the interface, where the back reaction, called the va-

por thrust (or vapor recoil) represents a force on the interface. The dynamic pressure at the gas side of the interface is much larger than that at the liquid side,

$$\rho_g v_{g,e}^2 = \frac{j^2}{\rho_g} \gg \rho_f v_{f,e}^2 = \frac{j^2}{\rho_f}, \tag{2.80}$$

where $v_{g,e}$ and $v_{f,e}$ are the normal components of vapor and liquid velocity relative to the interface. Consider a corrugated interface during evaporation/condensation. Points on the trough are closer to the hot/cold plate than are points on the crest, and so they have greater evaporation/condensation rates j. Momentum fluxes are thus greater at the troughs than at the crests of surface waves. As seen from Eq. (2.80), vapor thrust is destabilizing for either evaporation ($j>0$) or condensation ($j<0$) (Burelbach *et al.*, 1988). Vapor thrust is only important for cases of very high heat fluxes.

As noted above, vapor thrust exerts a reactive downward pressure on a horizontal evaporating film. Bankoff (1961) introduced the vapor thrust effect in analyzing the Rayleigh-Taylor instability of an evaporating liquid-vapor interface above a hot horizontal wall (film boiling). In this case the vapor thrust stabilizes the film boiling, since the reactive force is greater for the wave crests approaching the wall than for the troughs. Later, Bankoff (1971) extended the linear stability analysis of Yih (1955, 1963) and Benjamin (1957) to the instability of an evaporating thin liquid film on a hot, inclined wall. A critical heat flux was found above which the vapor thrust dominates the inertial effects.

The energy balance at $z=h$ is given by

$$j\left(L+\frac{1}{2}v_{g,e}^2-\frac{1}{2}v_{f,e}^2\right)+k_{\rm th}\vec{\nabla}\vartheta\cdot\vec{\mathbf{n}}-k_{{\rm th},g}\vec{\nabla}\vartheta_g\cdot\vec{\mathbf{n}} +2\mu\boldsymbol{\epsilon}_f\cdot\vec{\mathbf{n}}\cdot\vec{\mathbf{v}}_{f,e}-2\mu_g\boldsymbol{\epsilon}_g\cdot\vec{\mathbf{n}}\cdot\vec{\mathbf{v}}_{g,e}=0, \tag{2.81a}$$

where L is the latent heat of vaporization per unit mass, $k_{{\rm th},g}$, μ_g, and ϑ_g are, respectively, the thermal conductivity, viscosity, and temperature of the vapor, and $\boldsymbol{\epsilon}_f,\boldsymbol{\epsilon}_g$ are the rate-of-deformation tensors in the liquid and the vapor (Burelbach *et al.*, 1988).

The stress balance boundary condition that generalizes Eq. (2.12b) in the case of phase transformation is given by

$$j(\vec{\mathbf{v}}_{f,e}-\vec{\mathbf{v}}_{g,e})-(\mathbf{T}-\mathbf{T}_g)\cdot\vec{\mathbf{n}}=\kappa\sigma(\vartheta)\vec{\mathbf{n}}-\vec{\nabla}_s\sigma, \tag{2.81b}$$

where $\vec{\nabla}_s\sigma$ is the surface gradient of interfacial tension and $\mathbf{T}_g$ is the stress tensor in the vapor phase.

One needs to pose a constitutive equation relating the dependence of the interfacial temperature ϑ_i and the interfacial mass flux (Palmer, 1976; Plesset and Prosperetti, 1976; Sadhal and Plesset, 1979). Its linearized form is

$$\tilde{K}\, j=\vartheta_i-\vartheta_s\equiv\Delta\vartheta_i, \tag{2.82}$$

where

$$\tilde{K}=\frac{\vartheta_s^{3/2}}{\hat{\alpha}\rho_g L}\left(\frac{2\pi R_g}{M_w}\right)^{1/2},$$

ϑ_s is the absolute saturation temperature, $\hat{\alpha}$ is the accommodation coefficient, R_g is the universal gas constant, and M_w is the molecular weight of the vapor (Palmer, 1976; Plesset and Prosperetti, 1976). Note that the absolute saturation temperature ϑ_s serves now as the reference temperature ϑ_∞ in the nondimensionalization, Eq. (2.53). When $\Delta\vartheta_i=0$, the phases are in thermal equilibrium with each other, i.e., their chemical potentials are equal. In order for net mass transport to take place, a vapor pressure driving force must exist, given for ideal gases by kinetic theory (Schrage, 1953), and represented in the linear approximation by the parameter $\tilde{K}$ (Burelbach *et al.*, 1988). Departure of the parameter $\tilde{K}$ from ideal behavior is addressed by an accommodation coefficient depending on interface/molecule orientation and steric effects, which represents the probability of a vapor molecule's sticking upon hitting the liquid-vapor interface.

The balances discussed give rise to a "one-sided" model for evaporation or condensation (Burelbach *et al.*, 1988) in which the dynamics of the vapor are ignored, except that mass is conserved and one retains the effects of vapor thrust and the kinetic energy it produces. It is assumed that the density, viscosity, and thermal conductivity of the liquid are much greater than those in the vapor. Therefore the boundary conditions (2.81) are significantly simplified.

The energy balance relation (2.81a) becomes

$$-k_{\rm th}\partial_z\vartheta=jL, \tag{2.83}$$

meaning that all the heat conducted to the interface in the liquid is converted to latent heat of evaporation.

Next, the normal and tangential stress conditions at the free surface, given by Eq. (2.81b), are reduced to

$$-\frac{j^2}{\rho_g}-\mathbf{T}\cdot\vec{\mathbf{n}}\cdot\vec{\mathbf{n}}=\kappa\sigma(\vartheta), \tag{2.84a}$$

$$\mathbf{T}\cdot\vec{\mathbf{n}}\cdot\vec{\mathbf{t}}=\vec{\nabla}\sigma\cdot\vec{\mathbf{t}}. \tag{2.84b}$$

Finally, the remaining boundary conditions (2.79) and (2.82) are unchanged.

We now consider the nondimensional formulation for the two-dimensional case. The dimensionless mass balance Eq. (2.20) is modified by the presence of the nondimensional evaporative mass flux J,

$$EJ=(-\partial_T H-U\partial_X H+W)[1+(\partial_X H)^2]^{-1/2}, \tag{2.85a}$$

or at leading order of approximation

$$\partial_T H+\partial_X Q+EJ=0, \tag{2.85b}$$

where

$$Q(X,T)=\int_0^H U\,dZ \tag{2.85c}$$

is the scaled volumetric flow rate per unit width parallel to the wall, $J=(h_0 L/k_{\rm th}\Delta\vartheta)j$, $\Delta\vartheta\equiv\vartheta_0-\vartheta_s$, and $\rho=\rho_f$. The parameter E is an evaporation number

$$E=\frac{k_{\rm th}\Delta\vartheta}{\rho\nu L}, \tag{2.85d}$$

which represents the ratio of the viscous time scale $t_v=h_0^2/\nu$ to the evaporative time scale, $t_e=(\rho h_0^2 L/k_{\rm th}\Delta\vartheta)$ (Burelbach *et al.*, 1988). The latter is a measure of the time required for an initially stationary film to evaporate to dryness on a horizontal wall. For low evaporation rates E is small. The dimensionless versions of Eqs. (2.82) and (2.83) are

$$KJ=\Theta \quad \text{at } Z=H, \tag{2.86a}$$

$$\partial_Z\Theta=-J \quad \text{at } Z=H, \tag{2.86b}$$

where

$$K=\tilde{K}\frac{k_{\rm th}}{h_0 L}. \tag{2.86c}$$

Equations (2.25), (2.26), (2.57), (2.85c), (2.86a), and (2.86b) constitute the problem to be solved, whose solution is then substituted into Eq. (2.85b) to obtain the desired evolution equation. The general dimensionless evolution Eq. (2.27) will then contain an additional term EJ, stemming from the mass flux due to evaporation/condensation, which is expressed via the local film thickness H. This will be done below.

2. Mass loss/gain only

We first consider the case of an evaporating/condensing thin liquid layer lying on a rigid plane held at a constant temperature. Mass loss or gain is retained, while other effects are neglected.

Solving first Eq. (2.57) along with boundary conditions (2.55a) and (2.86) and eliminating the mass flux J from the latter yields the dimensionless temperature field and the evaporative mass flux through the interface

$$\Theta=1-\frac{Z}{H+K}, \quad J=\frac{1}{H+K}. \tag{2.87}$$

An initially flat interface will remain flat as evaporation proceeds and if surface tension, thermocapillary, and convective thermal effects are negligible, i.e., $M=\overline{C}^{-1}=\epsilon Re P_r=0$, it will give rise to a scaled evolution equation of the form

$$\partial_T H+\frac{\overline{E}}{H+K}=0, \tag{2.88}$$

where $\overline{E}=\epsilon^{-1}E$ and K, the scaled interfacial thermal resistance, is equivalent to the inverse Biot number B^{-1}. Physically, $K\neq 0$ represents a temperature jump from the liquid surface temperature to the uniform temperature of the saturated vapor, ϑ_s. The conductive resistance of the liquid film is proportional to H, and, assuming infinite thermal conductivity of the solid, the total thermal resistance is given by $(H+K)^{-1}$. For constant superheat temperature $\vartheta_0-\vartheta_s$, Eq. (2.88) represents a volumetric balance, whose solution, subject to $H(0)=1$, is

$$H=-K+[(K+1)^2-2\overline{E}\,T]^{1/2}. \tag{2.89a}$$

For $K\neq 0$ the film vanishes in finite time

$$T_e=\frac{2K+1}{2\overline{E}} \tag{2.89b}$$

and the rate of disappearance of the film at $T=T_e$ remains finite:

$$\left.\frac{dH}{dT}\right|_{T=T_e}=-\frac{\overline{E}}{K}. \tag{2.90}$$

The value of $\partial_T H$ remains finite because as the film thins the interface temperature ϑ_i, nominally at its saturation value ϑ_s, increases to the wall temperature. If $K=0$, $\vartheta_i=\vartheta_s$ and the temperature gradient $(\vartheta_0-\vartheta_s)/h\to\infty$, the thermal resistance vanishes and hence the mass flux will go to infinity as $h\to 0$. However, for large evaporation rates the interfacial temperature jump becomes significant, so that nonzero K is significant. Further, when the film gets very thin, a thermal disturbance develops in the solid substrate, reflecting the fact that the thermal conductivity of the solid is finite (see Sec. II.1). Hence the two thermal resistances, acting in series, prevent the evaporation rate from becoming infinite.

From Burelbach *et al.* (1988), the interfacial thermal resistance $K=10$ for a 10-nm-thick water film. Since K is inversely proportional to the initial film thickness, $K\sim 1$ for $h_0=100$ nm, so that $H/K\sim 1$ at this point. However, $H/K\approx 10^{-1}$ at $h_0=30$ nm, so the conduction resistance becomes small compared to the interfacial transport resistance shortly after van der Waals forces become appreciable.

Another contribution to the surface shear stress occurs when the vapor is flowing. Vapor molecules leaving the interface must be accelerated to the bulk vapor velocity v_g from the interfacial velocity component parallel to the wall. Similarly, the liquid molecules entering the interface have been accelerated from the bulk liquid velocity v_f to the interfacial tangential velocity. Thus the velocity profile in the base-state liquid film is given by

$$\mu u=\left[\tau_i-\frac{1}{2}j(v_g-v_f)\right]z+(-\partial_x p+\rho_f g)\left(h_0 z-\frac{1}{2}z^2\right).$$

The split in the evaporative shear stress between the bulk liquid and vapor is not readily determined and has been equally apportioned in the above equation (Wallis, 1969; Chung and Bankoff, 1980). The total interfacial shear stress is therefore continuous, but less than it would be in the absence of evaporation and greater than it would be in the absence of condensation. Here j is positive for evaporation and negative for condensation, and v_g and v_f are the tangential bulk velocity components. Often the convective shear stress, the first term on the right-hand side, is small, and we shall omit it in the subsequent discussion.

3. Mass loss/gain, vapor thrust, capillarity, and thermocapillarity

The dimensionless vapor thrust gives an additional normal stress at the interface, $\Pi_0=-\frac{3}{2}\overline{E}^{\,2}D^{-1}J^2$, where D is a unit-order scaled ratio between the vapor and liquid densities

$$D=\frac{3}{2}\epsilon^{-3}\frac{\rho_g}{\rho}$$

and can be calculated using Eq. (2.87). The resulting scaled evolution equation for a film evaporating on an isothermal horizontal surface is obtained by using the combination of Eqs. (2.27) and (2.88) with $\beta_0=\tau_0=0$, $\partial_X\Sigma=0$ (Burelbach *et al.*, 1988):

$$\partial_T H+\overline{E}\,(H+K)^{-1}+\partial_X\left[\overline{E}^{\,2}D^{-1}\left(\frac{H}{H+K}\right)^3\partial_X H+\frac{1}{3}\overline{C}^{\,-1}H^3\partial_X^3 H\right]=0. \tag{2.91}$$

Since usually $t_e\gg t_v$, $\overline{E}$ can itself be a small number and then can be used as an expansion parameter for slow evaporation compared to the nonevaporating base state (Burelbach *et al.*, 1988) appropriate to very thin evaporating films.

Taking into account van der Waals forces, Burelbach *et al.* (1988) gave the complete evolution equation for a heated or cooled thin film on a horizontal plane surface in the form

$$\partial_T H+\overline{E}\,(H+K)^{-1}+\frac{1}{3}\overline{C}^{\,-1}\partial_X(H^3\partial_X^3 H)+\partial_X\{[AH^{-1}+\overline{E}^{\,2}D^{-1}H^3(H+K)^{-3}+KMP_r{}^{-1}\times(H+K)^{-2}H^2]\partial_X H\}=0. \tag{2.92}$$

Here the first term represents the rate of volumetric accumulation, the second the mass loss, the third the stabilizing capillary term, and the fourth, fifth, and sixth the van der Waals, vapor thrust, and thermocapillary terms, respectively, all destabilizing. This is the first full statement of the possible competition among various stabilizing and destabilizing effects on a horizontal plate, with scaling to make them present at the same order. Joo *et al.* (1991) extended the work to an evaporating liquid film draining down a heated inclined plate or a condensing one on a cooled inclined plate. Figure 17 presents typical examples of the evolution of the film on the horizontal plane when all of the effects in Eq. (2.92) are taken into account. Figure 17(a) shows the case of an evaporating film, while Fig. 17(b) displays the case of condensation. The film evolution presented in Fig. 17(a) illustrates film rupture that occurs when all the liquid is driven out of the thin spot. In the case shown in Fig. 17(b) the stabilizing effects of mass gain (condensation) and thermocapillarity are considered. However, the destabilizing actions of the vapor thrust and the van der Waals forces are strong enough to lead to film rupture.

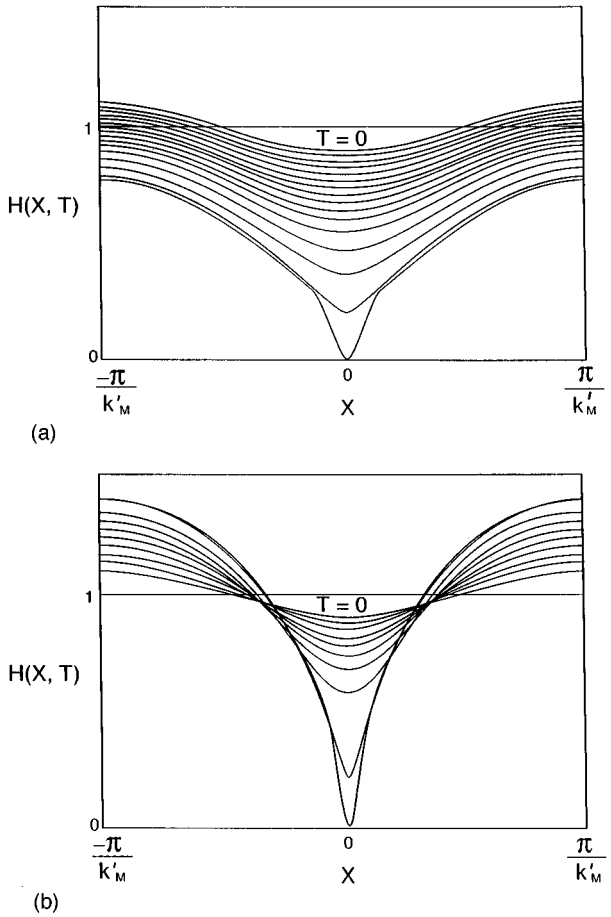

FIG. 17. Film profiles at different times: (a) quasiequilibrium evaporation, when vapor recoil and mass loss are both important, $A=1,\overline{C}^{\,-1}=1,K=0,\overline{E}=1,D=1$; (b) nonequilibrium condensation including mass gain, vapor recoil, and thermocapillarity, $\overline{E}=-0.1$, $\overline{E}^{\,2}D^{-1}=1$, $MP_r{}^{-1}=-1$, $A=1$, $\overline{C}^{\,-1}=1$, $K=0.1$. Copyright © 1988 Cambridge University Press. Reprinted with the permission of Cambridge University Press from Burelbach, Bankoff, and Davis (1988).

I. Liquid film on a thick substrate

The ideas described in the previous sections can be easily implemented in the case of a liquid film lying on top of a solid slab of thickness small compared to the characteristic wavelength of the interfacial disturbance (Oron *et al.*, 1996). A schematic of this configuration is shown in Fig. 18. In this case the thermal conduction equation in the solid has to be solved simultaneously with the energy equation in the liquid. This coupled thermal problem is written at leading order in ϵ as

$$\partial_Z^2\Theta_w=0,\quad -\frac{d_w}{h_0}\leqslant Z\leqslant 0, \tag{2.93a}$$

$$\partial_Z^2\Theta=0,\quad 0\leqslant Z\leqslant H, \tag{2.93b}$$

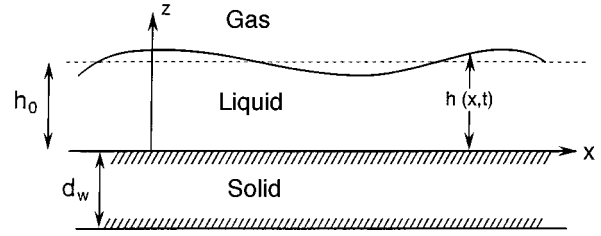

FIG. 18. Sketch of the liquid film on a thick substrate.

with the boundary conditions

$$\Theta_w=\Theta, \quad -k_{\mathrm{th},w}\partial_Z\Theta_w=-k_{\mathrm{th}}\partial_Z\Theta \quad \text{at } Z=0, \tag{2.94a}$$

$$\Theta_w=1 \quad \text{at } Z=-\frac{d_w}{h_0}, \tag{2.94b}$$

where Θ_w and d_w/h_0 are the dimensionless temperature and thickness, respectively, of the solid slab and $k_{\mathrm{th},w}$ is its thermal conductivity. Equation (2.94a) expresses the conditions of continuity of both the temperature and heat flux at the solid-liquid boundary, while Eq. (2.94b) prescribes a uniform temperature at the bottom of the solid substrate. Further boundary conditions have to be taken at the vapor-liquid interface. At leading order they can be either Eq. (2.58) in the nonvolatile case or the combination of Eqs. (2.86) in the case of a volatile liquid.

In the former case, the solution of Eqs. (2.93) and (2.94) results in

$$\Theta=1-\frac{B(\overline{\kappa}\,Z+d_w/h_0)}{\overline{\kappa}\,(1+BH)+Bd_w/h_0},$$

$$\Theta_w=1-\frac{B(Z+d_w/h_0)}{\overline{\kappa}\,(1+BH)+Bd_w/h_0}, \tag{2.95a}$$

with $\overline{\kappa}=k_{\mathrm{th},w}/k_{\mathrm{th}}$, which implies an interfacial temperature in the form

$$\Theta_i=\left[1+B\left(H+\frac{d_w/k_{\mathrm{th},w}}{h_0/k_{\mathrm{th}}}\right)\right]^{-1}. \tag{2.95b}$$

Comparing the expressions for the interfacial temperatures Θ_i as given by Eqs. (2.59) and (2.95b), one notices that, in addition to the thermal resistances due to conduction and convection at the interface in the former case, the latter contains a thermal resistance owing to conduction in the solid. The evolution equation, analogous to Eq. (2.62), will have the same form, except for the obvious change in the denominator of the second term.

In the case where evaporation is also considered, the scaled interfacial thermal resistance K appears in the results:

$$\Theta=1-\frac{\overline{\kappa}\,Z+d_w/h_0}{\overline{\kappa}\,(K+H)+d_w/h_0},$$

$$\Theta_w=1-\frac{Z+d_w/h_0}{\overline{\kappa}\,(K+H)+d_w/h_0},$$

$$\Theta_i=\frac{K}{K+H+\dfrac{d_w/k_{\mathrm{th},w}}{h_0/k_{\mathrm{th}}}}. \tag{2.96}$$

The resulting evolution equation then has the form of Eq. (2.91), where the denominators of the second and third terms contain an additional additive term $a\equiv(d_w/k_{\mathrm{th},w})/(h_0/k_{\mathrm{th}})$. This additional term represents the ratio between the thermal conductive resistances of the solid and the liquid. Figure 19 displays the interfaces

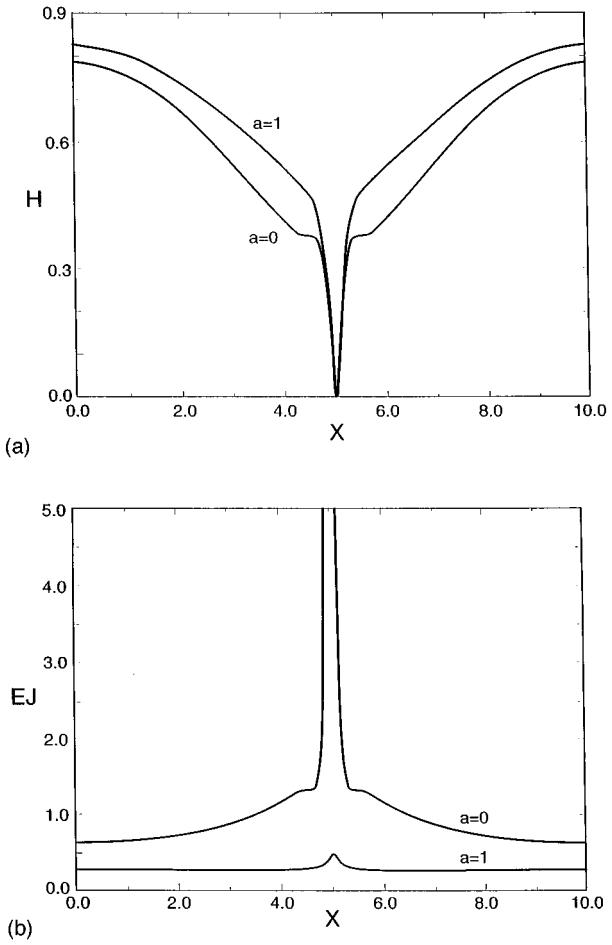

FIG. 19. Film profiles for rupture with evaporation. (a) The film interface at rupture for $a=0$ and $a=1$, as given by Eq. (2.91) with $A=1, K=0, \overline{E}=0.5, \overline{C}^{-1}=1$, (b) the evaporative mass flux $J=\overline{E}\,(H+a)^{-1}$ along the film interface, as calculated for the two cases shown in (a).

and the corresponding mass fluxes close to the moment of rupture for two values of the parameter a, $a=0$ and $a=1$. In the case of $a=0$, the flux $J\to\infty$ in the vicinity of the rupture point, indicating the emergence of a singularity. For $a\neq 0$, the flux J remains bounded everywhere.

Using Eqs. (2.96) one can derive the expressions for the temperatures along the gas-liquid (GL) and solid-liquid (SL) interfaces: $\Theta_{\mathrm{GL}}\equiv\Theta(H)$ and $\Theta_{\mathrm{SL}}\equiv\Theta_w(0)$. When the film ruptures, i.e., $H=0$, the values for Θ_{GL} and Θ_{SL} are equal, if K^{-1} is finite or if

$$a=\frac{d_w}{\overline{\kappa}\,h_0}\neq 0, \tag{2.97}$$

independent of the value of K. However, the temperature singularity $\Theta_{\mathrm{GL}}\neq\Theta_{\mathrm{SL}}$ emerges at the rupture point when both $K\to 0$ and $a=0$. Equation (2.97) is the sufficient condition to be satisfied in order to relieve this singularity (Oron *et al.*, 1996a). Indeed, if it is satisfied

$$\lim_{H\to 0}\{\lim_{K\to 0}\Theta_{\mathrm{GL}}\}=\lim_{H\to 0}\{\lim_{K\to 0}\Theta_{\mathrm{SL}}\}=0,$$

and the singularity is removed. The problematic case of $K\to 0$ arises if quasiequilibrium evaporation is present.

This case corresponds to the situation in which temperature at the free interface is effectively specified as the saturation temperature ϑ_s (Burelbach *et al.*, 1988). Such a situation leads to temperature singularities at rupture if condition (2.97) is not satisfied. In the evaporative case, an additional singularity of an infinite evaporative mass flux $\overline{E}\,\overline{J}=\overline{E}\,(H+a)^{-1}$ emerges at the rupture point if $a=0$.

J. Flows in a cylindrical geometry

In many technological applications, including coating of wires (e.g., creation of an insulator layer on a wire, protecting optical fibers, painting textile fibers, etc.), cooling of heated columns by falling liquid films, and others, one encounters a situation in which a thin liquid layer rests or flows on a cylindrical surface, which induces an extra component of curvature on the interface. This situation is similar to the one studied by Rayleigh (1894) in which thin liquid jets and liquid columns are subject to breakups driven by surface tension. Long-wave methods presented above can be applied in order to study the nonlinear evolution of these physical systems. Disintegration of liquid columns into drops was studied by Eggers (1993, 1995), Shi *et al.* (1994), and Eggers and Dupont (1994). In contrast to the case of liquid columns, the presence of a solid surface causes significant shear stress which can introduce some changes into the dynamics of the film, thus motivating the investigation of the cylindrical case. Long-wave methods discussed earlier can be applied here as well.

1. Capillary instability of a liquid thread

A problem of axisymmetric flow of two concentric fluids in a pipe was considered by Hammond (1983). If one neglects gravity and assumes that the outer film is much thinner and more viscous than the inner one,

$$\epsilon\equiv\frac{R-a}{R}\ll 1,\quad \epsilon\frac{\mu_i}{\mu_o}\ll 1, \tag{2.98}$$

then the two flows are decoupled. The equations can first be separately solved for the outer film, and an evolution equation can then be derived for the interface between the fluids:

$$r=R_0-h(x,t).$$

Here r and x are the radial and the axial directions of the cylindrical coordinates, R_0 is the radius of the pipe, $r=a$ is the undisturbed radius of the interface, and subscripts i and o denote the properties of the inner and outer layers, respectively.

Take the characteristic velocity as

$$U_0=\frac{\sigma}{\mu_o},$$

and scale the variables as follows:

$$x=R_0X,\quad r=R_0(1-\epsilon Z),\quad t=\epsilon^{-3}R_0U_0^{-1}T,$$
$$h=\epsilon R_0H,\quad u=\epsilon^3U_0U,\quad w=\epsilon^4U_0W, \tag{2.99}$$

$$p=\sigma R_0{}^{-1}(-1+\epsilon P), \tag{2.100}$$

where u, w, and p are, respectively, the axial and radial components of the flow field and the pressure in the outer layer. Upon introducing Eqs. (2.99) and (2.100) into the governing equations (2.10)–(2.12) written in cylindrical coordinates, with $\Phi=0$, and writing the dependent variables in perturbation series in ϵ, one obtains at leading order Eqs. (2.22). The boundary conditions, Eqs. (2.23) and (2.24) with $\beta_0=\tau_0=\Sigma=0$ and a modified Eq. (2.24b) with $\Pi_0=0$, give

$$P=-H-\partial_X^2H, \tag{2.101}$$

where $\overline{C}^{-1}=1$ due to the chosen scaling of the variables. The interfacial curvature in cylindrical coordinates is given by

$$\kappa=\frac{1}{R_0}\left(1-\frac{h}{R_0}-R_0\partial_x^2h\right)+\text{higher-order terms}. \tag{2.102}$$

Equation (2.102) shows that the curvature of the film interface is proportional to the sum of the curvature of the cylindrical substrate, the deflection of the interface in the radial direction, and its deformation in the axial direction. As a result, two terms appear in the expression for the capillary pressure in Eq. (2.101).

Solution of the Eqs. (2.22)–(2.24a) and (2.101) results in the evolution equation

$$\partial_TH+\frac{1}{3}\partial_X[H^3\partial_X(H+\partial_X^2H)]=0 \tag{2.103a}$$

or in dimensional form

$$\mu_o\partial_th+\frac{\sigma}{3R_0}\partial_x[h^3\partial_x(h+R_0^2\partial_x^2h)]=0. \tag{2.103b}$$

Comparison between Eqs. (2.37) and (2.103) reveals similarities, although they describe different physical effects. Owing to the thinness of the outer layer the axisymmetric dynamics is similar to that of a two-dimensional film, with one exception: the action of the additional term in the capillary pressure is analogous to that of the unstable density stratification in the gravity field leading to Rayleigh-Taylor instability. The capillary instability is generated by the curvature of the cylindrical interface. For the linear and nonlinear stability analyses the reader is referred to Sec. II.D and Hammond (1983). Figure 20 illustrates quasi-steady states obtained from the solution of Eq. (2.103a). It follows from Eq. (2.101) that the lobes with wave number larger than unity are at positive pressure, while those with wave number smaller than unity are at negative pressure. Therefore there is drainage from a narrow lobe to a wide one. If the gap between them does not thin too rapidly, the liquid will drain completely from the small lobe. However, if the thinning is fast, then at the final state both lobes will coexist (Hammond, 1983).

An evolution equation similar to Eq. (2.103), for a thin isothermal liquid film undergoing capillary instability on a surface of a cylinder, was derived by Yarin *et al.* (1993)

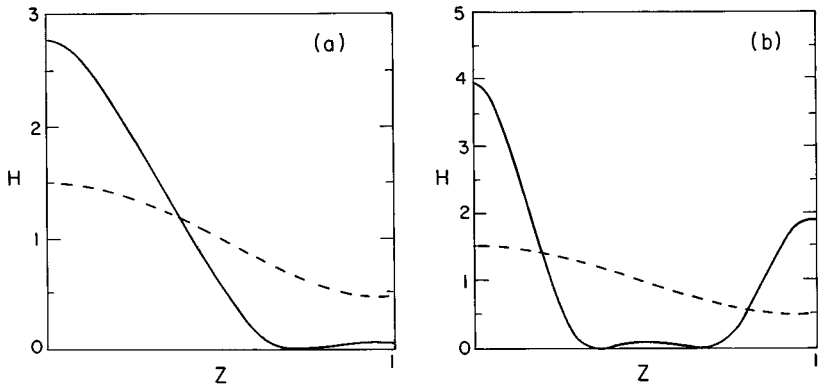

FIG. 20. Quasisteady long-time behavior of an annular film, Eq. (2.103a): (a) $\Delta=2^{3/2}\pi$; (b) $\Delta=6\pi$ and $Z=2X/\Delta$. Initial disturbances are represented by the dashed lines. The pressure within each of the lobes is almost constant; the small lobes are slowly draining into their larger neighbors. Only half a period is shown. Copyright © 1983 Cambridge University Press. Reprinted with the permission of Cambridge University Press from Hammond (1983).

$$\mu\partial_t h+\frac{\sigma}{6R_0}\partial_x\{h^2\partial_x[h^2+R_0^2\partial_x^2(h^2)]\}=0. \tag{2.104}$$

The dynamics of the interface, as described by Eqs. (2.103) and (2.104), are similar in most parametric regimes. The differences between the equations is due to the use of different methods for their derivation. [A method of control volumes was employed to derive Eq. (2.104).] The similarity of the solutions suggests that both methods preserve the main features of the flow. Yarin *et al.* (1993) also considered the influence of temperature-dependent viscosity on the evolution of a thin film on a cylindrical surface while solving the coupled thermal-hydrodynamic problem.

2. Flow on a horizontal cylinder

Lubrication theory can also be applied to the drainage of a thin, initially uniform film on a horizontal cylinder. This case is important in extrusion of pipe or wire coatings and film flow over tubes in heat transfer devices. Goren (1962) examined the linear instability of an isothermal annular coating on a wire, and found, when the film is very thin, that the most rapidly growing disturbance satisfies the condition $2\pi R_0/\lambda=0.707$. Xu and Davis (1985) studied the linear instability of capillary jets with thermocapillarity. They found that capillary breakup of the jet can be retarded or even suppressed for small Prandtl numbers P_r and large Biot numbers B. In the limiting case of $B\to\infty$ the jet becomes isothermal subject to the axial shear stress at the interface. In this case the capillary breakup can be entirely eliminated. Reisfeld and Bankoff (1992) developed the nonlinear evolution equation for a draining thin film on a horizontal cylinder, taking into account gravity, surface tension, thermocapillarity, and long-range molecular forces. The possibility of steady states for the film under a variety of thermal conditions, for both heating and cooling, was examined. The early-time dynamics of the film were also investigated. The roles of surface tension and gravity in determining the azimuthal location of local thinning and the influence of intermolecular forces in promoting rupture of these thin regions gave some unexpected film shapes. The problem geometry is shown in Fig. 21. Symmetry conditions are applied as

$$\partial_\theta H(0,T)=0,\quad \partial_\theta H(\pi,T)=0, \tag{2.105}$$

where θ is the azimuthal angle.

Conservation of fluid volume requires that

$$\int_0^{2\pi} H(\theta,t)\,d\theta=V_0, \tag{2.106}$$

where V_0 is the initial volume per unit width. Viscous scales are used for the radial and azimuthal velocities, ν/R_0 and ν/h_0, respectively, where R_0 is the cylinder radius and h_0 is the initial film thickness. The aspect ratio is

$$\epsilon=h_0/R_0\ll 1. \tag{2.107}$$

The derivation of the evolution equation follows along the same general lines as for a horizontal plane wall, with the added complication of the gravity force's being azimuthally position dependent. The evolution equation thus obtained is

$$\begin{aligned}\partial_T H+\partial_\theta\{&H^3[Gr\sin\theta+\overline{S}(\partial_\theta H+\partial_\theta^3 H)]\\&+BMP_r{}^{-1}H^2\partial_\theta H(1+BH)^{-2}+AH^{-1}\partial_\theta H\}\\&=0.\end{aligned} \tag{2.108}$$

Here

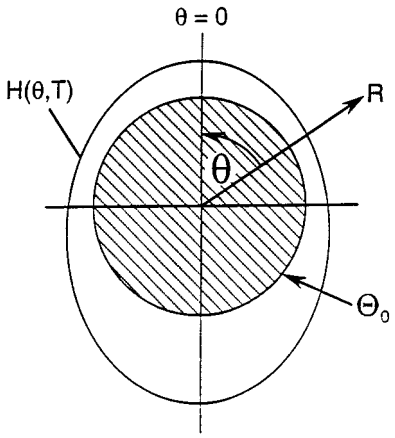

FIG. 21. Schematic representation of the problem of a film on a horizontal cylinder. Copyright © 1992 Cambridge University Press. Reprinted with the permission of Cambridge University Press from Reisfeld and Bankoff (1992).

$$S=\frac{\sigma h_0}{\rho\nu^2}\left(\frac{h_0}{R_0}\right)^3,$$

$S=\overline{S}\,\epsilon^{-3}$ in order to retain the effects of thermocapillary forces and surface tension at leading order. A compilation is given of the magnitudes of the various parameters for water and for mercury on a thin wire and a large tube. The gravity number Gr,

$$Gr=\frac{gh_0^3}{3\nu^2},$$

can be removed from Eq. (2.108) by rescaling the time variable. The Bond number Bo then appears in the equation

$$Bo=\frac{\rho g {R_0}^3}{3h_0\sigma}.$$

For unit-order Bond number Bo and $A=0$, one obtains by integrating and applying the symmetry condition (2.105)

$$\partial_\theta^2 H+H=Bo\cos\theta+\text{const}, \tag{2.109}$$

which has no 2π-periodic solutions, unless the gravity forces are negligible compared to surface tension, $Bo=0$. For $Bo>0$, one can obtain pendant-drop solutions. However, these are not well described by the lubrication approximation. For large Bond number and stabilizing van der Waals forces ($A<0$), a steady state is possible, as intermolecular forces counter the deformation due to gravity. If van der Waals forces are negligible, with $Bo^{-1}\to 0$, the isothermal equation becomes

$$\frac{1}{Gr}\partial_T H+\partial_\theta(H^2\sin\theta)=0. \tag{2.110}$$

Solution by the method of characteristics gives

$$H(\theta,T)=(1+2GrT)^{-1/2} \quad \text{for } \theta=\theta_0=0,$$

$$H(\theta,T)=(1-2GrT)^{-1/2} \quad \text{for } \theta=\theta_0=\pi,$$

$$H(\theta,T)=\left(\frac{\sin\theta_0}{\sin\theta}\right)^{1/3} \quad \text{for } 0<\theta<2\pi,\theta\neq\pi,$$

where $\theta=\theta(GrT),\theta_0\equiv\theta(T=0)$, and the time dependence is given implicitly by

$$F(g(\theta),\sin 75^\circ)-F(g(\theta_0),\sin 75^\circ)+48^{1/4}(\sin\theta_0)^{2/3}GrT=0. \tag{2.111}$$

Here $F(\phi,k)$ is an incomplete elliptic integral of the first kind,

$$F(\phi,k)=\int_0^\phi \frac{dx}{\sqrt{1-k^2\sin^2 x}},$$

and

$$g(\theta)=\arccos\left(\frac{\sqrt{3}-1+(\sin\theta)^{2/3}}{\sqrt{3}+1-(\sin\theta)^{2/3}}\right).$$

Figure 22 shows the time dependence of the local film thickness in this case. Equation (2.109) predicts that the film profile becomes singular at $\theta=\theta_0=\pi$ as $GrT\to 0.5$, so that the lubrication approximation is appropriate only for smaller times (approximately up to $GrT=0.47$).

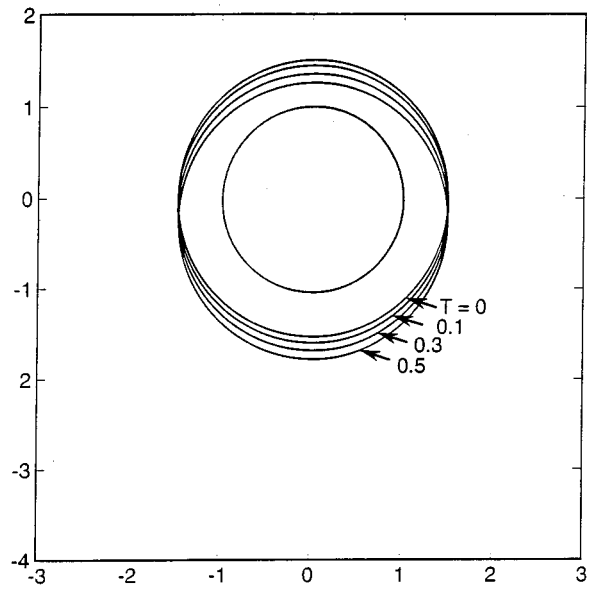

FIG. 22. Unsteady film flow for an isothermal film on a horizontal cylinder, $Bo^{-1}=0, A=0$. Copyright © 1992 Cambridge University Press. Reprinted with the permission of Cambridge University Press from Reisfeld and Bankoff (1992).

A cusp arises because the fourth-order spatial derivative term has been omitted when $Bo^{-1}=0$, so that a boundary layer develops at $\theta=\pi$. Using singular perturbation theory, one finds that the boundary layer thickness $\Delta=O(Bo^{-1/4})$ gives an indication of the region over which surface tension affects the shape of the thin layer. For small, but nonzero, Bo^{-1} Fig. 23 shows the expected unsteady film flow with a pendant-drop shape, where the weight of the fluid in the drop is balanced by the force of surface tension. With $A=0.1$, van der Waals forces cause rupture at a locally thin region whose azimuthal position depends on the Bond number. When the cylinder is heated, thermocapillary forces generate a flow that augments that due to gravity, while these same forces generate an opposing flow when the cylinder is cooled. These cause the film to thin at a location farther from or closer to the top of the cylinder for a given Bond number (Fig. 24), with $Bo^{-1}=0.1, \overline{M}/P_r Gr=5$, and $B=1$. Thus a wide variety of interfacial behavior is possible with a heated cylinder. For large Marangoni number, the film thickness can become very small locally, and for $A>0$, rupture occurs. However, by varying the physical properties of the fluid $(Bo, M/P_r Gr)$ it is possible to prevent or promote film rupture. With a cooled cylinder, thermocapillary forces oppose the drainage, and it is possible to restrain the flow even for large Bond numbers.

K. Flow on a rotating disc

The centrifugal spinning of volatile solutions has been found to be a convenient and efficient means of coating

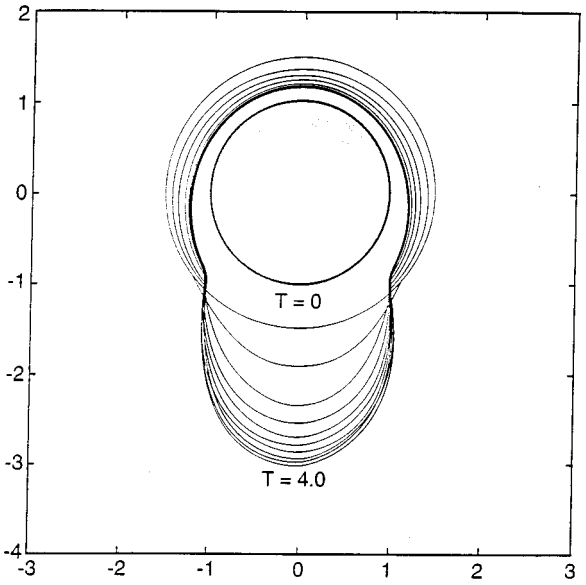

FIG. 23. Unsteady film flow for an isothermal film on a horizontal cylinder, $Bo^{-1}=0.25, A=0$. Copyright © 1992 Cambridge University Press. Reprinted with the permission of Cambridge University Press from Reisfeld and Bankoff (1992).

planar solids with thin films. This process, known as spin coating, has been widely used in many technological processes. Two important phases of the process are usually considered. Phase one occurs shortly after the liquid volume is delivered to the disk surface. At the outset of this phase the liquid film, assumed to be flat, is relatively thick (greater than 500 μm) so that the Reynolds number for the flow is appreciable. The film thins due to radial drainage and solvent evaporation. Inertial forces are important and may lead to the appearance of instabilities of the spinning film. Phase two occurs when the film has thinned to the point where inertia is no longer important (film thickness less than 100 μm), but corrugations to the fluid interface may still be present due to the instabilities that were generated during phase one. The film continues to thin due to radial drainage and evaporation until the solvent becomes depleted and the film ceases to flow.

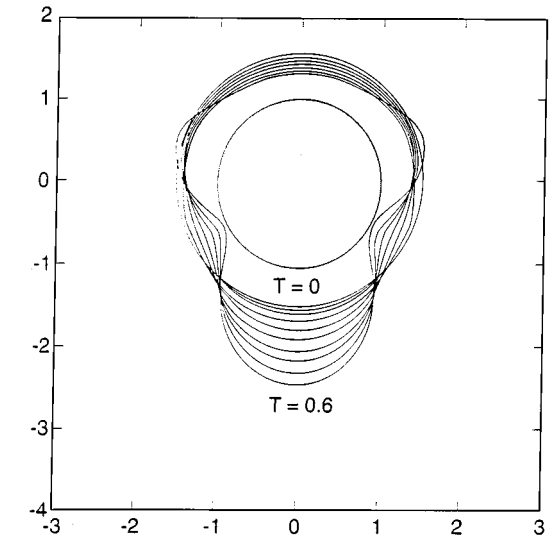

FIG. 24. Unsteady film flow and rupture for a heated film with $Bo^{-1}=0.1, M/P_rGr=5$. Copyright © 1992 Cambridge University Press. Reprinted with the permission of Cambridge University Press from Reisfeld and Bankoff (1992).

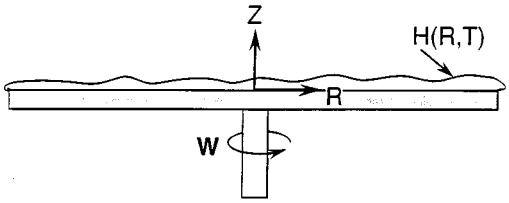

FIG. 25. Schematic representation of rotating liquid film. Reprinted with the permission of the American Institute of Physics from Reisfeld, Bankoff, and Davis (1991).

The isothermal, axisymmetric flow of an incompressible viscous liquid on a horizontal rotating disk was considered by Reisfeld *et al.* (1991). The fluid, consisting of dissolved or suspended solute in a volatile solvent, is evaporating due to the difference in the vapor pressure between the solvent species at the fluid-vapor interface and that present in the gas phase. The appropriate physical configuration is shown in Fig. 25. Cylindrical polar coordinates (r,θ,z) are used in a frame of reference rotating with the disk.

The liquid-vapor interface is located at $z=h(r,t)$. In the coordinate system chosen the outward unit normal vector $\vec{\mathbf{n}}$ and unit tangent vector $\vec{\mathbf{t}}$ are

$$\vec{\mathbf{n}}=\frac{(-\partial_r h,0,1)}{[1+(\partial_r h)^2]^{1/2}},\quad \vec{\mathbf{t}}=\frac{(1,0,\partial_r h)}{[1+(\partial_r h)^2]^{1/2}}. \tag{2.112}$$

The equations of motion analogous to Eqs. (2.10) and including the centripetal forces and Coriolis acceleration are written in the vector form as

$$\vec{\nabla}\cdot\vec{\mathbf{v}}=0, \tag{2.113a}$$

$$\rho(\vec{\mathbf{v}}+\vec{\mathbf{v}}\cdot\vec{\nabla}\vec{\mathbf{v}})=-\vec{\nabla}p+\mu\nabla^2\vec{\mathbf{v}}-\rho \times[\vec{\mathbf{g}}+2\vec{\mathbf{W}}\times\vec{\mathbf{v}}+\vec{\mathbf{W}}\times(\vec{\mathbf{W}}\times\vec{\mathbf{v}})]. \tag{2.113b}$$

Here $\vec{\mathbf{W}}$ is the angular velocity vector with the components $(0,0,\Omega)$. The boundary condition are given by Eqs. (2.12b) with $\partial_s\sigma=0$ and $\vec{\mathbf{f}}=0$ and Eq. (2.85), all written in cylindrical polar coordinates.

The characteristic length scale in the horizontal direction is chosen as the radius of the rotating disk L and the velocity scale is taken as $U_0=\Omega^2 L h_0^2/\nu$. A small parameter ϵ is defined in accord with Eq. (2.13a) as $\epsilon=h_0/L$.

The dimensionless parameters of the problem are the Reynolds number Re, as given in Eq. (2.18), the Froude number F,

$$F=\left(\frac{U_0^2}{gh_0}\right)^{1/2}, \tag{2.114}$$

and the evaporation number, which for a prescribed evaporative mass flux j (Levich, 1962) is defined as

$$E=\frac{3j}{2\epsilon U_0\rho}. \tag{2.115}$$

In contrast to the above discussions, two terms of the velocity are retained in the perturbation expansion. When these are substituted into the mass conservation Eq. (2.113a), one obtains the following evolution equation:

$$\partial_T H+\frac{2}{3}E+\frac{1}{3r}\left[r^2H^3+\epsilon Re\left(\frac{5}{12}Er^2H^4-\frac{34}{105}r^2H^7\right)\right]+\frac{\epsilon}{3}\partial_r\left\{Re\left(\frac{2}{5}r^3H^6-rF^{-2}H^3\right)\partial_r H+r\overline{C}^{-1}H^3\partial_r\left[\frac{1}{r}\partial_r(r\partial_r H)\right]\right\}=0. \tag{2.116}$$

If the order-ϵ terms were dropped in Eq. (2.116), only local mass loss and centripetal drainage would be modeled and no instabilities would result. When the order-ϵ terms are retained, inertia is included and kinematic waves can be amplified. See also Sec. VI for further discussions of such analyses.

For most spin coating applications, both $\overline{C}^{-1}$ and F^{-2} are very small, although they may be very important in planarization studies, in which the leveling of liquid films on rough surfaces is investigated. Equation (2.116) can be thus simplified

$$\partial_T H+\frac{2}{3}E+\frac{1}{3r}\partial_r\left[r^2H^3+\epsilon Re\left(\frac{5}{12}Er^2H^4-\frac{34}{105}r^2H^7+\frac{2}{5}r^3H^6\partial_r h\right)\right]=0. \tag{2.117}$$

This simplified equation can then be used for further analysis. Looking for flat basic states $H=\overline{H}(T)$, one derives from Eq. (2.117) the ordinary differential equation

$$\partial_T\overline{H}+\frac{2}{3}\left[E+\overline{H}^3+\epsilon Re\left(\frac{5}{12}E\overline{H}^4-\frac{34}{105}\overline{H}^7\right)\right]=0, \tag{2.118}$$

augmented with the initial condition $\overline{H}(0)=1$.

For the case where evaporation is negligible ($E=0$), the film thins due to centrifugal drainage, and the leading-order in ϵ solution is

$$\overline{H}=\left(1+\frac{4}{3}T\right)^{-1/2}, \tag{2.119}$$

which predicts a decrease of the thickness to zero as $T\to\infty$.

In the case of $E>0$, both evaporation and drainage cause thinning of the layer. Equation (2.118) predicts a film that thins monotonically to zero thickness in a finite time, T_d, as shown in Fig. 26. Explicit expressions for $\overline{H}(T)$ and for $T_d(E)$ are given in Reisfeld *et al.* (1991). In the case of absorption or condensation, $E<0$, drainage competes with absorption and inertia to thin the film. Initially, the film thins due to drainage, until the rate of mass gain due to absorption and the inertial contribution balances the rate of mass loss due to drainage. At this point the basic state reaches a steady state (Fig. 26). Far from the steady state, the film thins monotonically. Once the steady state is reached, the position of the basic state interface $\overline{H}_s$ satisfies the equation

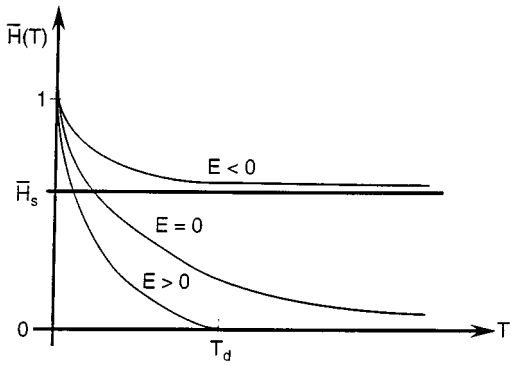

FIG. 26. Basic-state film thickness for principal values of the evaporation number E for rotating liquid films. Reprinted with the permission of American Institute of Physics from Reisfeld *et al.* (1991).

$$\overline{H}_s^3-|E|-\epsilon Re\overline{H}_s^4\left(\frac{5}{12}|E|+\frac{34}{105}\overline{H}_s^3\right)=0. \tag{2.120}$$

For small values of ϵ the approximate solution is

$$\overline{H}_s\sim|E|^{1/3}. \tag{2.121}$$

Linear stability analysis of flat base states is given in Reisfeld *et al.* (1991).

Stillwagon and Larson (1990) considered the spin coating process and leveling of a non-volatile liquid film over an axisymmetric, uneven solid substrate. For a given local dimensionless height of the substrate, $\ell(r)$, their equation, deduced from the Cartesian version valid for capillary leveling of a film in a trench, resembles Eq. (2.116) with $E=0$, where ϵRe is formally set to zero

$$\partial_T H+\frac{1}{3r}\partial_r[r^2H^3+r\overline{C}^{-1}H^3(\partial_r^3H+\partial_r^3 l)]=0. \tag{2.122}$$

Stillwagon and Larson (1990) calculated steady-state solutions for Eq. (2.122) for two different initial profiles, a flat film and one with a constant film thickness consistent with the unevenness of the substrate. These initial conditions led to the same final steady solutions. Experiments with liquid salt mixture films reported in Stillwagon and Larson (1990) demonstrated quantitative agreement between measured film profiles and those obtained from Eq. (2.122). The results of their experiments with volatile fluids showed that film shrinkage occurred, because of evaporation, and the final stage of film leveling was affected. Therefore it was suggested that the evolution of an evaporating spinning film be divided into two stages with fluid flow dominating the first stage and solvent evaporation dominating the second.

L. Summary

In this section we have presented the basics of the long-wave approach to the hydrodynamics of thin, bounded liquid films. The approach is shown to be intimately connected to that used in the theory of hydrodynamic lubrication. Using the long-wave approach we have derived a general evolution equation governing the spatiotemporal behavior of the interface of a thin liquid film subjected to several physical effects, such as surface tension, gravity, van der Waals attractions, thermocapillarity, temperature dependence of physical properties of the liquid, evaporation/condensation, finite thermal resistance of the solid substrate, rotation of the substrate, and an additional component of the interfacial curvature induced by the curvature of the solid substrate. The dynamics of the velocity, pressure, and temperature (in the case of nonisothermal films) within the fluid are shown to be directly determined from that of the interface. In each particular case considered here the appropriate evolution equation is derived from the general case, and its typical solutions are discussed. Linear stability analysis of various base-state solutions of these evolution equations is presented.

III. SPATIAL NONUNIFORMITIES AT THE BOUNDARIES

The full set of governing equations and boundary conditions can also be reduced to an evolution equation when the conditions specified at the boundaries vary slowly in space (or time).

A. Van der Waals forces, surface tension, thermocapillarity, and nonuniform temperature at the bottom

Here $\beta_0=\Pi_0=0, \Phi=\Phi_r+AH^{-3}+GH$, and $\tau_0=0$, where G is given by Eq. (2.37c). We also assume that the dimensionless temperature at the rigid boundary $Z=0$ is prescribed by a periodic function slowly varying with X,

$$\Theta=\Theta_b(X) \quad \text{at } Z=0. \tag{3.1}$$

Then, solving Eqs. (2.57), (2.58), and (3.1), one obtains the temperature distribution in the film

$$\Theta=\Theta_b(X)\left[1-\frac{BZ}{1+BH}\right]-\frac{B\delta Z}{1+BH}, \tag{3.2}$$

and at the interface,

$$\Theta_i=\frac{\Theta_b(X)-B\delta H}{1+BH}. \tag{3.3}$$

Here δ is the ratio of the difference between the average bottom and the gas-phase temperatures, and the variation of the temperature along the bottom, $\Delta\vartheta_b\equiv\vartheta_{b,\max}-\vartheta_{b,\min}$. Therefore the dimensionless interfacial shear stress $\partial_X\Sigma$ is given by

$$\partial_X\Sigma=-M\gamma(H)\partial_X\left[\frac{\Theta_b(X)-B\delta H}{1+BH}\right] \tag{3.4}$$

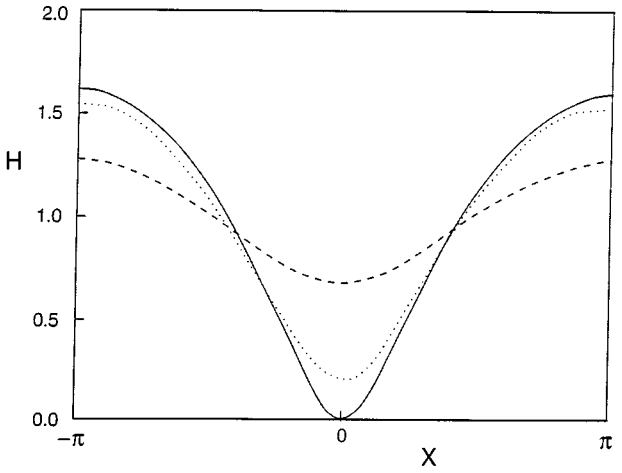

FIG. 27. Dimensionless steady layer profile $H(X)$ for various values of $B_{\rm dyn}$, for a fixed value of $\overline{C}^{-1}/G=0.6174$, calculated from Eq. (3.5) with $\Theta_b(X)=\frac{1}{2}\cos X$ and $B=0$; dashed line, $B_{\rm dyn}=0.627$; dotted line, $B_{\rm dyn}=1.255$; solid line $B_{\rm dyn}=1.445$. Reprinted with the permission of the American Institute of Physics from Tan *et al.* (1990).

and the resulting evolution equation (2.27) reads

$$\partial_T H+\partial_X\left[\left(AH^{-1}-\frac{1}{3}GH^3\right)\partial_X H\right]+\frac{M}{2}\partial_X\left\{H^2\gamma(H)\partial_x\left[\frac{\Theta_b(X)-B\delta H}{1+BH}\right]\right\}+\frac{1}{3}\overline{C}^{-1}\partial_X[H^3\partial_X^3 H]=0. \tag{3.5}$$

Note that $H=\text{const}$ is not a solution of Eq. (3.5) due to spatial nonuniformity of Θ_b. In Eq. (3.4), and consequently in Eq. (3.5), the δ term represents the contribution of the temperature drop across the layer, while the term containing Θ_b is due to the nonuniform temperature at the bottom. Equation (3.5) was obtained by Tan *et al.* (1990) for the case of surface tension linearly decreasing with temperature, $\gamma(H)=1$. They investigated possible steady states of Eq. (3.5) for $B\ll 1$. It was found that in the absence of van der Waals forces continuous steady states could be sustained only if the dynamic Bond number $B_{\rm dyn}$

$$B_{\rm dyn}=\frac{3\left(-\frac{\partial\sigma}{\partial\vartheta}\right)\Delta\vartheta_b}{2\rho g h_0^2} \tag{3.6}$$

did not exceed a certain value depending on the temperature distribution $\Theta_b(X)$. This predicts well the experimental observations of Burelbach *et al.* (1990; see Fig. 4 and Sec. VII below). The value of the dynamic Bond number $B_{\rm dyn}$ describes the relative magnitude of the destabilizing thermocapillary and stabilizing gravity terms proportional to M and G, respectively. Figure 27 reproduced from Fig. 3 in Tan *et al.* (1990) displays possible steady states for a fixed value of $\overline{C}^{-1}/G$ and vari-

ous values of $B_{\rm dyn}$ calculated for $\Theta_b(X)=\frac{1}{2}\cos X$. The minimal thickness of the film in its steady state decreases when $B_{\rm dyn}$ increases.

B. Van der Waals forces, surface tension, thermocapillarity, evaporation, and nonuniform heat flux at the bottom

The heat flux per unit length of the bottom plane is now prescribed as a smooth, slowly varying function $qQ(X)$, where $Q(X)$ is a dimensionless function and q is a characteristic value of heat flux, such as its amplitude. The temperatures in the governing set of equations and boundary conditions can then be scaled in units of $qh_0/k_{\rm th}$. The thermal part of the problem consists of Eq. (2.57) with the boundary conditions (2.86a) and (2.86b),

$$\partial_Z\Theta=-Q(X) \quad \text{at } Z=0. \tag{3.7}$$

The solution for both the temperature field and the evaporative mass flux is given by

$$\Theta=Q(X)[H-Z+K], \quad J=Q(X). \tag{3.8}$$

Following the steps outlined in the derivation of Eqs. (2.91) and (2.92) with $\partial_X\Sigma=-(MK/P_r)\partial_XQ(X)$ and $\Pi_0=-E^2D^{-1}Q^2$ accounting for the thermocapillary effect and vapor recoil, respectively, one obtains (Oron *et al.*, 1997)

$$\partial_TH+EQ(X)+\frac{1}{3}\overline{C}^{-1}\partial_X(H^3\partial_X^3H)+\partial_X\left[\left(AH^{-1}-\frac{1}{3}GH^3\right)\partial_XH\right]-\frac{MK}{2P_r}\partial_X(H^2\partial_XQ)-E^2D^{-1}\partial_X[H^3\partial_X(Q^2)]=0. \tag{3.9}$$

In the particular case of a spatially uniform heat flux $Q=\text{const}$ at the bottom. Equation (3.9) reduces to the one appearing in Burelbach *et al.* (1988),

$$\partial_TH+EQ+\frac{1}{3}\overline{C}^{-1}\partial_X(H^3\partial_X^3H)+\partial_X\left[\left(AH^{-1}-\frac{1}{3}GH^3\right)\partial_XH\right]=0. \tag{3.10}$$

In this particular case the interfacial temperature and the evaporative mass flux are uniform, $\Theta_i=KQ, J=Q$, as given by Eq. (3.8), and therefore both vapor thrust and thermocapillary effect are absent. The heat flux utilized was chosen as

$$Q(X)=\exp\left[-a\left(X-\frac{1}{2}\Delta\right)^2\right], \tag{3.11}$$

where Δ is the length of the periodic domain and a is a positive constant. The trough is generated around the location of the maximum heat flux where the rate of evaporation is the largest. In the simplest case of no vapor thrust and no thermocapillarity, there is monotonic thinning of the film, which resembles topologically the pattern shown in Fig. 12. The emergence of a satellite drop or drops at the late stage of evolution for moderate a, as shown in Fig. 28, is due to the thermocapillarity (mainly) and vapor thrust.

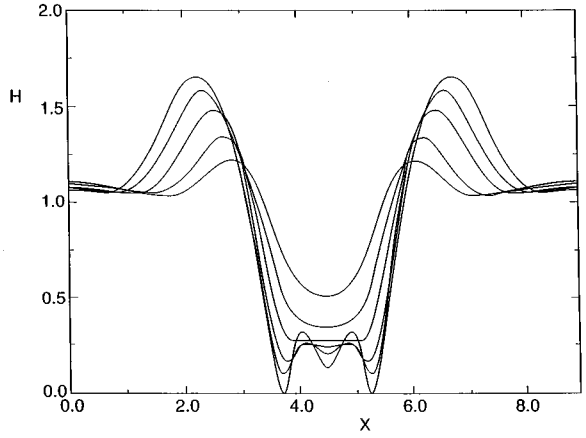

FIG. 28. Evolution of the dimensionless layer profile $H(X)$ for a film heated by spatially nonuniform heat flux. The evolution is described by Eqs. (3.9) and (3.11), with $E=0, A=1, G=0, \overline{C}^{-1}=1, a=1.\ D^{-1}=0, MKP_r^{-1}/2=40$. A satellite drop splits into two partially coalesced drops.

C. Summary

In this section we have considered physical problems associated with slowly varying spatial nonuniformities at the boundaries. The long-wave approach has been applied to these problems, and typical solutions of the resulting evolution equations have been discussed. The examples discussed include the cases of spatially nonuniform temperature and heat flux.

IV. PROBLEMS REDUCING TO SETS OF EVOLUTION EQUATIONS

A. Free films

1. Evolution equation

Free films of liquid are bounded by two interfaces between liquid and gas or liquid and two other liquids. Examples of such a configuration may be provided by two bubbles in a liquid or two drops of different liquids suspended in a third liquid. A liquid film confined between these is then a free film. Therefore, in order to study the behavior of such a free film, one needs to formulate the interfacial boundary conditions at both the interfaces, given by $z=h^{(1)}(x,t)$ and $z=h^{(2)}(x,t)$. The governing equations (2.10) in the bulk, however, remain unchanged. The boundary conditions read, at $z=h^{(i)}\times(x,t)$,

$$w=\partial_th^{(i)}+u\partial_xh^{(i)}, \tag{4.1}$$

$$\mathbf{T}\cdot\vec{\mathbf{n}}^{(i)}=-\kappa^{(i)}\sigma^{(i)}\vec{\mathbf{n}}^{(i)}+(\partial_s\sigma^{(i)})\vec{\mathbf{t}}^{(i)}+\vec{\mathbf{f}}^{(i)}, \tag{4.2}$$

where the index i refers to the ith interface. The unit vectors $\vec{\mathbf{n}}^{(i)}$ and $\vec{\mathbf{t}}^{(i)}$ are given by

$$\vec{\mathbf{n}}^{(1)}=\frac{(-\partial_x h^{(1)},1)}{[1+(\partial_x h^{(1)})^2]^{1/2}},\quad \vec{\mathbf{t}}^{(1)}=\frac{(1,\partial_x h^{(1)})}{[1+(\partial_x h^{(1)})^2]^{1/2}}, \tag{4.3a}$$

$$\vec{\mathbf{n}}^{(2)}=\frac{(\partial_x h^{(2)},-1)}{[1+(\partial_x h^{(2)})^2]^{1/2}},\quad \vec{\mathbf{t}}^{(2)}=\frac{(1,\partial_x h^{(2)})}{[1+(\partial_x h^{(2)})^2]^{1/2}}. \tag{4.3b}$$

Going to the long-wave limit of the governing set of dimensionless equations and boundary conditions, as in Sec. II, yields the system consisting of Eqs. (2.15) and the following boundary conditions. At $Z=H^{(1)}(X,T)\equiv h^{(1)}/h_0$,

$$\partial_T H^{(1)}+U\partial_X H^{(1)}=W, \tag{4.4a}$$

$$\{(U_Z+\epsilon^2\partial_X W)[1-\epsilon^2(\partial_X H^{(1)})^2]-4\epsilon^2(\partial_X H^{(1)})\partial_X U\} =\tau_0^{(1)}[1+\epsilon^2(\partial_X H^{(1)})^2] +(\partial_X\Sigma^{(1)})[1+\epsilon^2(\partial_X H^{(1)})^2]^{1/2}, \tag{4.4b}$$

$$-P-\Pi_0^{(1)}+\frac{2\epsilon^2}{[1+\epsilon^2(\partial_X H^{(1)})^2]}\{\partial_X U[\epsilon^2(\partial_X H^{(1)})^2-1] -\partial_X H^{(1)}(\partial_Z U+\epsilon^2\partial_X W)\}=\frac{C_1^{-1}\epsilon^3\partial_X^2 H^{(1)}}{[1+\epsilon^2(\partial_X H^{(1)})^2]^{3/2}}, \tag{4.4c}$$

and at $Z=H^{(2)}(X,T)\equiv h^{(2)}/h_0$,

$$\partial_T H^{(2)}+U(\partial_X H^{(2)})=W, \tag{4.5a}$$

$$\{(\partial_Z U+\epsilon^2\partial_X W)[1-\epsilon^2(\partial_X H^{(2)})^2]-4\epsilon^2(\partial_X H^{(2)})\partial_X U\} =-\tau_0^{(2)}[1+\epsilon^2(\partial_X H^{(2)})^2] -(\partial_X\Sigma^{(2)})[1+\epsilon^2(\partial_x H^{(2)})^2]^{1/2}, \tag{4.5b}$$

$$-P-\Pi_0^{(2)}+\frac{2\epsilon^2}{[1+\epsilon^2(\partial_X H^{(2)})^2]}\{(\partial_X U)[\epsilon^2(\partial_X H^{(2)})^2-1] -(\partial_X H^{(2)})(\partial_Z U+\epsilon^2\partial_X W)\}=\frac{C_2^{-1}\epsilon^3\partial_X^2 H^{(2)}}{[1+\epsilon^2(\partial_X H^{(2)})^2]^{3/2}}, \tag{4.5c}$$

where the

$$C_i=\frac{U_0\mu}{\sigma_0^{(i)}} \tag{4.6}$$

are the corresponding capillary numbers.

Let

$$\overline{C}_i=C_i\epsilon^{-3},\quad i=1,2 \tag{4.7}$$

with $\overline{C}_i=O(1), i=1,2$ and $\epsilon\to 0$, which yields a system analogous to Eqs. (2.22)–(2.24):

$$\partial_Z^2 U=\partial_X P+\partial_X\Phi, \tag{4.8a}$$

$$0=\partial_Z P+\partial_Z\Phi, \tag{4.8b}$$

$$\partial_X U+\partial_Z W=0, \tag{4.8c}$$

at $Z=H^{(1)}(X,T)$:

$$\partial_T H^{(1)}+U\partial_X H^{(1)}=W, \tag{4.8d}$$

$$\partial_Z U=\tau_0^{(1)}+\partial_X\Sigma^{(1)}, \tag{4.8e}$$

$$-\Pi_0^{(1)}-P=\overline{C}_1^{-1}\partial_X^2 H^{(1)}, \tag{4.8f}$$

at $Z=H^{(2)}(X,T)$:

$$\partial_T H^{(2)}+U\partial_X H^{(2)}=W, \tag{4.8g}$$

$$\partial_Z U=-\tau_0^{(2)}-\partial_X\Sigma^{(2)}, \tag{4.8h}$$

$$-\Pi_0^{(2)}-P=\overline{C}_2^{-1}\partial_X^2 H^{(2)}. \tag{4.8i}$$

This set of equations can, in principle, be solved and further reduced to a single (or a set of) evolution equation(s), as shown in Sec. II. Several particular cases are discussed next.

2. Van der Waals forces and constant surface tension in a free film

A planar film of liquid with van der Waals attractions and interfaces of constant surface tension is a simple model of the bridge between two gas bubbles which at rupture results in the coalescence of the bubbles. Here $\tau_0^{(i)}=0$, $\Pi_0^{(i)}=0$, $\partial_X\Sigma^{(i)}=0$, and $\Phi=\Phi_r+A(H^{(1)}-H^{(2)})^{-3}$.

To simplify the problem given by Eqs. (4.8) one may consider the varicose or "squeeze" mode, where $H\equiv H^{(1)}=-H^{(2)}$ along with symmetric interfacial tractions. Then, instead of boundary conditions at one of the interfaces, one formulates the symmetry conditions at the midplane $Z=0$ (Prevost and Gallez, 1986; Erneux and Davis, 1993),

$$W=0,\quad \partial_Z U=0\quad \text{at } Z=0. \tag{4.9}$$

The problem is thus governed by the set of Eqs. (4.8a)–(4.8f) and (4.9).

Prevost and Gallez (1986) solved the problem of the evolution of a free film in the squeeze mode, assuming that the interface is immobile. This condition replaces Eq. (4.8e) by

$$U=0\quad \text{at } Z=H, \tag{4.10}$$

where $H\equiv H^{(1)}$. Equations (4.8a)–(4.8d), (4.8f), (4.9), and (4.10) are then solved and the resulting evolution equation reads

$$\partial_T H-\frac{1}{3}\partial_X[H^3\partial_X\overline{P}]=0, \tag{4.11}$$

where $\overline{P}$ is again given by Eq. (2.25).

Erneux and Davis (1993) studied the varicose mode of evolution of a free film, relaxing the immobility condition (4.10) at the interfaces employed by Prevost and Gallez (1986). The solution of these equations does not provide us with the value of the tangential velocity $U=U(X,T)$, leaving it unknown at this stage:

$$\partial_T H+\partial_X(UH)=0. \tag{4.12a}$$

Closure is not achieved by using only the leading-order terms, and so has to proceed to the next order of approximation. Assume small Reynolds number

$$Re=\epsilon\overline{Re},\quad \overline{Re}=O(1) \tag{4.12b}$$

and small capillary number

$$C=\epsilon\overline{C}, \quad \overline{C}=O(1). \tag{4.12c}$$

The set of governing equations is next solved at order ϵ to obtain the needed closure. As a result, the evolutionary set comprises Eq. (4.12a) and

$$H[\overline{R}\,e(\partial_T U+U\partial_X U)+\partial_X\Phi-\overline{C}^{-1}\partial_X^3 H] =4\partial_X(H\partial_X U). \tag{4.12d}$$

Prevost and Gallez (1986) studied a special case of this problem, in which the surface viscosity of the film interface is much more important than the viscosity of the liquid, and the set of evolution equations (4.12a) and (4.12d) derived by Erneux and Davis (1993) reduces to Eq. (4.11). On the other hand, when the surface viscosity of the film interface is negligible, Eqs. (4.12a) and (4.12d) reduce to Eq. (2.41b) for a bounded film, as derived by Williams and Davis (1982).

Linearization of Eqs. (4.12a) and (4.12d) around the state $U=0, H=1/2$ yields a characteristic equation of the form

$$\overline{R}\,e\omega^2+4k'^2\omega+k'^2(\overline{C}^{-1}k'^2-3A)=0, \tag{4.13}$$

which implies that instability is possible only if the last term in Eq. (4.13) is negative. It thus follows that, as in the case of the bounded film (Sec. II.C), surface tension stabilizes the film, whereas the negative disjoining pressure $A>0$ destabilizes it, and the cutoff wave number is given by

$$k_c'=\sqrt{6A\overline{C}}. \tag{4.14}$$

Weakly nonlinear analysis of Eqs. (4.12a) and (4.12d) by Erneux and Davis reveals that, as in the case of the free film, nonlinear effects accelerate the rupture process of the film. The degree of augmentation was also estimated. Sharma *et al.* (1995) considered the role of various nonlinearities on rupture of free thin films based on Eqs. (4.12a) and (4.12d). Inertial and nonlinear viscous corrections were found to have minor effects on the evolution of a film perturbed with the small-amplitude, fastest-growing mode. When $k'>k_c'$, linearized theory shows that the film is stable to infinitesimal disturbances. However, weakly nonlinear theory shows that if disturbances have large enough amplitude, then subcritical instabilities (see, for example, Seydel, 1988) are still possible when $k'>k_c'$. When the threshold amplitude is exceeded, there is a sudden change from the planar film to the ruptured film.

Ida and Miksis (1996) solved Eqs. (4.12a) and (4.12d) numerically and determined that the film evolves toward rupture. In the neighborhood of the rupture point they found a similarity solution in the form

$$H=(T_R-T)^m f_1(\xi), \quad U=(T_R-T)^n f_2(\xi),$$

where $\xi=X(T_R-T)^{-p}$. By balancing the viscous and van der Waals (Φ) terms in Eq. (4.12d), they found $m=1/3$ and $n=p-1$. The values of n and p remain undetermined, presumably determined by an asymptotic matching to the solution far from the point of rupture.

B. Thermocapillarity in a free film

Oron (1997) considered the nonlinear dynamics of a free liquid film subject to the thermocapillary effect induced by the transverse temperature gradient applied to the film. The varicose mode of the instability was handled in a way similar to that used by Erneux and Davis (1993) in the case of the isothermal film. The thermal part of the problem was treated similarly to what has been shown in Sec. II.F.

The resulting set of evolution equations is (Oron, 1997)

$$\partial_T H+\partial_X(HU)=0, \tag{4.15a}$$

$$H(\partial_T U+U\partial_X U-\overline{C}^{-1}\partial_X^3 H) =4\partial_X(H\partial_X U)+\frac{MP_r^{-1}B}{2}\frac{\partial_X H}{(1+BH)^2}. \tag{4.15b}$$

Numerical solutions of Eqs. (4.15) suggest that evolution of the film leads to rupture. In many cases a thin neck is formed in the film prior to rupture.

C. Bounded films with interfacial viscosities and van der Waals forces

If one has a fluid/fluid interface that is "clean," then there is little or no measurable interfacial resistance to shear or dilation. However, if the interface is contaminated or else is intentionally covered with a surface-active material, then such resistances are present. These then result in new interfacial properties such as surface viscosities. Consider the case $\Pi_0^{(1)}=0$, $\partial_X\Sigma^{(1)}=0$, and $\Phi=\Phi_r+AH^{-3}$.

In the presence of interfacial viscosities, and in two dimensions, the shear stress balance, Eq. (2.24), has a component which reads at leading order as (Ruckenstein and Jain, 1974; Jain and Ruckenstein, 1976; Edwards and Oron, 1995)

$$\tau_0=B_q\partial_X^2 U, \tag{4.16}$$

where B_q is the total Boussinesq number measuring the relative magnitude of the total interfacial and liquid viscosities,

$$B_q=\frac{(\mu_s+\kappa_s)h_0}{\mu}, \tag{4.17}$$

and where μ_s and κ_s are, respectively, interfacial shear and dilatational viscosities.

Integrating Eqs. (2.22a) and (2.23) with $\beta_0=0$ and (4.16) yields the X component of the flow field, U,

$$U=\frac{1}{2}Z^2\partial_X\overline{P}+FZ, \tag{4.18}$$

and an equation that relates two unknown functions, $F(X,T)$ and H (Edwards and Oron, 1995):

$$H\partial_X\overline{P}+F=\frac{1}{2}B_qH^2\partial_X^3\overline{P}+B_qH\partial_X^2F. \tag{4.19a}$$

The kinematic condition (2.22c) provides upon substitution of Eq. (4.18) the closure of the problem (Edwards and Oron, 1995),

$$\partial_T H+\frac{1}{2}\partial_X(FH^2)+\frac{1}{6}\partial_X(H^3\partial_X\overline{P})=0. \tag{4.19b}$$

Thus the evolutionary system is given by Eqs. (4.19) for F and H, provided that $\overline{P}$ is determined by Eq. (2.25).

As in the problem considered in Sec. IV.A, a set of two coupled differential equations has arisen from the full governing equations and boundary conditions. In the limiting case of zero interfacial viscosity, Eqs. (4.19) lead to a single evolution equation (2.41b), derived by Williams and Davis (1982). On the other hand, the limiting case of infinitely large interfacial viscosity, causing immobility of the interface ($U=0$ at $Z=H$), leads again to a single evolution equation,

$$\partial_T H-\frac{1}{12}\partial_X[H^3\partial_X\overline{P}]=0. \tag{4.20}$$

Linearization of Eqs. (4.19) around $H=H_0$ results in the characteristic equation given by Edwards and Oron (1995) in the form

$$\omega=\frac{1}{4H_0}k'^2\left(A-\frac{1}{3}\overline{C}^{-1}H_0^4k'^2\right)\left[\frac{4+B_qH_0k'^2}{1+B_qH_0k'^2}\right]. \tag{4.21}$$

Equation (4.21) shows that interfacial viscous stress does not alter the stability properties of the modes in comparison to the case with zero interfacial viscosity, but only the growth rate of the perturbations. In the limit of infinite Boussinesq number, it follows from Eq. (4.21) that interfacial viscosity has at most a fourfold damping effect (Jain and Ruckenstein, 1976).

Numerical solutions of Eqs. (4.19) show that the damping effect caused by interfacial viscous stress is much larger than the maximum fourfold damping effect predicted by the linear theory. Moreover, the rate of film thinning is strongly dependent on the value of the Boussinesq number. Figure 29, taken from Edwards and Oron (1995), presents the spatiotemporal evolution of the film interface, as described by Eqs. (4.19) and (2.25b) for $\overline{C}^{-1}=0.01, A=1/2\pi$, and for two different values of the Boussinesq number B_q. Figure 30 displays the time evolution of the minimal film thickness for different values of B_q, along with the evolution predicted by the linear theory, corresponding to the fastest-growing mode for a fixed value of $\overline{C}^{-1}, \overline{C}^{-1}=0.01$ and $A=1/2\pi$. The curve corresponding to a pure interface with no interfacial viscosity, $B_q=0$, represents the result of Williams and Davis (1982). In the presence of interfacial viscous stress, the film rupture process is retarded from the beginning of the evolution. This retardation effect increases with increasing B_q.

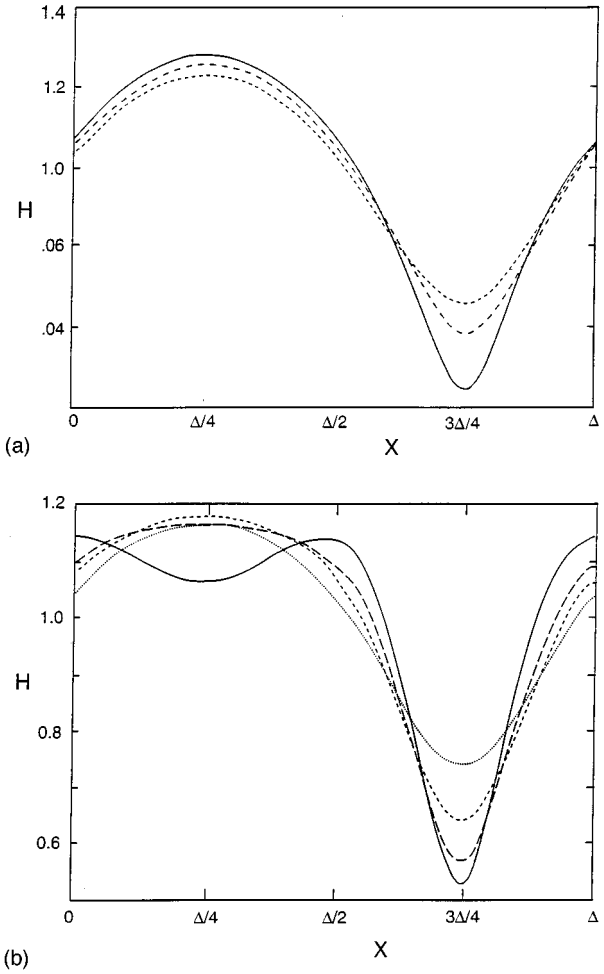

FIG. 29. Spatiotemporal evolution of a film with interfacial viscous stress, as described by Eqs. (4.19) and (2.25b) for $\overline{C}^{-1}=0.01$ and $A=1/2\pi$.: (a) the Boussinesq number $B_q=0.1$. The lowest curve is topologically similar to the steady solution; (b) $B_q=1.0$. The curves correspond to the interfacial shapes calculated with a uniform time step. Diminution of the rate of film rupture can be clearly seen.

D. Surfactants

Consider a situation in which the presence of a surface-active agent (surfactant) affects the local surface tension of the interface. The local concentration of the adsorbed surfactant is unknown and is part of the solution of the mathematical problem. The situation is complicated by the fact that all surfactants exhibit some solubility in the bulk liquid. Hence there is an equilibrium balance between the adsorbed surfactant at the surface and the dissolved concentration in the bulk liquid at the surface, given by a partition coefficient, representing the ratio of the forward and backward rate constants [k_1 and k_2 in Eq. (4.24) below]. If equilibrium is not established immediately, the sorption kinetics must be taken into account. Thus, in the general case, such as soap and water, *three* coupled evolution equa-

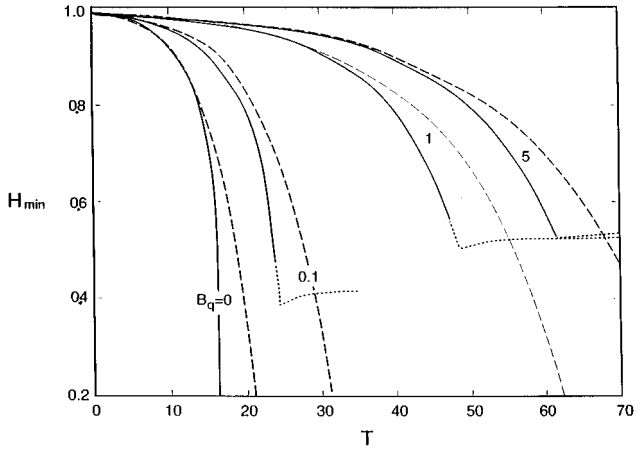

FIG. 30. Temporal evolution of the minimum film thickness H_{min} for $\overline{C^{-1}}=0.01$ and for various values of B_q: solid curves, nonlinear evolution as described by Eqs. (4.19); dashed curves, linear evolution in accordance with Eq. (4.21) for the fastest-growing mode; dotted curves, stage of evolution that is beyond the range of validity of the long-wave theory. Copyright © 1995 Cambridge University Press. Reprinted with the permission of Cambridge University Press from Edwards and Oron (1995).

tions are required for the determination of the interfacial concentration, the bulk concentration, and the local film thickness (Jensen and Grotberg, 1993).

1. Soluble surfactants

Consider the case of a finite-area soluble surfactant placed on a thin liquid film resting on a horizontal substrate. The spreading coefficient S is the difference between the surface tension of the gas-liquid interface with no surfactant and that with an adsorbed monolayer of surfactant (see de Gennes, 1985). The depth of the layer, h_0, can be taken to be small compared to the horizontal extent of the surfactant distribution (Jensen and Grotberg, 1993), of magnitude h_0/ϵ where $\epsilon \ll 1$, for the spreading problem. For a perturbation to the film with an initially uniform surface distribution, the characteristic length in the horizontal direction is $\lambda = h_0/\epsilon$, where λ is the wavelength. Instead of a thermocapillary effect, there is now a solutocapillary effect, owing to the variation of surface tension with adsorbed concentration:

$$\sigma = \sigma_0 - \sigma_\Gamma \Gamma, \tag{4.22a}$$

where $\sigma_\Gamma = -(\partial\sigma/\partial\Gamma)$ at $\Gamma = 0$. Usually $\Sigma_\Gamma > 0$, although there are cases, such as with dissolved salts, where $\Sigma_\Gamma < 0$. Define $\mathbf{\Gamma}(X,T) = \Gamma/\Gamma_0$, where Γ_0 is the initial adsorbate concentration at the surface and $\Sigma = \sigma/(\Gamma_0\sigma_\Gamma)$. The adsorbate concentration and surface-tension gradients are related and in dimensionless form give

$$\partial_X \Sigma = -\partial_X \mathbf{\Gamma}. \tag{4.22b}$$

By neglecting capillarity one can derive [similarly to Eq. (2.62) with $\gamma(H)=1$ and $B \ll 1$] the evolution equation

$$\partial_T H - \frac{1}{2}\partial_X (H^2 \partial_X \Gamma) = 0. \tag{4.23}$$

If one assumes that the surfactant is initially deposited on the interface as a monolayer, there is a transient period during which surfactant enters the bulk liquid. First-order kinetics are employed for the forward and backward reactions:

$$j(\Gamma, c_s) = k_1 c_s - k_2 \Gamma, \tag{4.24}$$

where j is the net flux of dissolved surfactant at the interface with concentration c_s into the adsorbed monolayer of concentration Γ, and k_1 and k_2 are constants. If the flux were controlled by diffusion at the surface, then

$$j = -D_b(\vec{\mathbf{n}}\cdot\vec{\nabla})c,$$

where D_b is the bulk diffusion coefficient. When $j \to 0$, indicating balancing of the adsorptive and desorptive fluxes,

$$\Gamma = K c_s, \quad K = k_1/k_2,$$

where K is the equilibrium partition coefficient. This occurs after a time period of $O(K^{-1})$, where $K = k_2 t_s$, which is the ratio of the time scale of the flow, $t_s = \epsilon^{-2} h_0 \mu S^{-1}$, to the time scale for desorption. When one scales the solute concentration $C = c/c_0 = (k_1/k_2\Gamma_0)C$, Eq. (4.24) becomes at $Z = H$

$$J = K(C_s - \mathbf{\Gamma}) = -\frac{1}{K_0}\left(\frac{\delta}{\epsilon^2}\partial_Z C - \delta(\partial_X H)(\partial_X C)\right), \tag{4.25}$$

where

$$J = j t_s/\Gamma_0, \quad \delta = \mu D_b/(S h_0), \quad K_0 = \Gamma_0/(h_0 c_0) = K/h_0. \tag{4.26}$$

Note that K has dimensions of length, since Γ is the concentration per unit area, while c is the concentration per unit volume. The parameter δ is an inverse Peclet number, and K_0 is a dimensionless partition coefficient reflecting the solubility of the surfactant in the bulk liquid and the film thickness.

The dimensionless transport equations then become

$$\partial_T \mathbf{\Gamma} + \partial_X(U_s \mathbf{\Gamma}) = D' \partial_X^2 \mathbf{\Gamma} + J, \tag{4.27}$$

where $D' = \mu D_s/(S h_0)$, D_s being the surface diffusivity, U_s the tangential component of the flow field at the interface, and

$$\partial_T C + \partial_X(UC) + \partial_Z(WC) = \delta \partial_X^2 C + \delta\epsilon^{-2}\partial_Z^2 C. \tag{4.28}$$

Conservation of surfactant per unit width, with an impermeable wall and zero bulk mean flow, requires that

$$\int_0^\lambda dX\left(\mathbf{\Gamma} + \delta\int_0^H C\,dZ\right)$$

be constant with time.

By assuming $\epsilon^2\delta^{-1} \ll 1$, so that vertical diffusion acts rapidly, Jensen and Grotberg (1993) decomposed the bulk concentration into a component independent of Z and a small fluctuation:

$$C(X,Z,T)=C_0(X,T)+\epsilon^2\delta^{-1}C_1(X,Z,T),$$

where

$$\overline{C}_1\equiv\frac{1}{H}\int_0^H C_1 dZ=0.$$

With the further simplification that $\delta=O(1)$ and neglecting terms of $O(\epsilon^2)$, they obtained three coupled equations for the local film thickness, surface, and bulk concentrations:

$$\partial_T H-\frac{1}{2}\partial_X(H^2\partial_X\Gamma)=0, \tag{4.29a}$$

$$\partial_T\Gamma-\partial_X(H\Gamma\partial_X\Gamma)=D'\partial_X^2\Gamma+K(C_0-\Gamma), \tag{4.29b}$$

$$\partial_T C_0-\frac{1}{2}H(\partial_X\Gamma)(\partial_X C_0)=\frac{\delta}{H}\partial_X(H\partial_X C_0)-\frac{K\delta}{H}(C_0-\Gamma)-\frac{\alpha_p}{H}C_0, \tag{4.29c}$$

where α_p is a measure of the permeability of the substrate wall at $Z=0$:

$$\alpha_p=\left(\frac{\epsilon^2}{\delta}C\right)^{-1}\partial_Z C|_{Z=0}.$$

For $\alpha_p=0$ the wall is impermeable. Thus, if $K=0$, no sorption occurs and Eq. (4.29b) describes the transport of a passive scalar by a surfactant-driven flow (Jensen and Grotberg, 1993). If $K\to\infty,\Gamma=C_0(X,T)$ to leading order, which requires a fast diffusive flux between surface and bulk in order to maintain local equilibrium. When the flux terms are eliminated between the surface and bulk transport equations, Eqs. (4.29) become to leading order

$$\partial_T H-\frac{1}{2}\partial_X(H^2\partial_X C_0)=0, \tag{4.30a}$$

$$H\left[\partial_T C_0-\frac{1}{2}H(\partial_X C_0)^2-\frac{\delta}{H}\partial_X(H\partial_X C_0)+\frac{\alpha_p}{H}C_0\right]+K_0[\partial_T C_0-\partial_X(HC_0\partial_X C_0)-D'\partial_X^2 C_0]=0. \tag{4.30b}$$

When $K_0\to\infty$, Eq. (4.30b) reduces to the transport equation for an insoluble surfactant (Gaver and Grotberg, 1992; Jensen and Grotberg, 1992). For smaller values of K_0 the influences of advection and diffusion in the substrate manifest themselves. For $K_0=0$ the surface flow becomes unimportant compared to the bulk flow for transport of a passive scalar and hence can be equally well used to describe heat transport from a line source at the free surface.

Consider now the case of a finite strip of surfactant placed on a clean interface. Immediately after this placement the fronts spread rapidly. For small D' and $K_0\to\infty$, the width of the spreading monolayer strip grows proportionally to $T^{1/3}$ (Jensen and Grotberg, 1993). This scaling also turns out to be convenient when the surfactant is soluble. Similarity solutions for Eqs. (4.30) are sought in the form

$$\xi=\frac{X}{T^{1/3}},\quad \tau=T,\quad H(\xi,\tau)=H(X,T),$$

$$F(\xi,\tau)=C_0(X,T)T^{1/3}. \tag{4.31}$$

One sees that the effects of horizontal diffusion grow with time and ultimately dominate the advection terms. Figure 1 in Jensen and Grotberg (1993) shows numerical solutions of Eqs. (4.30) and (4.31) for an insoluble surfactant ($K_0\to\infty$) and small surface diffusion ($D'=0.01$), with initial condition of $H(\xi,1)=1$ and

$$F(\xi,1)=\frac{1}{2}\left[1-\tanh\left(\frac{\xi-\xi_m}{\xi_N}\right)\right], \tag{4.32}$$

where $\xi_m=0.5$ and $\xi_N=0.1$. A shock in the film height occurs at the leading edge of the monolayer, which advances to a nearly stationary position in the transformed frame. The shock is smoothed by surface diffusion on a length scale proportional to $D'T^{1/3}$, so that with advancing time the shock widens and decays. The small-slope requirement of lubrication theory can thus be met.

A large amount of literature has been developed for simplified models, particularly for insoluble surfactants, obtained by considering limiting values of the parameters. Besides the spreading-strip problem noted above, Grotberg and co-workers have made extensive studies relevant to the delivery of surfactants and drugs in the human lung. Interesting phenomena are predicted and, in some cases, experimentally verified. These include similarity solutions giving the time behavior of spreading for planar semi-infinite initial film distributions, kinematic shock waves at the surfactant front, possible film rupture owing to depletion of surfactant at the center, development of a leading-edge hump behind the front, reverse flow when gravity is important, reduction of wave-front magnitude due to surface diffusion and preexisting surfactant, and fingering due to front instability. A synopsis of this work is given by Grotberg and Gaver (1996).

2. Insoluble surfactants

de Witt *et al.* (1994) considered the evolution of a free film with insoluble surfactants and subject to long-range molecular forces. The interfacial shear stress arises due to the spatial variation of the surfactant concentration Γ along the interfaces.

Surface tension is assumed to decrease linearly with surfactant concentration, $\Sigma=\Sigma_0-M_s\Gamma$, where Σ_0 is the surface tension at equilibrium concentration and M_s is the solutal version of the Marangoni number, proportional to $\Gamma_0\partial\sigma/\partial\Gamma$. The set of governing equations and boundary conditions consists of Eqs. (4.8a)–(4.8f) and (4.9) with $\tau_0^{(1)}=0,\Pi_0^{(1)}=0,\partial_X\Sigma^{(1)}=-M_s\partial_X\Gamma$, $\Phi=\Phi_r+A(2H)^{-3}$, and the surface diffusion Eq. (4.27) with $J=0$.

The same scalings are used here that led to the derivation of the set of evolution equations (4.12a) and

(4.12d) in the case of a free film subject to van der Waals forces (see Sec. IV.A). The desired set of three evolution equations is obtained upon resolving the governing equations to zeroth and first orders of approximation in ϵ in terms of three unknown functions—the thickness H, the surfactant concentration $\mathbf{\Gamma}$, and the velocity U:

$$\partial_T H+\partial_X(UH)=0, \tag{4.33a}$$

$$H[\overline{R}\,e(\partial_T U+U\partial_X U)+\partial_X\Phi-\overline{C}^{-1}\partial_X^3 H] =\partial_X(-M_s\mathbf{\Gamma}+4H\partial_X U), \tag{4.33b}$$

$$\partial_T\mathbf{\Gamma}+\partial_X(\mathbf{\Gamma}U)=D'\partial_X^2\mathbf{\Gamma}. \tag{4.33c}$$

Linear stability analysis of the motionless steady state $H=1/2,\mathbf{\Gamma}=1$, and $U=0$ reveals that the cutoff wave number k_c' is given by Eq. (4.14), which coincides with the results of Erneux and Davis (1993) for the film devoid of surfactant. The cutoff wave number is found to be independent of the Marangoni number M_s, although the growth rate of the perturbations decreases with increase of M_s.

Nonlinear solutions of Eqs. (4.33) evolve to rupture. The surfactant concentration at rupture points is zero due to its transport by the induced flow in the direction of the interfacial crests [Fig. 3 in de Witt *et al.* (1994)].

The dynamics of a thin liquid film with insoluble surfactants was considered by Paulsen *et al.* (1996) in the context of bubble/particle flotation. The authors considered the coupled evolution of the film thickness and the surfactant concentration when the film was subjected the action of both van der Waals and hydrophobic attraction forces. In this case the dimensionless potential for the disjoining pressure is given by

$$\Pi_0=\Pi_r+AH^{-3}+l_1\exp(-H/l_2), \tag{4.34}$$

where A is the dimensionless Hamaker constant, Eq. (2.41c), Π_r is the reference value, and l_1 and l_2 are, respectively, the magnitude of the hydrophobic attractive force and its length of decay, both dimensionless. The coupling between the hydrodynamics and the surfactant concentration is due to the surface boundary condition (4.22). A set of governing equations in this case consists of Eqs. (2.27) and (2.25b) with $\beta_0=\tau_0=\Phi=0$, $\partial_X\Sigma=-\partial_X\mathbf{\Gamma}$,

$$\partial_T H+\frac{1}{2}\partial_X(H^2\partial_X\mathbf{\Gamma})+A_l\partial_X[H^3\exp(-H/l_2)\partial_X H] +A\partial_X(H^{-1}\partial_X H)+\frac{1}{3}\overline{C}^{-1}\partial_X(H^3\partial_X^3 H)=0, \tag{4.35}$$

and the transport equation for the insoluble surfactant, Eq. (4.27) with $J=0$. Here the value of the constant A_l is

$$A_l=\frac{l_1}{3l_2}. \tag{4.36}$$

It is possible now to evaluate the tangential component of the flow field U_s at the interface $Z=H$ using Eq. (2.26),

$$U_s=-H\partial_X\mathbf{\Gamma}-\frac{1}{2}H^2\partial_X\overline{P}. \tag{4.37}$$

By substituting Eq. (4.37) into Eq. (4.27), one obtains

$$\partial_T\mathbf{\Gamma}-\partial_X(H\mathbf{\Gamma}\partial_X\mathbf{\Gamma})+\frac{1}{2}\overline{C}^{-1}\partial_X(\mathbf{\Gamma}H^2\partial_X^3 H) -\frac{3}{2}A\partial_X(\mathbf{\Gamma}H^{-2}\partial_X H)-\frac{3}{2}A_l\partial_X \times[\mathbf{\Gamma}\exp(-H/l_2)\partial_X H]=D'\partial_X^2\mathbf{\Gamma}. \tag{4.38}$$

The set of evolution equations (4.35), (4.38), which determines the spatiotemporal behavior of the local film thickness H and the surfactant concentration $\mathbf{\Gamma}$, was not actually solved by Paulsen *et al.* (1996). Instead, they considered the case of a zero-stress interface with constant Σ, which leads to decoupling of Eq. (4.35) from Eq. (4.38). Equation (4.35) without the $\mathbf{\Gamma}$ term is then solved in order to study the process of film rupture.

Dagan and Pismen (1984) studied the waves on the surface of a thin liquid film driven by the solutal Marangoni effect and induced by chemical reaction of an insoluble surfactant, subject to a specified longitudinal concentration gradient. Following the steps of the derivation of the evolution equations, similar to those described above for Eqs. (4.29), they obtained (in different units)

$$\partial_T H-\frac{1}{2}\partial_X(H^2\partial_X\mathbf{\Gamma})=0, \tag{4.39a}$$

$$\partial_T\mathbf{\Gamma}-\partial_X[H(\mathbf{\Gamma}+c')\partial_X\mathbf{\Gamma}]=D'\partial_X^2\mathbf{\Gamma}+F(\mathbf{\Gamma}), \tag{4.39b}$$

where c' is the normalized concentration gradient and $F(\mathbf{\Gamma})$ is the chemical-reaction term. They showed that if surface tension decreases with concentration $\mathbf{\Gamma}$ then the film becomes thinner when the wave propagates in the direction of higher concentrations and thicker when it propagates in the direction of lower concentrations.

Schwartz *et al.* (1995, 1996) studied the process of leveling of thin liquid films with surfactant and discussed the implications of the results to coating of surfaces. A dimensional set of evolution equations was found to be

$$\partial_t h+\frac{1}{3\mu}\partial_x[h^3\partial_x(\sigma\partial_x^2 h)]-\frac{\sigma_\Gamma}{2\mu}\partial_x(h^2\partial_x\Gamma)=0, \tag{4.40a}$$

$$\partial_t\Gamma+\frac{1}{2\mu}\partial_x[\Gamma h^2\partial_x(\sigma\partial_x^2 h)]-\frac{\sigma_\Gamma}{\mu}\partial_x(h\Gamma\partial_x\Gamma) -D_b\partial_x^2\Gamma-D_s(1-\Gamma)=0. \tag{4.40b}$$

A linear theory based on Eqs. (4.40) showed that the base state $\Gamma=1,h=h_0$ is stable to sinusoidal perturbations, which decay with time. This decay, called leveling, was studied with respect to the "surfactant strength" proportional to σ_Γ. The main result is that a decrease of σ_Γ would not necessarily lead to an increase in the rate of the leveling of the film, as would be expected. The reason for such unusual behavior is the presence of surface-tension gradients induced by the variation of the

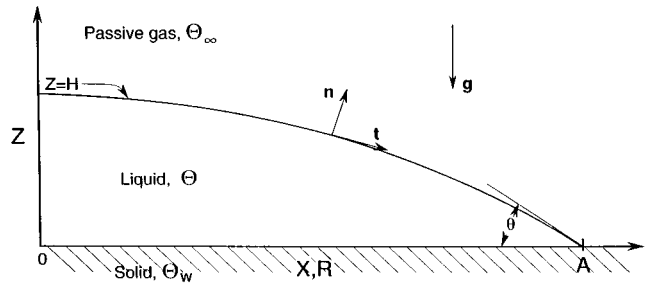

FIG. 31. Sketch of the problem geometry. Copyright © 1991, Cambridge University Press. Reprinted with the permission of Cambridge University Press from Ehrhard and Davis (1991).

surfactant concentration Γ. A nonlinear study of Eqs. (4.40) with no surface diffusion, $D_s=0$, and with constant surface tension, $\sigma=$const, in both of the second terms of Eqs. (4.40a) and (4.40b), was carried out by Schwartz *et al.* (1996), and the results were compared with the solutions of the full governing equations found numerically by using the finite-element method. A substantial agreement over a range of parameters was established among the solutions found by different methods.

E. Summary

The long-wave approach has been applied to a class of physical problems that do not reduce to a single evolution equation but rather to a set of two or three equations. Among problems of this class we have considered free films, bounded films with interfacial rheological viscosities, and the dynamics of surfactants in bounded and free films. Typical solutions of the nonlinear evolution equations have been discussed. Results of the linear stability analysis have also been presented.

V. SPREADING

A. The evolutionary system

In Sec. II lubrication asymptotics were used to convert the system governing interfacial instabilities of thin films to a single evolution equation, thereby bypassing the free-boundary nature of the problem. This was possible to do because the instabilities that occur in this system all have long-scale forms. Precisely the same scheme can be used to describe the spreading of liquid drops on solid surfaces. Here the parameter is the static contact angle θ_s which, if small, will guarantee that the slopes everywhere on the drop will likewise be small, for reasonable initial conditions.

Consider a drop as shown in Fig. 31. The contact lines at $X=\pm A(T)$ move and, if the no-slip condition is applied at the liquid-solid boundary, the contact line will be the site of a nonintegrable shear-rate singularity (Dussan V. and Davis, 1974). The presence of this singularity makes it impossible to enforce a boundary condition at the contact line relating the slope of the interface and the (given) contact angle.

A number of measures have been used in the literature to overcome this deficiency of the model. The first and the most common is to introduce on the solid-liquid interface near the contact line *apparent slip* through the posing of an *ad hoc* model. For example, if one sets at $z=0$,

$$u=\beta\partial_z u, \quad w=0, \tag{5.1}$$

where the solid is impermeable, and the slip velocity u is proportional to the shear stress through the scalar β. In this Navier slip model, β is taken to be numerically small, and so the slip is negligible except near the contact lines where $\partial_z u$ is large.

The evolution equation in two dimensions for the spreading drop will again be Eq. (2.27), with $\Phi_0=\tau_0=\partial_X\Sigma=0$ and with $\overline{P}$ given by Eq. (2.25b),

$$\overline{C}_m\partial_T H+\partial_X\left[\left(\frac{1}{2}H^2+\beta_0 H\right)(\tau_0+\partial_X\Sigma)\right] -\partial_X\left[\left(\frac{1}{3}H^3+\beta_0 H^2\right)\partial_X\overline{P}\right]=0. \tag{5.2}$$

In three dimensions the evolution equation has the form

$$\overline{C}_m\partial_T H+\vec{\nabla}_1\cdot\left[\left(\frac{1}{2}H^2+\beta_0 H\right)(\vec{\tau}_0+\vec{\nabla}_1\Sigma)\right] -\vec{\nabla}_1\cdot\left[\left(\frac{1}{3}H^3+\beta_0 H^2\right)\vec{\nabla}\overline{P}\right]=0, \tag{5.3}$$

where the mobility capillary number $\overline{C}_m$ appears as

$$\overline{C}_m=\frac{\mu K_{\mathrm{CL}}}{\sigma_0\theta_s^{3-m}}. \tag{5.4}$$

The mobility coefficient K_{CL} of the contact line is either K_A or K_R, defined below in Eqs. (5.8), as is the mobility exponent m.

The appearance of the coefficient $\overline{C}_m$ in Eqs. (5.2) and (5.3) is due to the use of a different time scale from that employed in Eqs. (2.27) and (2.28), as discussed below. Equation (5.2) should be augmented by a gross mass balance and by contact-line conditions that describe the mechanics of spreading:

$$\int_{-A}^{A} H\,dX=1. \tag{5.5}$$

The conditions of contact are

$$H[\pm A(T),T]=0, \tag{5.6}$$

which give compatibility between H, the nondimensional interface shape, and the time-dependent contact-line position $A=A(T)$.

Finally, one poses contact-angle conditions of the form

$$\partial_X H(\pm A,T)=\mp\tan\theta. \tag{5.7}$$

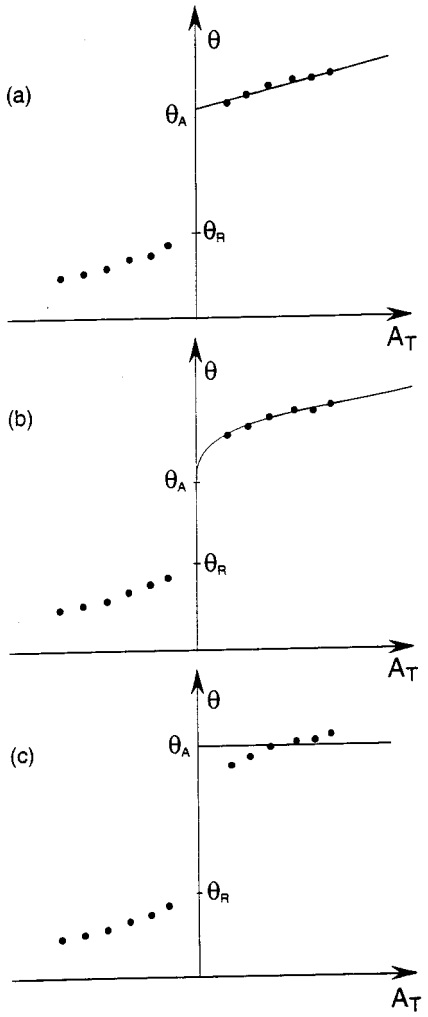

FIG. 32. Typical measurements of contact angle after Dussan V. (1979). $\partial_T A \equiv u_{\mathrm{CL}}$ is the speed of the contact line. Symbols represent experimental data, solid lines correspond to various mobility exponents m in the model of Eqs. (5.8): (a) $m=1$; (b) $m=3$; (c) $m=\infty$. Copyright © 1991 Cambridge University Press. Reprinted with the permission of Cambridge University Press from Ehrhard and Davis (1991).

Remark: *It is the choice of the slip law, here Eq. (5.1), and the function θ, which relates the angle to the contact line speed, say, that models the small-scale physics near the contact line, such as the roughness and the chemical inhomogeneity of the substrate. Equations (5.1) and (5.7) then relate the small scales to the macroscopic behavior of the system.*

When contact angles are measured through a light microscope, it is found that the data are well described by the relations (Dussan V., 1979)

$$u_{\mathrm{CL}} = K_A(\theta - \theta_A)^m, \quad \theta > \theta_A, \tag{5.8a}$$

$$u_{\mathrm{CL}} = -K_R(\theta_R - \theta)^m, \quad \theta < \theta_R, \tag{5.8b}$$

where K_A, K_R, and m are positive and θ_A and θ_R are called the advancing and receding contact angles, respectively, each measured in the liquid. These data, shown in Fig. 32 for various m, display a monotonically increasing dependence of the angle on the speed u_{CL} of the contact line. When liquid displaces gas, $\partial_T A > 0$, the front steepens as the speed increases, and when gas displaces liquid, $\partial_T A < 0$, the angle decreases with speed. Further, the data display contact-angle hysteresis, which means that for θ in the interval $[\theta_R, \theta_A]$ the contact-line speed is zero and hence the static angle depends on the history of the motion.

A major contribution of Dussan V. and her coworkers was to argue and show both theoretically and experimentally that measured angles, given by Eq. (5.8), are *not material constants* but are affected by the outer flows and hence the geometries of the systems. The departures of measured angles from the microscopic angles are due to viscous bending of the interface near the contact line. For capillary numbers $C = U_{\mathrm{CL}}\mu/\sigma$ small, these departures are small. In order to obtain a geometry-invariant θ, one has to go to smaller scale and use the intermediate angle θ_I. Ngan and Dussan V. (1989) and Dussan V. *et al.* (1991) excise a small neighborhood of the contact line and on the arc of the sector prescribe the flow at $r=R$ and $\theta=\theta_I$, which results from an asymptotic theory for $\beta_0 \to 0$.

In all the descriptions, the local region near the contact line supplies the outer field with a one-parameter family of solutions. They can be named by the value of slip length β_0 or by the angle θ_I at $r=R$.

De Gennes (1985) and Troian *et al.* (1989) envision the existence of a precursor film on the solid ahead of the front. Then in effect one has macroscopic spreading over a prewetted surface. The precursor film may have finite or infinite extent but in either case its existence removes from view the problem of a contact line. Thus, rather than a slip coefficient β_0, one has a precursor film thickness δ that names the local solution at the front. Comparable outer fields result from the two approaches if $\beta_0 \approx \delta$ (Spaid and Homsy, 1996).

The results from these approaches will be discussed below. In what follows it will be supposed that the apparent and microscopic contact angles have similar functional forms of contact-line speed and hence Eqs. (5.8) will be used for the discussion. Of course, the coefficients K_A, K_R, and m are not directly known but have to be inferred. Hocking (1983) assumes that the microscopic contact angle contains hysteresis but is independent of speed u_{CL} and deduces forms like Eqs. (5.8) for the apparent angle. His model can be obtained as a limiting case, $K_{\mathrm{CL}} \to \infty$, in form (5.8).

Recently, there has been some evidence to suggest that the *microscopic* contact angle depends on speed. Jin *et al.* (1996) used molecular dynamics to show this. Willson (1995) finds a similar result by measurement of the liquid/vapor interface shape within 20 microns of the contact line and fitting to the analytic model for that shape (Rame, Dussan, and Garoff, 1991). That model connects parameters derived from the experiment to the microscopic contact angle of any slip model. For a series of polymer melts spreading on glass, his results are not compatible with a constant microscopic angle and suggest that the capillary number which is appropriate for

scaling the contact line velocity further from the contact line is not appropriate for scaling the velocity in the slipping region.

The scaling used in system (5.1)–(5.8) follows Ehrhard and Davis (1991), Ehrhard (1993), and Smith (1995). From Eq. (5.5) the fixed volume per unit width V_0 is unity. The longitudinal scale L is given by $L=(V_0\theta_s)^{1/2}$. The vertical length scale is $\theta_s L$ and so the small parameter is θ_s. Time is scaled on $L/K_{\rm CL}\theta_s^m$, (u,w) is scaled on $K_{\rm CL}\theta_s^m(1,\theta_s)$, and pressure is scaled on $\mu K_{\rm CL}\theta_s^{m-2}/L$, where for a spreading drop $\theta_s=\theta_A$, for a receding drop $\theta_s=\theta_R$, and $K_{\rm CL}=K_A$ or $K_{\rm CL}=K_R$ depending on θ. The exponent m can be determined empirically (Hoffman, 1975; Ehrhard and Davis, 1991) or by theoretical arguments (De Gennes, 1985) and is found to be about $m=3$.

The evolutionary system (5.2) and (5.4)–(5.8) for spreading has altered the free-boundary nature of the interface (described by H), but it remains a free-boundary problem because $A=A(T)$ is *a priori* unknown.

The constant $\overline{C}_m$ is a scaled ratio of speeds, contact-line spreading versus σ_0/μ associated with capillary pressures driven by changes in curvature of the interface. As Rosenblat and Davis (1985) have discussed, the spreading results from two phenomena. There is "capillary push" associated with a noncircular interface generating pressure gradients and viscous flow that drive the bulk drop. And there is "contact-line pull" associated with the difference between the static and actual contact angles driving local spreading. The mobility capillary number measures the relative importance of these. When $\overline{C}_m$ is small, the interface is a circle that quasistatically evolves due to contact-line pull. When $\overline{C}_m$ is large, there are significant distortions of the interface and $\theta=\theta_s$ always.

B. Constant surface tension only

The simplest spreading problem involves a viscous fluid with constant physical properties. In this case $\Pi_0=\Phi_0=\tau_0=0$. Equation (5.2) then becomes

$$\overline{C}_m\partial_T H+\partial_X\left[\left(\frac{1}{3}H^3+\beta_0 H^2\right)\partial_X^3 H\right]=0. \tag{5.9}$$

If the functional $\beta_0=\beta_* H^{-1}$, where β_* is a constant, this equation becomes that first formulated by Greenspan (1978). With any form for β_0, one can seek approximate solutions for $\overline{C}_m\to 0$. In this case

$$\partial_X^2 H=-\kappa(T), \tag{5.10}$$

which shows that the interface is the arc of a parabola (the lubrication limit of a circle) and κ is the curvature. This "circle" develops quasistatically as time progresses. Here $\overline{C}_m\ll\beta_0\sim 1$.

When one solves Eq. (5.10) subject to conditions (5.5) and (5.6), one obtains

$$H=\frac{3}{4A^3}(A^2-X^2). \tag{5.11}$$

Finally, form (5.11) is substituted into the contact-angle condition (5.8) with $\dot{A}=u_{\rm CL}$ to obtain a differential equation for the contact-line position $A(T)$,

$$\dot{A}=K_A\left[\left(\frac{3}{2A^2}\right)^m-\theta_A^m\right],\quad \theta>\theta_A, \tag{5.12a}$$

$$\dot{A}=-K_R\left[\theta_R^m-\left(\frac{3}{2A^2}\right)^m\right],\quad \theta<\theta_R, \tag{5.12b}$$

where $K_A, K_R>0$. Equations (5.12) can be used to monitor drops that expand, contract, or a combination of both. For example, when there is pure spreading $\theta\geqslant\theta_A>0$, a drop will equilibrate at $A=A_\infty$, where $A_\infty=\sqrt{3/2\theta_A}$. By examining the equation at long times one can determine the rate of approach to the steady state.

For pure spreading with $\theta_A=0$, Eq. (5.12a) gives a simple power law for long times,

$$A\sim T^q. \tag{5.13}$$

For example, for $\theta_A=0$ and $m=3$, one obtains $q=1/7$. A list of such theoretical and experimental power laws is given in Table I. The theory and experiment agree well in terms of the exponents, though the multiplicative constant in Eq. (5.13) is not well tested.

An alternative approach is that of Hocking (1983) in which θ is taken to be either θ_A or θ_R but in either case is independent of $u_{\rm CL}$. This corresponds to $\overline{C}_m\to\infty$ in Eqs. (5.2) and (5.3), which is accomplished by rescaling T to $\overline{C}_m^{-1}T$. The result is Eqs. (5.2) and (5.3) with $\overline{C}_m$ set to unity and

$$\theta=\theta_A,\quad \dot{A}>0, \tag{5.14}$$

$$\theta=\theta_R,\quad \dot{A}<0.$$

For constant $\beta_0\to 0, \overline{C}_m=O(1)$, i.e., $\beta_0\ll\overline{C}_m$, Hocking (1995a) finds that the apparent angle θ satisfies

$$\theta^3=\theta_0^3+u_{\rm CL}[K_A^{-1}+9\overline{C}_m\ln(h_m/\beta_0)]. \tag{5.15}$$

This is obtained at second order in β_0 through matched asymptotic expansions with a double boundary layer near the contact line. Thus, if $K_A^{-1}\gg 9\overline{C}_m\ln(h_m/\beta_0)$, then the results given above hold since then the effects of slip appear only as a first correction and spreading is controlled by the angle versus speed characteristic. On the other hand, if $K_A^{-1}\ll 9\overline{C}_m\ln(h_m/\beta_0)$, the Hocking theory applies and the spreading is controlled by slip.

If the Hocking model is used, it is found that the power laws (5.13) for large T correspond to the exponents in Table I for $m=3$. Only the constant multipliers differ between the predictions of the two theories. Hocking (1995a) argues that the multiplier for spreading oils is numerically closer to that of the Hocking theory.

If one takes the view that the local physics near the contact line is "unknown" as seen by the macroscopic viewer, one can "excise" a neighborhood of the contact line and instead match an outer solution, which solves the evolution equation with a local (singular) wedge

TABLE I. Isothermal spreading results. The symbols ST and G denote surface tension and gravity dominance, respectively. The asterisk indicates that error bars were not given. Copyright © 1991 Cambridge University Press. Reprinted with the permission of Cambridge University Press from Ehrhard and Davis (1991).

Reference	Plane, $A\sim T^q$ q	Axisymmetric, $A\sim T^q$ q	Dominant force
Experiments:			
Tanner (1979)	0.148	0.106-0.112	ST
Cazabat and Cohen Stuart (1986)		$\frac{1}{10}$*	ST
		$\frac{1}{8}$*	G
Chen (1988)		0.080-0.135	ST
Theory:			
Lopez *et al.* (1976)	$\frac{1}{5}$	$\frac{1}{8}$	G
Tanner (1979)	$\frac{1}{7}$	$\frac{1}{10}$	ST
Starov (1983)		$\frac{1}{10}$	ST
Greenspan (1978), $m=1$	$\frac{1}{3}$	$\frac{1}{4}$	ST
Ehrhard and Davis (1991), $m=1$	$\frac{1}{3}$	$\frac{1}{4}$	ST
	$\frac{1}{2}$	$\frac{1}{3}$	G
Ehrhard and Davis (1991), $m=3$	$\frac{1}{7}$	$\frac{1}{10}$	ST
	$\frac{1}{4}$	$\frac{1}{7}$	G

flow that has the additional information of $\theta_I=\theta_I(R)$. Here the angle θ_I is an intermediate angle inferred from the asymptotics of Hocking for $\beta_0\to 0$ as a function of distance R from the contact line. Ngan and Dussan V. (1989) obtained this relation in the form

$$\theta_I\sim\theta_s+C\left[\frac{2\sin\theta_s}{\theta_s-\sin\theta_s\cos\theta_s}\left(\ln\frac{R}{\beta}+1\right)+l(\theta_s)\right]+\cdots, \tag{5.16}$$

where β is the slip length scale, $R/\beta\to\infty$, $l(\theta_s)$ depends directly on the form of the slip boundary condition, and C is capillary number

$$C=\frac{\mu u_{\mathrm{CL}}}{\sigma}. \tag{5.17}$$

Note that Eq. (5.16) is valid in the limit of $\beta_0\ll C\ll 1$. Dussan V. *et al.* (1991) show good agreement with predictions from this theory by measurements in mutual displacement systems.

Another approach to spreading for $\theta_A=0$ is that of De Gennes (1985), who wished to examine the small-scale physics of contact lines. He reasoned that with "perfect" spreading there should be a nearly uniform precursor foot ahead of the droplet in which attractive van der Waals forces are effective. In such a "foot" he takes

$$\phi=\phi_r+\frac{A'}{6\pi h^3},\quad A'<0, \tag{5.18a}$$

as the potential for these forces. He analyzes the thick drop that smoothly blends into the foot, which extends far forward along the substrate. On the one hand there is no longer a contact line nearby to consider, and, on the other hand, the actual contact line at the edge of the foot is not considered. This model is able to predict an apparent contact angle θ satisfying Eq. (5.8a) with $\theta_A=0$ and $m=3$.

When $\theta_A>0$, the model (5.18a) no longer holds and one must use a van der Waals model appropriate to a wedge-shaped region. Hocking (1995a) showed that in this case

$$\phi=\phi_R+\frac{A'}{6\pi h^3}[(\partial_x h)^4-\theta_A^4],\quad A'<0, \tag{5.18b}$$

where A' is a modified Hamaker constant. In Hocking's theory θ_A is constant, and when he solves the spreading-

drop problem with such a force potential, he finds that the contact-angle condition emerges as a natural boundary condition; the power laws (5.13) remain unchanged, though the multipliers do change slightly. His conclusion is that the presence of the van der Waals potential does not have a significant effect on the spreading process for $\theta_A > 0$.

As discussed above, the macroscopic dynamics of spreading drops, and hence spreading in general, is connected to the microscale physics and chemistry of the system by the conditions at the contact line, namely, the slip condition (5.1) and the contact-angle condition (5.7). Great progress has been made in recent years, beginning with the work of de Gennes (1985), on the underlying mechanisms present in a small region near the contact line. This work was recently reviewed by Leger and Joanny (1992), who carefully discuss the origin of contact-angle hysteresis by roughness (defects) and chemical inhomogeneity of the surface including the possibility of irregular jump motions of the contact line. They further discuss the possibility of "layered" potentials for the van der Waals forces [see for example, Eq. (2.48e)] in complete spreading. Such studies are essential for understanding the macroscale dynamics, since they supply the bases for the slip models and $\theta = \theta(u_{\mathrm{CL}})$.

There is quite an interesting effect of gravity on the spreading of droplets. Assume that gravity acts vertically downward as shown in Fig. 31. Ehrhard and Davis (1991) and Smith (1995) derive the evolution equation

$$\overline{C}_m \partial_T H + \partial_X \left[\left(\frac{1}{3} H^3 + \beta_0 H^2 \right) \partial_X (\partial_X^2 H - GH) \right] = 0, \tag{5.19}$$

where the Bond number G is

$$G = \frac{\rho g L^2}{\sigma}. \tag{5.20}$$

When the drop is initially "thick," hydrostatic pressure will of course tend to flatten the drop and enhance its spreading rate. When the drop thins as it spreads, hydrostatic effects become negligible. However, at yet later times, as shown by Ehrhard and Davis (1991), hydrostatic effects reemerge as being important, since at very long times the curvature $\partial_X^2 H \to 0$ more quickly than $H \to 0$. This is in agreement with the observations of Cazabat and Cohen-Stuart (1986). These power laws are also given in Table I.

Brenner and Bertozzi (1993) showed that the similarity solution given by Starov (1983) is linearly stable with respect to perturbations vanishing outside the area of the drop. By doing this they showed why the experimental spreading law, Eq. (5.13), given by Tanner (1979) and Lopez *et al.* (1976) is observed. They also showed that the spreading time scale exhibits a dependence on the microscopic length scale in the vicinity of the contact line.

C. Thermocapillarity

Consider now the case of a spreading droplet on a uniformly heated plate. Here $\Pi_0 = \tau_0 = 0$, β_0 is constant,

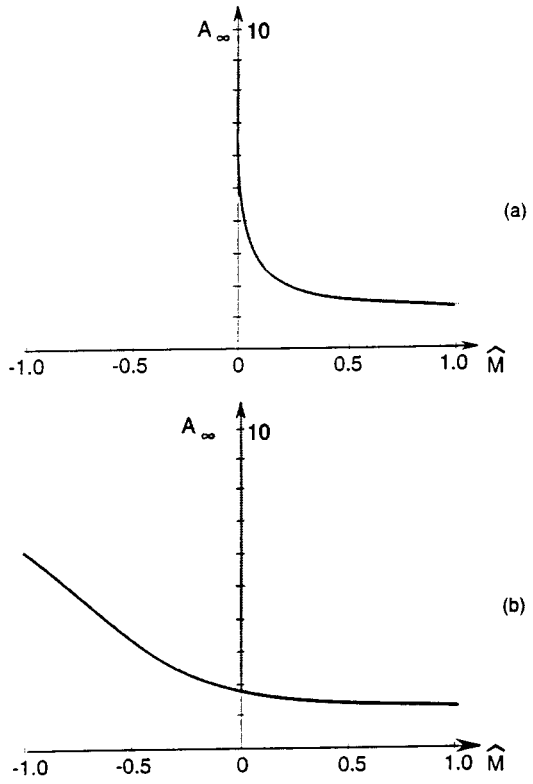

FIG. 33. Final spreading: final drop widths A_∞ as functions of Marangoni number $\hat{M}$ for $G=0$ and $B \ll 1$, for two different advancing contact angles: (a) $\theta_A = 0$; (b) $\theta_A = 0.5$. The curves are obtained from Eq. (5.21). Copyright © 1991 Cambridge University Press. Reprinted with the permission of Cambridge University Press from Ehrhard and Davis (1991).

but $\sigma = \sigma(\vartheta)$. Thermocapillarity creates a flow in the drop that can augment or retard the spreading. As in Sec. II.F one can solve first for the temperature ϑ as a functional of H and hence determine the thermocapillary shear stress $\partial_X \Sigma$ on the interface. One can then obtain the evolution equation (2.63) with $\gamma(H) = 1$, except that now slip must be retained. Ehrhard and Davis (1991) found that

$$\overline{C}_m \partial_T H + \partial_X \left[\left(\frac{1}{3} H^3 + \beta_0 H^2 \right) \partial_X (\partial_X^2 H - GH) \right] + \partial_X \left[\frac{\hat{M}}{(1+BH)^2} \left(\frac{1}{2} H^2 + \beta_0 H \right) \partial_X H \right] = 0, \tag{5.21}$$

where $\hat{M}$ is the effective Marangoni number. The contact-line conditions are identical to those given above.

Ehrhard and Davis (1991) showed that, for $\overline{C}_m \to 0$, heating retards the spreading; even if $\theta_A = 0$, the heated drop will cease spreading at a finite width. Of course, this final state is a dynamical one involving circulation of the liquid. Figure 33, taken from Fig. 8 of Ehrhard and Davis (1991), shows how heating, $\hat{M} > 0$, retards spreading, while cooling, $\hat{M} < 0$, promotes spreading. In neither case does the spreading follow a power law. Transient

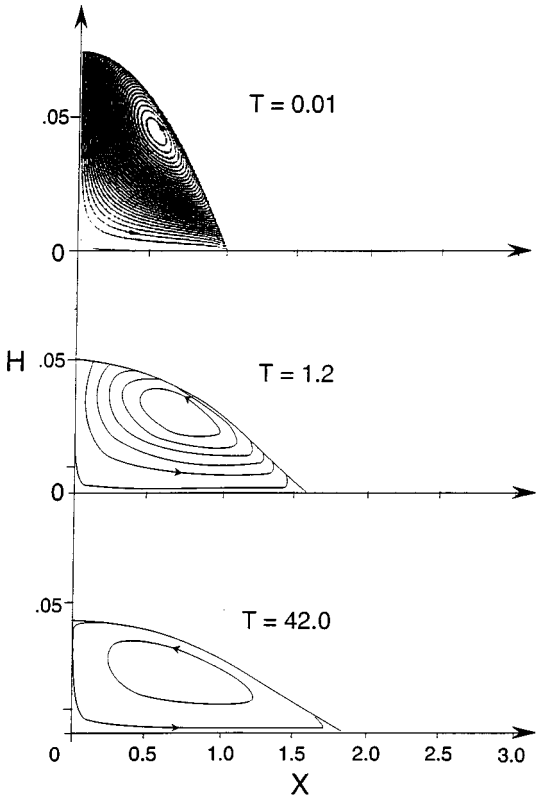

FIG. 34. Nonisothermal spreading: evolution of the stream function with $\hat{M}=0.2, \theta_A=0.25$, $B \ll 1$, and $G=0$. Instantaneous streamlines are given in steps of $\Delta\psi=0.01$. Copyright © 1991 Cambridge University Press. Reprinted with the permission of Cambridge University Press from Ehrhard and Davis (1991).

behavior for $\hat{M}>0$ is shown in Fig. 34. The evolution to the final shape involves the spreading flow along a heated substrate and a counterflow up the interface driven by thermocapillarity.

D. Evaporation/condensation

If a droplet is composed of a volatile liquid, the spreading and mass loss can compete to determine the dynamics of the drop.

The governing evolution equation is Eq. (2.92), but with slip retained:

$$\partial_T H + \frac{E}{H+K} + \partial_X\left[\overline{C}_m^{-1}\left(\frac{1}{3}H^3+\beta_0 H^2\right)\partial_X^3 H\right] + \partial_X\left[MKP_r^{-1}\frac{(\frac{1}{2}H^2+\beta_0 H)\partial_X H}{(H+K)^2} + \frac{4}{3}E^2 D^{-1}\frac{(\frac{1}{3}H^3+\beta_0 H^2)\partial_X H}{(H+K)^3}\right]=0, \tag{5.22}$$

with the edge conditions at $X=\pm A$

$$H=0 \tag{5.23}$$

and

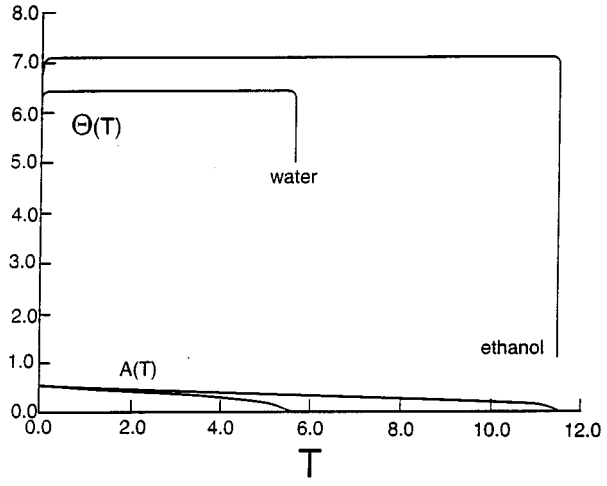

FIG. 35. The angle θ and the location of the contact line A in a spreading drop as functions of time T. Reprinted with the permission of the American Institute of Physics from Anderson and Davis (1995).

$$\partial_X H = \mp \tan\theta. \tag{5.24}$$

Anderson and Davis (1995) further allowed the apparent contact angle to depend explicitly on the mass transport due to phase transformation and hypothesized the edge condition

$$\frac{dA}{dT} = -\frac{\epsilon}{\hat{K}\theta(T)} + \overline{\eta}\, f(\theta), \tag{5.25}$$

where $\overline{\eta}$ is constant and $f(\theta)=(\theta-\theta_A)^m$ for $\theta>\theta_A$, $f(\theta)=0$ for $\theta_R<\theta<\theta_A$, and $f(\theta)=(\theta-\theta_R)^m$ for $\theta<\theta_R$, in which the contact line moves by the joint effects of spreading and mass loss. This results in an increase in the apparent contact angle as a function of the rate of heating. Thus heating directly affects both the evolution equation and the edge condition.

One result of following the evolution in time of a spreading drop is that, for nearly the full lifetime of the drop, there is a balance between the mass loss and the spreading, giving a drop with a nearly constant contact angle significantly larger than that given by the thermodynamics for the evaporation-free case. Figure 35, taken from Fig. 10 of Anderson and Davis (1995), shows the angle in a spreading drop as a function of time.

Hocking (1995b) took the microscopic angle to be constant (unaffected by mass transport) and analyzed a steady version of the above system with mass loss present in the evolution equation but absent in the edge condition. He found the same qualitative effects of evaporation as Anderson and Davis (1995), although the magnitudes of the steepening are smaller.

Wayner (1982, 1993, 1994) has proposed and observed experimentally a means for the propagation of the contact line by a mass-transfer processes in which liquid evaporates from the drop and condenses on the substrate ahead of the drop. This process might be especially effective in heated systems.

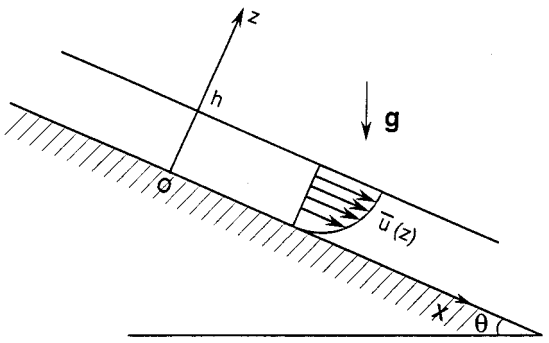

FIG. 36. Schematic of the problem for a falling film.

VI. RELATED TOPICS

A. Introduction

The approach to the analysis of thin films as described depends on the use of lubrication scalings to derive strongly nonlinear evolution equations that contain sufficient dynamics. This approach is applicable to a great number of related problems that will not be described in detail here. However, a few of these shall be sketched with the aim of providing the reader entries into the literature. The problems illustrate some of the different phenomena that may be addressed.

B. Falling films

Consider a thin liquid layer flowing down a plane inclined to the horizontal by angle θ as shown in Fig. 36. The equations are consistent with a uniform film of depth h_0 in parallel flow with profile

$$\overline{u}(z)=\frac{\rho g\sin\theta}{\mu}\left(h_0 z-\frac{1}{2}z^2\right) \tag{6.1a}$$

and hydrostatic pressure distribution

$$\overline{p}(z)=p_a+\rho g\cos\theta(h_0-z). \tag{6.1b}$$

This layer is susceptible to long-surface-wave instabilities, as discovered by Yih (1955, 1963) and Benjamin (1957) using linear stability theory; the neutral curve is shown in Fig. 37. Benney (1966) extended the theory into the nonlinear regime by deriving a nonlinear evolution equation for the interface shape $z=h(x,t)$. There have been a number of extensions of this work, as discussed by Lin (1969), Gjevik (1970), Roskes (1970), Atherton and Homsy (1976), Krishna and Lin (1977), Pumir *et al.* (1983), and Lin and Wang (1985). Nakaya (1975, 1978, 1981, 1983, 1989), among others, examined various dynamics in the nonlinear range.

For three-dimensional waves and $Z=H(X,Y,T)$, the dimensionless evolution equation, which we shall call the Benney equation, has the form (Roskes, 1970; Lin and Krishna, 1977; see also Joo and Davis, 1992a, 1992b for the case of a vertical plane, $\theta=\pi/2$)

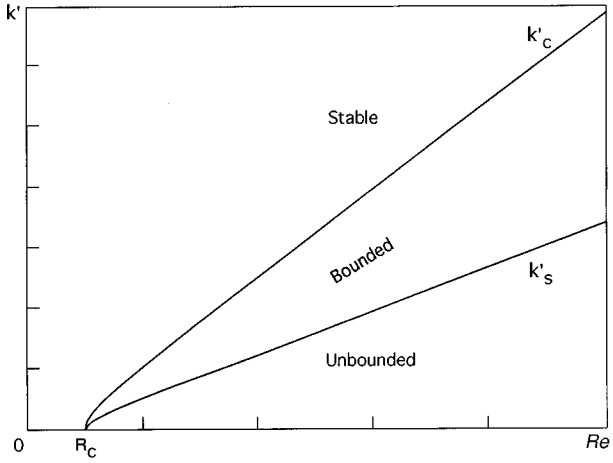

FIG. 37. Phase diagram for the Benney equation (6.2). $R_c=\frac{5}{2}\cot\theta$ is the critical value of the Reynolds number Re. For $Re<R_c$ the state $H=1$ is stable. If $Re>R_c$ then (i) for $k'<k'_s$ two-dimensional waves blowup in a finite time; (ii) for $k'_s<k'<k'_c$ two-dimensional waves saturate; (iii) for $k'>k'_c$ initial perturbations of $H=1$ decay. Here $k'_c=[\frac{2}{15S}Re(Re-R_c)]^{1/2}$ and $k'_c=2k'_s$.

$$\partial_T H+ReH^2H_X+\epsilon\partial_X\left[\frac{2}{15}Re^2(H^6\partial_X H)\right]$$
$$-\frac{1}{3}G\cos\theta\vec{\nabla}_1\cdot(H^3\vec{\nabla}_1 H)+S\vec{\nabla}_1\cdot(H^3\vec{\nabla}_1\nabla_1^2 H)=O(\epsilon^2), \tag{6.2}$$

where

$$G=\frac{\rho^2 h_0^3 g}{\mu^2},\quad Re=G\sin\theta,\quad S=\epsilon^2\frac{\rho\sigma h_0}{3\mu^2}=O(1), \tag{6.3}$$

and Re is the Reynolds number.

Notice that the unit-order terms of Eq. (6.2) contain no instabilities but generate waves that propagate and steepen as they travel. This can be easily seen, since the first two unit-order terms of Eq. (6.2) constitute a well-known first-order nonlinear wave equation (see, for example, Whitham, 1974). One must retain $O(\epsilon)$ terms in order to find an instability which is given by the third term. The hydrostatic-pressure and surface-tension effects are conveniently postponed to $O(\epsilon)$ in order to compete with the surface-wave growth.

Notice also that the mean flow, driven by the component of gravity down the plate, gives the wave propagation (term No. 2) and the wave instability (term No. 3) preferred orientations but leaves the surface tension (term No. 5) and hydrostatic pressure (term No. 4) isotropic in X and Y.

Linear theory of the film of unit thickness leads to waves that propagate at linearized phase speed c_L,

$$c_L=Re, \tag{6.4}$$

and growth rate

$$\omega=\epsilon k'^2\left(\frac{2}{15}Re^2-\frac{1}{3}G\cos\theta-Sk'^2\right). \tag{6.5}$$

Here the dimensionless wave vector is written $\mathbf{k}'=k'(\cos\theta_k,\sin\theta_k)$ so that by linear theory only two-dimensional waves are preferred, i.e., $\theta_k=0$ maximizes ω. Figure 37 shows for $\theta_k=0$ the neutral curves of k' versus Re. The figure also shows the result of a weakly nonlinear analysis of Eq. (6.2). See Lin (1969) and Gjevik (1970), in which a two-dimensional theory is developed. Here all dependent variables of the disturbance equations, say, $p=\mathsf{A}p_1+\mathsf{A}^2p_2+\cdots$ and the amplitude $\mathsf{A}(t)$ are found to satisfy a Landau equation,

$$\dot{\mathsf{A}}=\mathsf{A}-\delta|\mathsf{A}|^2\mathsf{A}. \tag{6.6}$$

Here A is the complex amplitude of the unstable wave, depending on the slow time t, and δ is positive above and negative below the curve $k_s'(Re)$, indicating bifurcation that is supercritical when positive and subcritical when negative. Subcritical bifurcation indicates a jump transition to surface-wave instabilities while supercritical bifurcation indicates a smooth transition (see, for example, Seydel, 1988).

The results based on the numerical solution of Eq. (6.2) are that if k' is the initial wavelength, there exists a value k_s' such that

(i) For $k_c'>k'>k_s'$, two-dimensional waves saturate (Gjevik, 1970).
(ii) For $k'<k_s'$, two-dimensional waves blow up in a finite time (Gjevik, 1970).
(iii) For the vertical plate case ($\theta=\pi/2$), all two-dimensional equilibrated waves are unstable to disturbances spatially synchronous downstream, leading to periodic, cross-stream, complex three-dimensional patterns (Joo and Davis, 1992a).
(iv) For the vertical plate, all two-dimensional equilibrated waves are unstable to two-dimensional disturbances spatially subharmonic downstream (Joo and Davis, 1992b). Here for the vertical plane $k_c'=\sqrt{2G^2/15S}$ is the cutoff wave number found from the linear theory and $k_s'=k_c'/2$. See also Prokopiou *et al.* (1991) for comparable and more extensive results at higher Re. Liu *et al.* (1995) have examined transitions to three dimensions at higher Reynolds number and on a plate with small inclination (see Fig. 1). Results similar to (i) and (ii) were also obtained by Rosenau *et al.* (1992).

Equation (6.2) in two dimensions ($\partial/\partial Y=0$) can be reduced to a weakly nonlinear equation as shown by Sivashinsky and Michelson (1980), if one writes $H=H_0+\epsilon\overline{H}(\xi,\tau)$, and if H_0 is constant, with a slow time $\tau=\epsilon T$, and translates with the linear phase speed c_L, $\xi=X-ReH_0^2T$. The resulting system is

$$\partial_\tau\overline{H}+2ReH_0\overline{H}\,\partial_\xi i\overline{H}+\gamma\partial_\xi^2\overline{H}+SH_0^3\partial_\xi^4\overline{H}=0, \tag{6.7}$$

known as the Kuramoto-Sivashinsky equation (Nepomnyashchy, 1974; Kuramoto and Tsuzuki, 1975, 1976; Sivashinsky, 1977). Here $\gamma=2Re^2H_0^6/15-GH_0^3\cos\theta/3$. This is a well-studied equation (see Hyman and Nicolaenko (1986); Kevrekidis *et al.* (1990)], which has only bounded solutions that are steady, time-periodic, quasi-periodic, or chaotic. Different equations displaying breaking waves and related to Eq. (6.7) were given by Oron and Rosenau (1989) and Rosenau and Oron (1989).

In the derivation of Eq. (6.2), the inertial terms, which are multiplied by Re, are considered small at leading order and enter the evolution equation at $O(\epsilon)$. As we shall shortly see, this restricts the validity of Eq. (6.2) to Re numerically small. If one wishes to describe flows at large Re, one must retain inertia at leading order, i.e., the downstream component of the momentum balance that needs to be solved is

$$\epsilon Re(\partial_T H+U\partial_X H)=-\partial_X P+\partial_Z^2 U, \tag{6.8}$$

with the pressure P satisfying a hydrostatic balance. This is a boundary-layer problem [when $\epsilon Re=O(1)$], which has been solved approximately by Prokopiou *et al.* (1991) by using a Karman-Pohlhausen method in which one presumes a Z profile for U and Eq. (6.8) is replaced by its Z-averaged version. The results are not asymptotic but do give better predictions of flows at higher Reynolds numbers than does Eq. (6.2). Rather than a simple equation, one obtains a complicated system,

$$\partial_T H+\partial_X q=0, \tag{6.9a}$$

$$F(H,q)=0, \tag{6.9b}$$

where $q=\int_0^H U\,dZ$ is the volumetric flow rate per unit-span width, and F is a pseudo-differential operator (Shkadov, 1967, 1968; Alekseenko *et al.*, 1985; Chang *et al.*, 1993; Chang, 1994).

Clearly, one can couple the dynamics of the falling film with the phenomena earlier explored, viz., heat and mass transfer, van der Waals attractions, etc. Rather than give the details, we only list a few references: Lin (1974), Sreenivasan and Lin (1978), Kelly *et al.* (1986), Joo *et al.* (1991,1997), and Oron and Rosenau (1992).

C. Falling sheets

Again consider a plane inclined to the horizontal by angle θ as shown in Fig. 38. Now, however, one begins with a dry plane and opens a gate at $x=0$ that allows the viscous liquid to flow down the plate with a straight contact line that moves in the positive x direction. The supply of liquid can be infinite (see Fig. 38, curve 1) or the gate can be shut in a finite time, creating a trailing contact line on a sheet of a fixed volume, analogous to a two-dimensional drop rolling down the plate (Fig. 38, curve 3).

Huppert (1982b) showed experimentally in the latter case that the leading edge becomes unstable in either of two ways, both periodic in the cross-stream direction y. Either long fingers develop with sides parallel to the x direction with the roots fixed to the plate or triangular fingers form, traveling downward with their roots moving downward as well (see Fig. 2). Further experiments

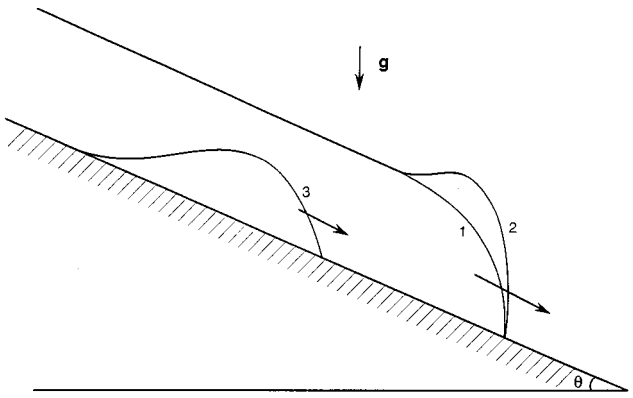

FIG. 38. Schematic of the problem for a falling sheet (curves 1, 2) and liquid ridge (curve 3). Arrows indicate the direction of the flow.

by Silvi and Dussan V. (1985) show that the magnitude of the contact angle determines which type of finger appears.

The basic state of the infinite sheet is shown in Fig. 38; as the sheet moves downward, a bead or ridge forms behind the leading edge (see Fig. 38, curve 2), giving rise to what appears to be a section of a quasisteady cylinder. This is formed because in a frame of reference moving with the contact line there is a recirculating flow down along the free surface toward the contact line and returning along the plate. The recirculation is caused by the presence of the contact line, slowing the drainage of the film. The return flow is generated by an induced pressure gradient due to the downstream "wall," the leading edge of the film. The induced high pressure near the contact line deforms the interface producing the ridge (Spaid and Homsy, 1996). On a vertical wall, the ridge is present. As the tilt angle of the plate is decreased, hydrostatic pressures will cause the ridge to decrease in size. For plates at small angles the ridge may be very small or absent.

The governing lubrication equation for this system is given by Hocking (1990),

$$\partial_T H+\frac{1}{3}G\partial_X[H^2(H+\beta_0)]\sin\theta+\vec{\nabla}_1\cdot\Big[H^2(H+\beta_0)\times\vec{\nabla}_1\Big(S\vec{\nabla}_1^{2H-\frac{1}{3}GH\cos\theta}\Big)\Big]=0, \tag{6.10}$$

where G and S are given by Eq. (6.3) and β_0 is the constant slip coefficient [see Eq. (2.16)]. Appropriate edge conditions are posed as well as periodicity in Y.

Hocking (1990) considered a falling ridge, i.e., a sheet with two contact lines. He points out that the similarity solution found by Huppert (1982b) is not valid at the trailing edge and that the similarity solution ends abruptly at a nonzero height and therefore cannot represent the liquid ridge in the whole domain. These deficiencies call for the construction of two inner solutions, one at each edge of the ridge. These are constructed as similarity solutions for Eq. (6.10) while using a slip condition and an assumption of quasisteady state at the leading edge. The solution exhibits a bulge near the leading edge of the sheet. Hocking suggested that the instability of the leading edge is related to the fluid flow in the bulge. He also established linear instability to spanwise disturbances of a fluid ridge moving with both contact lines straight.

Troian *et al.* (1989) considered the fingering instability of falling sheets as an instability of the self-similar basic state (Huppert, 1982b), represented by a balance between gravity and viscous forces that blends into a very thin precursor film of uniform thickness running ahead of the contact line. Linear stability analysis shows that the fastest growth of the disturbances occurred near the "virtual contact line," where capillary forces were comparable to viscous and gravitational forces. A preferred wavelength, weakly dependent on the thickness of the thin precursor film for linear stability, is predicted and agrees well with their experimental data. Brenner (1993) studied the growth in time of the most unstable wavelength. He derived analytical expressions in good qualitative agreement with the experimental results of de Bruyn (1992) for a liquid sheet of fixed volume proceeding down an inclined plane. Lopez *et al.* (1996) used a slip model for a liquid sheet of fixed flow rate, and hence of constant far-field thickness, and predicts fastest-growing wave numbers in good agreement with (although somewhat lower than) the wave numbers of fully developed rivulets measured by Johnson *et al.* (1996). The fully nonlinear lubrication calculation was in better agreement with the data than the linear theory.

The nonlinear evolution of a liquid ridge moving down an incline was examined by Hocking and Miksis (1993). The study was based on a quasisteady hypothesis and the assumption of the dynamic variation of the contact angle given by Eq. (5.8a). It was found that fluid is transferred laterally into growing lobes at the expense of thinner parts of the ridge. The process continues until the leading and the trailing edges meet. Using the linear stability theory, presented earlier by Hocking (1990), they reconsidered the problem, taking the presence of contact lines into account instead of using a quasisteady assumption. The results indicate that a preferred wavelength exists, and to this extent they parallel the results of Troian *et al.* (1989). In both cases the wavelength is not completely determined, being weakly dependent on the thickness of the precursor film (Troian *et al.*, 1989) or logarithmically dependent on the value of the slip coefficient (Hocking and Miksis, 1993). It should be noted that the thickness ratio of the precursor layer to the bulk film far from the contact region may be $O(10^{-5})$ to $O(10^{-6})$, which suggests that intermediate scaling may be needed for asymptotic consistency.

Moriarty *et al.* (1991) developed a spreading theory for a falling-liquid ridge in the case of small surface tension. The solution for the corresponding evolution equation was constructed using the method of matched asymptotic expansions. At the front the flow was shown to be governed by a balance between viscous, gravitational, and capillary forces, while away from it the mo-

tion is governed by the balance between viscous and gravitational forces. The authors used the concept of the precursor film to model the behavior of the contact line. Various problems related to the effective slip in the vicinity of the moving contact line were discussed by Tuck and Schwartz (1990) and Moriarty and Schwartz (1992).

The ridge behind the leading edge might be susceptible to Rayleigh-Taylor-type instability see (Chandrasekhar, 1961) or capillary instability (Rayleigh, 1894), but Spaid and Homsy (1996) showed by examining the energy balances in the linear stability theory that a kinematic mechanism is responsible, i.e., a perturbed capillary ridge subject to the body force $\rho g \sin\theta$ has thicker regions of liquid advancing more rapidly than the thinner regions. Small scale cross-stream perturbations are stabilized by surface tension.

Spaid and Homsy (1996) analyzed the film in two ways: (i) with a contact line and slip and (ii) with a precursor layer and no contact line. These two models produce similar ridges, and the instability depends only on the shape of the ridge.

D. Hele-Shaw flows

Slow flows of a viscous fluid between two closely spaced plates are Hele-Shaw flows. In such a case the flow field is approximately plane Poiseuille flow. In the absence of gravity the velocity components are proportional to the pressure gradients in the respective directions. Extensive treatment of Hele-Shaw flows was presented in Bensimon *et al.* (1986) and Homsy (1987). In the case of a horizontal one-dimensional Hele-Shaw flow, the longitudinal component of the flow field is given by

$$u = -\frac{b^2}{12\mu}\partial_x p, \tag{6.11}$$

where b is the width of the gap between the plates. If two immiscible fluids of greatly different viscosities are placed within a Hele-Shaw cell, the pressure p_a in the less viscous fluid can be assumed to be uniform in space. The dynamics of the interface separating these two fluids can also be described using the lubrication approximation.

When a thin liquid neck of a local thickness $2h(x,t)$ bounded by the other fluid on both sides is considered to be symmetrical, the location of the interfaces is at $z=\pm h$. The total liquid volumetric flux per unit depth through the cross section of the neck is uh, and therefore it follows from the continuity equation that

$$\partial_t h + \partial_x(uh) = 0. \tag{6.12}$$

The substitution of Eq. (6.11) into Eq. (6.12) and the use of the boundary condition for the balance of the normal stresses at the interface

$$p_a - p = \sigma \partial_x^2 h, \tag{6.13}$$

yield the evolution equation (Constantin *et al.*, 1993)

$$\mu \partial_t h + \frac{b^2\sigma}{12}\partial_x(h\partial_x^3 h) = 0. \tag{6.14}$$

This is analogous to Eq. (2.31) for surface tension only and $\tau=0$, but with h^3 replaced by h.

If one considers the effect of gravity on Hele-Shaw flows, the evolution equation will contain a linear advective term proportional to $\partial_x h$, which can be removed by introducing a moving frame of reference. It is found that at a late stage of evolution the minimal thickness of a neck decreases with time as t^{-4}, and breakup is achieved at infinite time (Constantin *et al.*, 1993). Finite-time rupture in the droplet-breakup problem in the Hele-Shaw cell was investigated in the context of Eq. (6.14) solved given a smooth initial condition (Dupont *et al.*, 1993). They also found that at the time of pinchoff the width of the neck grows quadratically as one moves away from the point of breakup.

Almgren (1996) studied rupture in Hele-Shaw flows and tested the validity of Eq. (6.14) near those points by comparing its solutions with the solutions of the Hele-Shaw approximation of the Navier-Stokes problem. Both approaches showed the appearance of rupture in finite times. It was concluded that the lubrication approximation, Eq. (6.14), is a faithful one and reproduces well the regime of rupture.

Traveling-wave solutions for a general equation of the type

$$\partial_t h + \partial_x(h^n \partial_x^3 h) = 0, \tag{6.15}$$

where n is constant, were studied by Boatto *et al.* (1993). It was found that transitions between different qualitative behaviors occurred at n=3, 2, 3/2, and 1/2. Soliton-like localized waves were determined to be possible only for $n<3$. The generic solution that represents a receding front is present for all $n>0$.

Consideration of density-stratified Hele-Shaw flows leads to the dimensionless evolution equation (Goldstein *et al.*, 1993) of the form

$$\partial_T H + B_d \partial_X(H\partial_X H) + \partial_X(H\partial_X^3 H) = 0, \tag{6.16}$$

where B_d is a Bond number relating the density jump effects to those due to capillarity,

$$B_d = \frac{2g\Delta\rho b}{\sigma}, \tag{6.17}$$

with b being the width of the Hele-Shaw cell. Equation (6.16) is analogous to Eq. (2.31) with H^3 replaced by H in the fourth-order term. Rupture was studied by Goldstein *et al.* (1995).

VII. SUMMARY

Several closing remarks are now in order. First of all, like any other theory, the long-wave theory of evolution of liquid films has to be verified against the results of experimental studies.

Several experimental works that have appeared in the literature support the theory and provide encouraging results even beyond the formal range of its validity. Bu-

relbach *et al.* (1990) performed a series of experiments in an attempt to check the long-wave theory developed by Tan *et al.* (1990) for steady thermocapillary flows due to nonuniform heating of the solid substrate. The measured steady shapes were tested against theoretical predictions, and good agreement was found for layers less than 1 mm thick under moderate heating conditions, where the temperature difference along the plate was 50 °C over a 5-cm length. The relative error was large for conditions near rupture (where the long-wave theory is not valid; see Burelbach *et al.*, 1988), but in all other cases the predicted and measured minimum film thicknesses agreed to within 20%. The theory (Tan *et al.*, 1990) also predicts rupture when the parameter $B_{\rm dyn}$ of Eq. (3.6) exceeds a certain critical value $B^c_{\rm dyn}$ and steady patterns for $B_{\rm dyn}<B^c_{\rm dyn}$. Experimental results (Burelbach *et al.*, 1990; see Fig. 1) showed that $B_{\rm dyn}$ is an excellent qualitative indicator of whether or not the film ruptures. This confirmed validity of the thermocapillary theory is a good indication that long-wave analysis should also be valid for more general systems with phase transformation (evaporation/condensation) and also for transient states of the film.

van Hook *et al.* (1995) performed experiments on the onset of the long-wavelength instability in a thin layer of silicone oil of thickness ranging between 0.005 cm and 0.025 cm and aspect ratio between 150 and 750 when the temperature drop across the layer was between 0.05 °C and 5 °C. A formation of ''dry spots'' at randomly varying locations was found above the critical temperature difference across the layer. The experimental results were checked versus solutions of one- and two-dimensional versions for the evolution equation (2.63) with $\gamma(H)=1$. A qualitative agreement of the structure of the dry spots with corresponding numerical simulations was found. van Hook *et al.* (1996) developed a two-layer model taking into consideration the change in the temperature profile in the air due to deformation of the interface. This two-layer model reduces to the one-layer model given by Eq. (2.63) in an appropriate limit. The experimental results of van Hook *et al.* (1996) are found to agree quantitatively with a two-layer model for certain liquid depths.

A theoretical study of the Rayleigh-Taylor instability in an extended geometry (Fermigier *et al.*, 1992) on the basis of the long-wave equation shows the tendency of hexagonal structures to emerge as a preferred pattern, in agreement with their experimental observations.

Goodwin and Homsy (1990) analyzed the falling sheet by direct integration of the Stokes flow (creeping flow) equations and found good agreement with the lubrication theory when the contact angle was small, i.e., when for $C\to 0$, $C^{-1}\theta_s^3\sim 1$.

In some cases experiments run ahead of theory. Thinning by evaporation of completely wetting thin water films was studied experimentally by Elbaum and Lipson (1994). Dewetting of the substrate was found to begin with nucleation and spreading of dry spots in which the film thickness ranged typically tens of Angströms. Toroidal rims forming around circular dry patches underwent a sequence of instabilities and collapsed into a series of droplets behind the drying front. Further study of the late stage of the breakup was done by Elbaum and Lipson (1995). They found that the wavelength of the patterns at the initial stage of instability of the rim was comparable to its diameter. That suggests that the initial stage of the breakup is governed by the capillary instability. However, at long times the characteristic wavelength is different, which leads to the conclusion that other than capillary mechanisms are involved in the process. A theoretical explanation of the phenomenon has not yet been found.

Another test for the validity of an asymptotic theory, such as the long-wave theory presented here, is via comparison of the solutions given by the long-wave evolution equations and the numerical solutions for the full original free-boundary problem from which the evolution equation was derived. Given the intrinsic complexity of the latter, there is only a limited number of such comparative studies. Krishnamoorthy *et al.* (1995) studied the spontaneous rupture of thin liquid films due to thermocapillarity. A full-scale direct numerical simulation of the governing equations was performed, and its results were found to exhibit very good qualitative agreement, except for times very close to rupture. More tests done for different aspects of falling films are mentioned below.

As an attempt to extend long-wave theories to falling-film flows, terms of higher order than unity are retained. As discussed in Sec. VI.B, such efforts have led to the discovery of new phenomena. Such Benney-type equations for falling films have unbounded solutions in certain parametric domains and bounded solutions in others. This was demonstrated by Pumir *et al.* (1983) and Rosenau *et al.* (1992) for the Benney equation. Clearly, solutions of a large, or infinite, amplitude do not describe real physical effects and are artifacts of the approximation that led to the specific evolution equations being solved. This suggests that some formally small terms of higher order neglected by the asymptotic expansion become significant. Therefore the ordering of the asymptotic series breaks down, and this results in a failure of the evolution equation derived to represent a rightful limiting case of the original set of governing equations. Frenkel (1993) argues that evolution equations of the Benney type are not uniformly valid in time. One of the reasons for this is that the expansion parameter ϵ employed in the asymptotic series is based on the initial characteristic wavelength λ of the disturbance. However, as a result of nonlinear interaction the effective value of ϵ increases as a result of decrease of λ, and thus after some time its initial value becomes irrelevant.

Several authors have tested the results of the two-dimensional version of Eq. (6.2) in the domain of saturating solutions, $k_s'<k'<k_c'$ (see Sec. VI.B), against direct numerical solutions of the Navier-Stokes equations. A few early results were given by Ho and Patera (1990) and Salamon *et al.* (1994). They reported good agreement between the long-wave theory and the full problem. A systematic study has recently appeared by

Ramaswamy *et al.* (1996), who examined the two-dimensional vertically falling film and showed that there was a very good quantitative agreement with the results of Eq. (6.2) for $k > k_s$ and $G \leqslant 5$, and poorer agreement thereafter, when $SG^{-1/3} = 100$. [The reader should not forget that the Benney equation holds for $G = O(1)$.]

Kim *et al.* (1992) studied the effect of an electrostatic field on the dynamics of a film flow down an inclined plane. They compared the results given by the long-wave evolution equation with those of the Karman-Pohlhausen approach, Eqs. (6.9), and direct numerical computations of the full free-boundary problem. Their long-wave evolution equation was similar to Eq. (6.2) but contained an extra term, corresponding to the applied electrostatic field. Solutions for the models and the full problem were qualitatively similar for the surface deformations and pressures, when the Reynolds number was relatively low, $Re \sim 5$. For larger Re, a boundary-layer approach using the Karman-Pohlhausen approximation was found very good in its prediction of steady states of the film. The transient states of the Karman-Pohlhausen model and the full problem, although qualitatively similar, had quantitative differences.

A somewhat easier, but less conclusive, test of the theory would be to solve the asymptotic hierarchy of the equations to one order higher than that at which closure of the problem and the evolution equation are attained. By solving the evolution equation and substituting its solution into the next-order terms of the asymptotic expansions for the dependent variables, e.g., velocity, pressure, temperature, etc., one can determine whether they constitute a small correction for the leading-order terms. A positive answer validates the results of the expansion and thus the asymptotic correctness of the resulting evolution equation.

The possibility of the emergence of nonphysical solutions degrades to a certain extent the usefulness of the Benney equation in studying the behavior of a falling film. As an alternative one may consider using the ''boundary-layer'' approach of Eqs. (6.9). Another alternative is to reduce the strongly nonlinear Benney equation to a weakly nonlinear Kuramoto-Sivashinsky equation (6.7) whose solutions are bounded and smooth at all times. This reduction, however, is rigorously valid for interfacial deflections that one very small compared to the average film thickness.

A reason for caution, as mentioned above, is the emergence of higher Fourier modes in the solutions, which are fed by the strongly nonlinear nature of the equations. These long-wave equations are derived under the assumption that the average thickness of the fluid layer will be small with respect to the characteristic wavelength of the interfacial perturbations, and thus the spatial gradients along the interface will also be small. However, the presence of higher subdominant modes in the solution giving multihumped patterns similar to that displayed in Fig. 28, does not preclude their relevance, as shown by Krishnamoorthy *et al.* (1995) for horizontal layers, Ramaswamy *et al.* (1996) Krishnamoorthy *et al.* (1997a) for two-dimensional heated falling films, and Krishnamoorthy *et al.* (1997b) for three-dimensional heated falling films. Comparison between solutions of the long-wave equations and the full direct simulations of the original free-boundary problem clearly supports the existence of such multihumped structures and demonstrates their qualitative similarity.

The evolution equations discussed in this review are generally known to be well balanced in the sense of boundedness of their solutions. Yet rigorous mathematical treatment of these equations is in its infancy. In fact, whether or not they can exhibit unphysical, unbounded solutions remains an open mathematical question.

The examples discussed in this review suggest generalizations in two directions. On the one hand, one can delve more deeply into the stated physical systems and create new models when the dynamics cease to be well described. On the other hand, one can broaden the existing models to include new physical effects that couple with those already understood. These two alternatives will be discussed.

Burelbach *et al.* (1988) showed that just before film rupture by van der Waals attractions, inertial effects become important, so that one cannot strictly predict dryout. In order to follow the dynamics to dryout one must retain the inertial terms and solve a ''boundary-layer problem.'' When rupture occurs, contact lines are formed and one must establish contact-line boundary conditions in order to follow the opening of the dry patch. Since negative disjoining pressures are associated with poorly wetting liquids, the ruptured interface would likely turn under the liquid as the patch opens, invalidating the lubrication approximation. This scenario of rupture and opening is a prototype of a class of problems in which the connectivity of the domain changes in time. The ability to describe such evolutions is extremely important. Upgrading the importance of inertia has been shown to be crucial in the study of falling films; see Chang (1994) for a view of this.

In this review some thermal and solutal phenomena have been described in terms of thermocapillary, solutocapillary, and evaporative effects. These are among situations in which new physico-chemical effects (i.e., surface physics) can be incorporated. One can study the coupling of heterogeneous chemical reactions with film dynamics [e.g., see Meinkohn and Mikhailov (1993)]. During the process of welding, or soldering, the molten metal can react chemically with the substrate which yields new reaction products [e.g., see Braun *et al.* (1995)]. Multiple component and multiphase systems can be approached. Structural effects such as those present in lipid bilayer cell membranes and rheologically complex fluid films can be addressed (see, for example, Gallez *et al.*, 1993). When moving contact lines are present, one should devise a model of van der Waals attractions valid for geometries more complex than uniform films or wedges and so be able to study the effects of contact lines on spreading at arbitrary contact angles. The slip model and the contact angle θ deal with macroscopic effects linked to the microscopic physics near

the contact line θ. More work needs to be done on the description of the microscopics. This could then give a deduced slip law and a deduced $\theta = \theta(u_{CL})$. There seems to be very little information on the contact angle in systems involving phase change: evaporation/condensation, solidification, etc. Anderson and Davis (1995) supposed that the apparent angle depends on the local mass transport, but does the microscopic angle?

Clearly, careful experimental investigations are needed to verify phenomena and to give data that can be used to test the theories. This review stands as a call for such experiments.

ACKNOWLEDGMENTS

It is a pleasure to thank L. M. Hocking for a careful reading of the manuscript and for sharing with us his comments, remarks, and suggestions. We also are grateful to A. L. Frenkel for his suggestions. A. O. acknowledges the hospitality of the Department of Engineering Sciences and Applied Mathematics at Northwestern University, where this work was done. This work was partially supported by the Office of Basic Energy Science, U.S. Department of Energy, Award No. DE-FG02-ER 13641-07.

REFERENCES

Alekseenko, S. V., V. Ye. Nakoryakov, and B. G. Pokusaev, 1985, "Wave formation on a vertical falling liquid film," AIChE. J. **31,** 1446-1460.

Almgren, R., 1996, "Singularity formation in Hele-Shaw bubbles," Phys. Fluids A **8,** 344-352.

Anderson, D. M., and S. H. Davis, 1995, "The spreading of volatile liquid droplets on heated surfaces," Phys. Fluids A **7,** 248-265.

Atherton, R. W., and G. M. Homsy, 1976, "On the derivation of evolution equations for interfacial waves," Chem. Eng. Commun. **2,** 57-77.

Babchin, A. J., A. L. Frenkel, B. G. Levich, and G. I. Sivashinsky, 1983, "Nonlinear saturation of Rayleigh-Taylor instability," Phys. Fluids **26,** 3159-3161.

Bankoff, S. G., 1961, "Taylor instability of an evaporating plane interface," AIChE. J. **7,** 485-487.

Bankoff, S. G., 1971, "Stability of liquid film down a heated inclined plane," Int. J. Heat Mass Transf. **14,** 377-385.

Bankoff, S. G., 1994, "Significant questions in thin liquid film heat transfer," Trans. ASME, J. Heat Transf. **116,** 10-16.

Bankoff, S. G., and S. H. Davis, 1987, "Stability of thin films," PhysChem. Hydrodynamics **9**, 5-7.

Benjamin, T. B., 1957, "Wave formation in laminar flow down an inclined plane," J. Fluid Mech. **2,** 554-574.

Benney, D. J., 1966, "Long waves on liquid films," J. Math. Phys. (N.Y.) **45,** 150-155.

Bensimon, D., L. P. Kadanoff, S. Liang, B. I. Shraiman, and C. Tang, 1986, "Viscous flows in two dimensions," Rev. Mod. Phys. **58**, 977–999.

Bikerman, J. J., 1973, *Foams* (Springer, New York).

Boatto, S., L. P. Kadanoff, and P. Olla, 1993, "Traveling-wave solutions to thin-film equations," Phys. Rev. E **48,** 4423-4431.

Braun, R. J., B. T. Murray, W. J. Boettinger, and G. B. McFadden, 1995, "Lubrication theory for reactive spreading of a thin drop," Phys. Fluids **7,** 1797-1810.

Brenner, M. P., 1993, "Instability mechanism at driven contact lines," Phys. Rev. E **47,** 4597-4599.

Brenner, M., and A. Bertozzi, 1993, "Spreading of droplets on a solid surface," Phys. Rev. Lett. **71,** 593-596.

Burelbach, J. P., S. G. Bankoff, and S. H. Davis, 1988, "Nonlinear stability of evaporating/condensing liquid films," J. Fluid Mech. **195,** 463-494.

Burelbach, J. P., S. G. Bankoff, and S. H. Davis, 1990, "Steady thermocapillary flows of thin liquid layers. II. Experiment," Phys. Fluids A **2,** 322-333.

Cahn, J. W., 1960, "On spinodal decomposition," Acta. Metall. **9,** 795-801.

Cazabat, A. M., and M. A. Cohen Stuart, 1986, "Dynamics of wetting: effects of surface roughness," J. Phys. Chem. **90,** 5845-5849.

Chandrasekhar, S., 1961, *Hydrodynamic and Hydromagnetic Stability* (Clarendon, Oxford).

Chang, H. -C., 1994, "Wave evolution on a falling film," Annu. Rev. Fluid Mech. **26,** 103-136.

Chang, H.-C., E. A. Demekhin, and D. I. Kopelevich, 1993, "Nonlinear evolution of waves on a vertically falling film," J. Fluid Mech. **250,** 443-480.

Chen, J. D., 1988, "Experiments on a spreading drop and its contact angle on a solid," J. Colloid Interface Sci. **122,** 60-72.

Chung, J. C., and S. G. Bankoff, 1980, "Initial breakdown of a heated liquid film in cocurrent two-component annular flow: II. Rivulet and dry patch models," Chem. Eng. Commun. **4,** 455-470.

Constantin, P., T. D. Dupont, R. E. Goldstein, L. P. Kadanoff, M. J. Shelley, and S.-M. Zhou, 1993, "Droplet breaking in a model of the Hele-Shaw cell," Phys. Rev. E **47,** 4169-4181.

Dagan, Z., and L. M. Pismen, 1984, "Marangoni waves induced by a multistable chemical reaction on thin liquid films," J. Colloid Interface Sci. **99,** 215-225.

Davis, S. H., 1983, "Rupture of thin films," in *Waves on Fluid Interfaces*, edited by R. E. Meyer (Academic, New York), p. 291-302.

Davis, S. H., 1987, "Thermocapillary instabilities," Annu. Rev. Fluid Mech. **19,** 403-435.

de Bruyn, J. R., 1992, "Growth of fingers at a driven three-phase contact line," Phys. Rev. A **46,** 4500-4503.

De Gennes, P. G., 1985, "Wetting: statics and dynamics," Rev. Mod. Phys. **57,** 827-863.

Deissler, R. J., and A. Oron, 1992, "Stable localized patterns in thin liquid films," Phys. Rev. Lett. **68,** 2948-2951.

de Witt, A., D. Gallez, and C. I. Christov, 1994, "Nonlinear evolution equations for thin liquid films with insoluble surfactants," Phys. Fluids **6**, 3256-3266.

Dowson, D., 1979, *History of Tribology* (Longmans, Green, London/New York).

Dupont, T. F., R. E. Goldstein, L. P. Kadanoff, and S.-M. Zhou, 1993, "Finite-time singularity formation in Hele-Shaw systems," Phys. Rev. E **47,** 4182-4196.

Dussan V., E. B., 1979, "On the spreading of liquids on solid surfaces: static and dynamic contact lines," Annu. Rev. Fluid Mech. **11,** 371-400.

Dussan V., E. B., and S. H. Davis, 1974, "On the motion of fluid-fluid interface along a solid surface," J. Fluid Mech. **65,** 71-95.

Dussan V., E. B., E. Ramé, and S. Garoff, 1991, "On identifying the appropriate boundary conditions at a moving contact line: an experimental investigation," J. Fluid Mech. **230,** 97-116.

Dzyaloshinskii, I. E., E. M. Lifshitz, and L. P. Pitaevskii, 1959, "Van der Waals forces in liquid films," Zh. Eksp. Teor. Fiz. **37**, 229-241 [Sov. Phys. JETP **10,** 161-170 (1960)].

Edwards, D. A., H. Brenner, and D. T. Wasan, 1991, *Interfacial Transport Phenomena* (Butterworth-Heineman, Boston).

Edwards, D. A., and A. Oron, 1995, "Instability of a nonwetting film with interfacial viscous stress," J. Fluid Mech. **298,** 287-309.

Eggers, J., 1993, "Universal pinching of 3D axisymmetric free-surface flow," Phys. Rev. Lett. **71,** 3458-3461.

Eggers, J., 1995, "Theory of drop formation," Phys. Fluids **7,** 941-953.

Eggers, J., and T. F. Dupont, 1994, "Drop formation in a one-dimensional approximation of the Navier-Stokes equation," J. Fluid Mech. **262,** 205-221.

Ehrhard, P., 1993, "Experiments on isothermal and non-isothermal spreading," J. Fluid Mech. **257,** 463-483.

Ehrhard, P., and S. H. Davis, 1991, "Non-isothermal spreading of liquid drops on horizontal plates,' J. Fluid Mech. **229,** 365-388.

Elbaum, M., and S. G. Lipson, 1994, "How does a thin wetted film dry up?," Phys. Rev. Lett. **72,** 3562-3565.

Elbaum, M., and S. G. Lipson, 1995, "Pattern formation in the evaporation of thin liquid films," Isr. J. Chem. **35,** 27-32.

Erneux, E., and S.H. Davis, 1993, "Nonlinear rupture of free films," Phys. Fluids A **5,** 1117-1122.

Fermigier, M., L. Limat, J. E. Wesfreid, P. Boudinet, and C. Quilliet, 1992, "Two-dimensional patterns in Rayleigh-Taylor instability of a thin layer," J. Fluid Mech. **236,** 349-383.

Frenkel, A. L., 1993, "On evolution equations for thin liquid films flowing down solid surfaces," Phys. Fluids A **5,** 2343-2347.

Frenkel, A. L., A. J. Babchin, B. G. Levich, T. Shlang, and G. I. Sivashinsky, 1987, "Annular flow can keep unstable flow from breakup: nonlinear saturation of capillary instability," J. Colloid Interface Sci. **115,** 225-233.

Gaines, G. L., 1966, *Insoluble monolayers at liquid-gas interfaces* (Interscience, New York).

Gallez, D., N. M. Costa Pinto, and P. M. Bisch, 1993, "Nonlinear dynamics and rupture of lipid bilayers," J. Colloid Interface Sci. **160,** 141-148.

Garoff, S., 1996, private communication.

Gaver, D. P. III, and J. B. Grotberg, 1992, "Droplet spreading on a thin viscous film," J. Fluid Mech. **235,** 399-414.

Gjevik, B., 1970, "Occurrence of finite-amplitude surface waves on falling liquid films," Phys. Fluids **13,** 1918-1925.

Goldstein, R. E., A. I. Pesci, and M. J. Shelley, 1993, "Topology transitions and singularities in viscous flows," Phys. Rev. Lett. **70,** 3043-3046, and references therein.

Goldstein, R. E., A. I. Pesci, and M. J. Shelley, 1995, "Attracting manifold for a viscous topology transition," Phys. Rev. Lett. **75,** 3665-3668, and references therein.

Goodwin, R., and G. M. Homsy, 1990, "Viscous flow down a slope in the vicinity of a contact line," Phys. Fluids A **3,** 515-528.

Goren, S. L., 1962, "The instability of an annular thread of fluid," J. Fluid Mech. **12,** 309-319.

Greenspan, H. P., 1978, "On the motion of a small viscous droplet that wets a surface," J. Fluid Mech. **84,** 125-143.

Grotberg, J. B., 1994, "Pulmonary flow and transport phenomena," Annu. Rev. Fluid Mech. **26,** 529-571.

Grotberg, J. B., and D. P. Gaver, 1996, "A synopsis of surfactant spreading research," J. Colloid Interface Sci. **178,** 377-378.

Halpern, D., and J. B. Grotberg, 1992, "Dynamics and transport of a localized soluble surfactant on a thin fluid," J. Fluid Mech. **237,** 1-11.

Hammond, P. S., 1983, "Nonlinear adjustment of a thin annular film of viscous fluid surrounding a thread of another within a circular cylindrical pipe," J. Fluid Mech. **137,** 363-384.

Ho, L.-W., and A. T. Patera, 1990, "A Legendre spectral element method for simulation of unsteady incompressible viscous free-surface flow," Comput. Methods Appl. Mech. Eng. **80,** 355-366.

Hocking, L. M., 1983, "The spreading of a thin drop by gravity and capillarity," Q. J. Mech. Appl. Math. **36,** 55-69.

Hocking, L. M., 1990, "Spreading and instability of a viscous fluid sheet," J. Fluid Mech. **211,** 373-392.

Hocking, L. M., 1995a, "The wetting of a plane surface by a fluid," Phys. Fluids **7,** 1214-1220.

Hocking, L. M., 1995b, "On contact angles in evaporating liquids," Phys. Fluids **7,** 2950-2955.

Hocking, L. M., and M. J. Miksis, 1993, "Stability of a ridge of fluid," J. Fluid Mech. **247,** 157-177.

Hoffman, R. L., 1975, "A study of the advancing interface. I. Interface shape in liquid-gas systems," J. Colloid Interface Sci. **50,** 228-241.

Homsy, G. M., 1987, "Viscous fingering in porous media," Annu. Rev. Fluid Mech. **19,** 271-311.

Huh, C., and L. E. Scriven, 1971, "Hydrodynamic model of a steady movement of a solid/liquid/fluid contact line," J. Colloid Interface Sci. **35,** 85-101.

Huppert, H. E., 1982a, "The propagation of two-dimensional and axisymmetric viscous gravity currents over a rigid horizontal surface," J. Fluid Mech. **121,** 43-58.

Huppert, H. E., 1982b, "Flow and instability of a viscous gravity current down a slope," Nature (London) **300,** 427-429.

Huppert, H. E., and J. E. Simpson, 1980, "The slumping of gravity currents," J. Fluid Mech. **99,** 785-799.

Hyman, J. M., and B. Nicolaenko, 1986, "The Kuramoto-Sivashinsky equation: A bridge between PDE's and dynamical systems," Physica D **18,** 113-126.

Ida, M. P., and M. J. Miksis, 1996, "Thin film rupture," Appl. Math. Lett. **9**, 35-40.

Israelachvili, J. N., 1995, *Intermolecular and Surface Forces* (Academic, London).

Jain, R. K., and E. Ruckenstein, 1976, "Stability of stagnant viscous films on a solid surface," J. Colloid Interface Sci. **54,** 108-116.

Jameel, A. T., and A. Sharma, 1994, "Morphological phase separation in thin liquid films," J. Colloid Interface Sci. **164,** 416-427.

Jensen, O. E., and J. B. Grotberg, 1992, "Insoluble surfactant spreading on a thin viscous film: shock evolution and film rupture," J. Fluid Mech. **240,** 259-288.

Jensen, O. E., and J. B. Grotberg, 1993, "The spreading of a heat or soluble surfactant along a thin liquid film," Phys. Fluids A **5,** 58-68.

Jin, W., J. Koplik, and J. R. Banavar, 1996, private communication.

Johnson, M. F. G., R. A. Schluter, and S. G. Bankoff, 1997, "Fluorescent imaging system for free surface flow," Rev. Sci. Instrum. (to be published).

Joo, S. W., and S. H. Davis, 1992a, "Irregular waves on viscous falling films," Chem. Eng. Commun. **118,** 111-123.

Joo, S. W., and S. H. Davis, 1992b, "Instabilities of three-dimensional viscous falling films," J. Fluid Mech. **242,** 529-549.

Joo, S. W., S. H. Davis, and S. G. Bankoff, 1991, "Long-wave instabilities of heated films: two dimensional theory of uniform layers," J. Fluid Mech. **230,** 117-146

Joo, S. W., S. H. Davis, and S. G. Bankoff, 1996, "A mechanism for rivulet formation in heated falling heated films," J. Fluid Mech. **321**, 279-298.

Kelly, R. E., S. H. Davis, and D. A. Goussis, 1986, "On the instability of heated film flow with variable surface tension," in *Proceedings of the 8th International Heat Transfer Conference*, edited by C. L. Tien, V. P. Carey, and J. K. Ferrell (Hemisphere, New York), v. 4, pp. 1937-1942.

Kevrekidis, I. G., B. Nicolaenko, and J. C. Scovel, 1990, "Back in the saddle again: a computer-assisted study of the Kuramoto-Sivashinsky equation," SIAM J. Appl. Math. **50**, 760-790.

Kheshgi, H. S., and L. E. Scriven, 1991, "Dewetting: nucleation and growth of dry regions," Chem. Eng. Sci. **46**, 519-526.

Kim, H., S. G. Bankoff, and M. J. Miksis, 1992, "The effect of an electrostatic field on film flow down an inclined plane," Phys. Fluids A **4,** 2117-2130.

Kopbosynov, B. K., and V. V. Pukhnachev, 1986, "Thermocapillary flow in thin liquid films," Fluid Mech.-Sov. Res. **15,** 95-106.

Krishna, M. V. G., and S. P. Lin, 1977, "Nonlinear stability of a viscous film with respect to three-dimensional side-band disturbances," Phys. Fluids **20,** 1039-1044.

Krishnamoorthy, S., B. Ramaswamy, and S. W. Joo, 1995, "Spontaneous rupture of thin liquid films due to thermocapillarity: A full-scale direct numerical simulation," Phys. Fluids **7,** 2291-2293.

Krishnamoorthy, S., B. Ramaswamy, and S. W. Joo, 1997a, "Nonlinear wave formation and rupture in heated falling films: A full-scale direct numerical simulation," J. Fluid Mech. (in press).

Krishnamoorthy, S., B. Ramaswamy, and S. W. Joo, 1997b, "Three-dimensional simulation of instabilities and rivulet formation in heated falling films," J. Comput. Phys. **131**, 70-88.

Kuramoto, Y., and T. Tsuzuki, 1975, "On the formation of dissipative structures in reaction-diffusion systems," Prog. Theor. Phys. **54,** 687-699.

Kuramoto, Y., and T. Tsuzuki, 1976, "Persistent propagation of concentration waves in dissipative media far from thermal equilibrium," Prog. Theor. Phys. **55,** 356-369.

Landau, L. D., and E. M. Lifshits, 1987, *Fluid Mechanics* (Oxford, London).

Leger, L., and J. F. Joanny, 1992, "Liquid spreading," Rep. Prog. Phys. **55,** 431-486.

Legros, J. C., 1986, "Problems related to non-linear variations of surface tension," Acta Astron. **13,** 697-703.

Legros, J. C., M. C. Limbourg-Fontaine, and G. Petre, 1984, "Influence of surface tension minimum as a function of temperature on the Marangoni convection," Acta Astron. **14,** 143-147.

Levich, V. G., 1962, *Physicochemical Hydrodynamics* (Prentice-Hall, Englewood Cliffs).

Lin, S.-P., 1969, "Finite amplitude stability of a parallel flow with a free surface," J. Fluid Mech. **36,** 113-126.

Lin, S.-P., 1974, "Finite amplitude side-band stability of a viscous film," J. Fluid Mech. **63,** 417-429.

Lin, S.-P., and M. V. G. Krishna, 1977, "Stability of a liquid film with respect to initially finite three-dimensional disturbances," Phys. Fluids **20,** 2005-2011.

Lin, S.-P., and C. Y. Wang, 1985, "Modeling wavy film flows," in *Encyclopedia of Fluid Mechanics*, edited by N. P. Cheremisinoff (Gulf, Houston), Vol. 1, p. 931-951.

Liu, J., J. B. Schneider, and J. P. Gollub, 1995, "Three-dimensional instabilities of film flows," Phys. Fluids **7,** 55-67.

Lopez, J., C. A. Miller, and E. Ruckenstein, 1976, "Spreading kinetics of liquid drops on solids," J. Colloid Interface Sci. **56,** 460-468.

Lopez, P. G., S. G. Bankoff, and M. J. Miksis, 1996, "Non-isothermal spreading of a thin liquid film on an inclined plane," J. Fluid Mech. **324,** 261-286.

Meinkohn, D., and A. Mikhailov, 1993, "Motion of thin wetting liquid films in the presence of surface chemical reactions," Physica A **198,** 25-45.

Miles, J. W., 1960, "The hydrodynamic stability of a thin film of liquid in uniform shearing motion," J. Fluid Mech. **8,** 593-610.

Mitlin, V. S., 1993, "Dewetting of solid surface: analogy with spinodal decomposition," J. Colloid Interface Sci. **156,** 491-497.

Mitlin, V. S., and N. V. Petviashvili, 1994, "Nonlinear dynamics of dewetting: kinetically stable structures," Phys. Lett. A **192,** 323-326.

Moriarty, J. A., and L. W. Schwartz, 1992, "Effective slip in numerical calculations of moving-contact-line problems," J. Eng. Math. **26**, 81-86.

Moriarty, J. A., L. W. Schwartz, and E. O. Tuck, 1991, "Unsteady spreading of thin liquid films with small surface tension," Phys. Fluids A **3,** 733-742.

Nakaya, C., 1975, "Long waves on a thin fluid layer flowing down an inclined plane," Phys. Fluids **15,** 1407-1412.

Nakaya, C., 1978, "Waves of large amplitude on a fluid film down a vertical wall," J. Phys. Soc. Jpn. **43,** 1821-1822.

Nakaya, C., 1981, "Stationary waves on a viscous fluid film down a vertical wall," J. Phys. Soc. Jpn. **50,** 2795-2796.

Nakaya, C., 1983, "Solitary waves on a viscous fluid film down a vertical wall," J. Phys. Soc. Jpn. **52,** 359-360.

Nakaya, C., 1989, "Waves on a viscous fluid film down a vertical wall," Phys. Fluids A **1,** 1143-1154.

Nepomnyashchy, A. A., 1974, "Stability of wave regimes in a film flowing down an inclined plane," Izv. Akad. Nauk SSSR, Mekh. Zhidk. Gaza, **3**, 28-34.

Ngan, C. G., and E. B. Dussan V., 1989, "On the dynamics of liquid spreading on solid surfaces," J. Fluid Mech. **209,** 191-226.

Oron, A., 1997, "Nonlinear dynamics of a free film subject to the Marangoni instability," unpublished.

Oron, A., and S. G. Bankoff, 1997, "Nonlinear dynamics of ultra-thin liquid films," unpublished.

Oron, A., S. G. Bankoff, and S. H. Davis, 1996, "Thermal singularities in film rupture," Phys. Fluids **8,** 3433-3435.

Oron, A., S. G. Bankoff, and S. H. Davis, 1997, "Evolution of a thin evaporating liquid film heated by a spatially nonuniform heat flux," unpublished.

Oron, A., and P. Rosenau, 1989, ''Nonlinear evolution and breaking of interfacial, Rayleigh-Taylor, waves,'' Phys. Fluids A **1,** 1155-1165.

Oron, A., and P. Rosenau, 1992, ''Formation of patterns induced by thermocapillarity and gravity,'' J. Phys. (France) II **2,** 131-146.

Oron, A., and P. Rosenau, 1994, ''On a nonlinear thermocapillary effect in thin liquid layers,'' J. Fluid Mech. **273,** 361-374.

Palmer, H. J., 1976, ''The hydrodynamic stability of rapidly evaporating liquids at reduced pressure,'' J. Fluid Mech. **75,** 487-511.

Paulsen, F. G., R. Pan, D. W. Bousfield, and E. V. Thompson, 1996, ''The dynamics of bubble/particle attachment and the application of two disjoining film rupture models to flotation,'' J. Colloid Interface Sci. **178,** 400-410.

Pimputkar, S. M., and S. Ostrach, 1980, ''Transient thermocapillary flow in thin liquid layers,'' Phys. Fluids **23,** 1281-1285.

Plesset, M. S., 1952, ''Note on the flow of vapor between liquid surfaces,'' J. Chem. Phys. **20,** 790-793.

Plesset, M. S., and A. Prosperetti, 1976, ''Flow of vapor in a liquid enclosure,'' J. Fluid Mech. **78,** 433-444.

Prevost, M., and D. Gallez, 1986, ''Nonlinear rupture of thin free liquid films,'' J. Chem. Phys. **84,** 4043-4048; **85,** 4757-4758(E).

Prokopiou, Th., M. Chen, and H.-C. Chang, 1991, ''Long waves on inclined films at high Reynolds number,'' J. Fluid Mech. **222,** 665-691.

Pumir, A., P. Manneville, and Y. Pomeau, 1983, ''On solitary waves running down an inclined plane,'' J. Fluid Mech. **135,** 27-50.

Ramaswamy, B., S. Chippada, and S. W. Joo, 1996, ''A full-scale numerical study of interfacial instabilities in thin Film flow,'' J. Fluid Mech. **325**, 163-194.

Rayleigh, Lord (J.W.S.), 1894, *Theory of Sound* (Macmillan, London).

Reisfeld, B., and S. G. Bankoff, 1990, ''Nonlinear stability of a heated thin film with variable viscosity,'' Phys. Fluids A **2,** 2066-2067.

Reisfeld, B., and S. G. Bankoff, 1992, ''Nonisothermal flow of a liquid film on a horizontal cylinder,'' J. Fluid Mech. **236,** 167-196.

Reisfeld, B., S. G. Bankoff, and S.H. Davis, 1991, ''The dynamics and stability of thin liquid films during spin-coating. I. Films with constant rates of evaporation or absorption,'' J. Appl. Phys. **70,** 5258-5266. ''II. Films with unit-order and large Peclet numbers,'' J. Appl. Phys. **70,** 5267-5277.

Reynolds, O., 1886, ''On the theory of lubrication and its application to Mr. Beauchamp Tower's experiments, including an experimental determination of the viscosity of olive oil,'' Philos. Trans. R. Soc. London **177,** 157-234.

Rosenau, P., and A. Oron, 1989, ''Evolution and Breaking of Liquid Film Flowing on a Vertical Cylinder,'' Phys. Fluids A **1,** 1763-1766.

Rosenau, P., A. Oron, and J. M. Hyman, 1992, ''Bounded and unbounded patterns of the Benney equation,'' Phys. Fluids A **4,** 1102-1004.

Rosenblat, S., and S. H. Davis, 1985, ''How do liquid drops spread on solids?'' in *Frontiers in Fluid Mechanics*, edited by S. H. Davis and J. L. Lumley (Springer, Berlin New York), pp. 171-183.

Roskes, G. J., 1970, ''Three-dimensional long waves on a liquid film,'' Phys. Fluids **13,** 1440-1445.

Ruckenstein, E., and R. K. Jain, 1974, ''Spontaneous rupture of thin liquid films,'' Chem. Soc. Faraday Trans. **270**, 132-137.

Sadhal, S. S., and M. S. Plesset, 1979, ''Effect of solid properties and contact angle in dropwise condensation and evaporation,'' J. Heat Transf. **101**, 48-54.

Salamon, T. R., R. C. Armstrong, and R. A. Brown, 1994, ''Traveling waves on vertical films: Numerical analysis using the Finite Elements Method,'' Phys. Fluids **6,** 2202-2220.

Scheludko, A. D., 1967, ''Thin liquid films,'' Adv. Colloid Interface Sci. **1,** 391-464.

Schlichting, H., 1968, *Boundary-layer Theory* (McGraw-Hill, New York).

Schrage, R. W., 1953, *A Theoretical Study of Interphase Mass Transfer* (Columbia University, New York).

Schramm, L. L., and F. Wassmuth, 1994, ''Foams: basic principles,'' in *Foams: Fundamentals and Applications in the Petroleum Industry*, edited by L. L. Schramm (American Chemical Society, Washington), pp. 3-46.

Schwartz, L. W., 1989, ''Viscous flows down an inclined plane: Instability and finger formation,'' Phys. Fluids A **1,** 443-445.

Schwartz, L. W., R. A. Cairncross, and D. E. Weidner, 1996, ''Anomalous behavior during leveling of thin coating layers with surfactants,'' Phys. Fluids **8,** 1693-1695.

Schwartz, L. W., D. E. Weidner, and R. R. Eley, 1995, ''An analysis of the effect of surfactant on the leveling behavior of a thin liquid coating layer,'' Langmuir **11,** 3690-3693.

Seydel, R., 1988, *From Equilibrium to Chaos: Practical Bifurcation and Stability Analysis* (Elsevier, New York).

Sharma, A., and A. T. Jameel, 1993, ''Nonlinear stability, rupture, and morphological phase separation of thin fluid films on apolar and polar substrates,'' J. Colloid Interface Sci. **161,** 190-208.

Sharma, A., C. S. Kishore, S. Salaniwal, and E. Ruckenstein, 1995, ''Nonlinear stability and rupture of ultrathin free films,'' Phys. Fluids **7,** 1832-1840.

Sharma, A., and E. Ruckenstein, 1986a, ''An analytical nonlinear theory of thin film rupture and its application to wetting films,'' J. Colloid Interface Sci. **113,** 456-479.

Sharma, A., and E. Ruckenstein, 1986b, ''Rupture of thin free films with insoluble surfactants: nonlinear aspects,'' AIChE Symp. Ser. **252**, 130-144.

Sharma, A., and E. Ruckenstein, 1988, ''Dynamics and lifetimes of thin evaporating liquid films: some non-linear effects,'' PhysChem. Hydrodynamics **10**, 675-691.

Sheludko, A., 1967, ''Thin liquid films,'' Adv. Colloid Interface Sci. **1,** 391-463.

Shi, X. D., M. P. Brenner, and S. R. Nagel, 1994, ''A cascade of structure in a drop falling from a faucet,'' Science **265,** 219-222.

Shkadov, V. Ya., 1967, ''Wave conditions in the flow of thin layer of a viscous liquid under the action of gravity,'' Izv. Akad. Nauk SSSR, Mekh. Zhidk. Gaza **1**, 43-50.

Shkadov, V. Ya., 1968, ''Theory of wave flows of thin layer of a viscous liquid,'' Izv. Akad. Nauk SSSR, Mekh. Zhidk. Gaza **2**, 20-26.

Silvi, V., and E. B. Dussan V., 1985, ''On the rewetting of an inclined solid surface by a liquid,'' Phys. Fluids **28**, 5–7.

Sivashinsky, G. I., 1977, ''Nonlinear analysis of hydrodynamic instability in laminar flames,'' Acta Astron. **4,** 1175-1206.

Sivashinsky, G. I., and D. M. Michelson, 1980, ''On irregular wavy flow of a liquid film down a vertical plane,'' Prog. Theor. Phys. **63,** 2112-2114.

Smith, M. K., 1995, "Thermocapillary migration of a two-dimensional liquid droplet on a solid surface," J. Fluid Mech. **294,** 209-230.

Smith, M. K., and S. H. Davis, 1982, "The instability of sheared liquid layers," J. Fluid Mech. **121,** 187-206.

Spaid, M. A., and G. M. Homsy, 1996, "Stability of Newtonian and viscoelastic dynamic contact lines," Phys. Fluids **8,** 460-478.

Sreenivasan, S., and S.-P. Lin, 1978, "Surface tension driven instability of a liquid film flow down a heated incline," Int. J. Heat Mass Transf. **21,** 1517-1526.

Starov, V. M., 1983, "Spreading of droplets of nonvolatile liquids over a flat surface," Coll. J. USSR **45**, 1009-1015.

Stillwagon, L. E., and R. G. Larson, 1988, "Fundamentals of topographic substrate leveling," J. Appl. Phys. **63,** 5251-5258.

Stillwagon, L. E., and R. G. Larson, 1990, "Leveling of thin films over uneven substrates during spin coating," Phys. Fluids A **2,** 1937-1944.

Tan, M. J., S. G. Bankoff, and S. H. Davis, 1990, "Steady thermocapillary flows of thin liquid layers," Phys. Fluids A **2,** 313-321.

Tanner, L. H., 1979, "The spreading of silicone oil on horizontal surfaces," J. Phys. D **12,** 1473-1484.

Teletzke, G. F., H. T. Davis, and L. E. Scriven, 1988, "Wetting hydrodynamics," Rev. Phys. Appl. **23,** 989-1007.

Troian, S. M., E. Herbolzheimer, S. A. Safran, and J. F. Joanny, 1989, "Fingering instabilities of driven spreading films," Europhys. Lett. **10,** 25-30.

Tuck, E. O., and L. W. Schwartz, 1990, "A numerical and asymptotic study of some third-order ordinary differential equations relevant to draining and coating flows," SIAM (Soc. Ind. Appl. Math.) Rev. **32,** 453-469.

van Hook, S. J., M. F. Schatz, W. D. McCormick, J. B. Swift, and H. L. Swinney, 1995, "Long-wavelength instability in surface-tension-driven Bénard convection," Phys. Rev. Lett. **75,** 4397-4400.

van Hook, S. J., M. F. Schatz, J. B. Swift, and H. L. Swinney, 1996, private communications.

Wallis, G. B., 1969, *One-dimensional Two-phase Flow* (McGraw Hill, New York).

Wasan, D. T., K. Koczo, and A. D. Nikolov, 1994, "Mechanisms of aqueous foam stability and antifoaming action with and without oil: a thin film approach," in *Foams: Fundamentals and Applications in the Petroleum Industry*, edited by L. L. Schramm (American Chemical Society, Washington), pp. 47-114.

Wayner, P. C., Jr, 1982, "Adsorption and capillary condensation at the contact line in change of phase heat transfer," Int. J. Heat Mass Transf. **25,** 707-713.

Wayner, P. C., Jr, 1993, "Spreading of a liquid film with a finite apparent contact angle by the evaporation/condensation process," Langmuir **9,** 294-299.

Wayner, P. C., Jr., 1994, "Thermal and mechanical effects in the spreading of a liquid film due to a change in the apparent finite contact angle," J. Heat Transf. **116**, 938-945.

Whitham, G. B., 1974, *Linear and Nonlinear Waves* (Wiley, New York).

Williams, M. B., 1981, "Nonlinear theory of film rupture," Ph.D. thesis (Johns Hopkins University).

Williams, M. B., and S. H. Davis, 1982, "Nonlinear theory of film rupture," J. Colloid Interface Sci. **90,** 220-228.

Willson, K. R., 1995, Ph.D. thesis, Carnegie Mellon University, "The dynamic wetting of polymer melts: An investigation of the role of material properties and the inner scale hydrodynamics."

Wong, H., C. J. Radke, and S. Morris, 1995, "The motion of long bubbles in polygonal capillaries. Part 1. Thin films," J. Fluid Mech. **292,** 71-94.

Wong, H., I. Fatt, and C. J. Radke, 1996, "Deposition and thinning of the human tear film," J. Colloid Interface Sci. **184,** 44-51, and references therein.

Xu, J.-J., and S. H. Davis, 1985, "Instability of capillary jets with thermocapillarity," J. Fluid Mech. **161,** 1-25.

Yarin, A. L., A. Oron, and P. Rosenau, 1993, "Capillary instability of thin liquid film on a cylinder," Phys. Fluids A **5,** 91-98.

Yiantsios, S. G., and B. G. Higgins, 1989, "Rayleigh-Taylor instability in thin viscous films," Phys. Fluids A **1,** 1484-1501.

Yiantsios, S. G., and B. G. Higgins, 1991, "Rupture of thin films: nonlinear stability analysis," J. Colloid Interface Sci. **147,** 341-350.

Yih, C.-S., 1955, "Stability of parallel laminar flow with a free surface," in *Proceedings of the 2nd US Congress on Applied Mechanics*, ASME New York, pp. 623-628.

Yih, C.-S., 1963, "Stability of parallel laminar flow down an inclined plane," Phys. Fluids **6,** 321-333.

Yih, C.-S., 1969, "Three-dimensional motion of liquid film induced by surface-tension variation or gravity," Phys. Fluids **12,** 1982-1987.